INTEGRATING SATELLITE-DERIVED PRECIPITATION MEASUREMENTS TO ASSESS WATER RESOURCES ON THE NAVAJO NATION AND THE FOUR CORNERS REGION

by

K. ANSLEY LONG

(Under the Direction of J. Marshall Shepherd)

ABSTRACT

The Four Corners Region of the southwestern United States is an arid and topographically complex region, with a majority of the annual precipitation occurring during the summer monsoon season and the winter months. The region is home to the Navajo Nation that spans roughly 27,500 square miles and nearly 174,000 people. Lack of infrastructure as a result of minimal economic resources confounded by environmental and climatic factors have limited access to a clean water supply for many Navajo. Access to water resources are critical for the Navajo's energy-water-food nexus (EWFN) and economic sectors, including agriculture. Currently, precipitation observations at the surface within Navajo reservation boundaries are sparse and radar coverage is insufficient. Limitations of surface precipitation observations distributed throughout the Navajo Nation make hydrologic assessments for water resources difficult. The use of space-borne precipitation observations is believed to provide the best spatial coverage for precipitation observations in the region. This research demonstrates using NASA's Integrated Multi-satellitE Retrievals for GPM (IMERG) that satellite-based rainfall estimates can be utilized for hydroclimate analysis for stakeholders in the Four Corners Region and for the Navajo Nation. With knowledge of the behavior of the satellite precipitation products, especially

on a monthly and seasonal basis, water resource managers in the region and on the Navajo reservation can have access to high-resolution precipitation observations to assess water resources and drought conditions. IMERG V06 is used with data from the North American Land Data Assimilation System (NLDAS-2) to conduct a geospatial water budget analysis for the Navajo reservation. The water budget analysis provides the Navajo Nation with a unique spatial analysis of surface hydrology and provides critical assessments of available water for the establishment of a novel precipitation metric. The precipitation per livestock (PPL) metric is developed using IMERG V06 and the Gridded Livestock of the World dataset to quantify spatial trends in available water through Precipitation-Evapotranspiration-Consumption maps. This research is a proof of concept and aims to provide ranchers and farmers as well as families that keep livestock for cultural traditional purposes to better understand the climatological water demands to maintain their herds.

INDEX WORDS: Satellite precipitation products, IMERG, water budget analysis, precipitation metrics, Navajo, water resources

INTEGRATING SATELLITE-DERIVED PRECIPITATION MEASUREMENTS TO ASSESS WATER RESOURCES ON THE NAVAJO NATION AND THE FOUR CORNERS REGION

by

K. ANSLEY LONG

B.S., University of Georgia, 2014

M.S., University of Utah, 2017

A Dissertation Submitted to the Graduate Faculty of The University of Georgia in Partial Fulfillment of the Requirements for the Degree

DOCTOR OF PHILOSOPHY

ATHENS, GEORGIA

2020

INTEGRATING SATELLITE-DERIVED PRECIPITATION MEASUREMENTS TO ASSESS WATER RESOURCES ON THE NAVAJO NATION AND THE FOUR CORNERS REGION

by

K. ANSLEY LONG

Major Professor: J. Marshall Shepherd

Committee: Jace Weaver
Andrew Grundstein
Jerry Shannon

Electronic Version Approved:

Ron Walcott
Interim Dean of the Graduate School
The University of Georgia
August 2020

DEDICATION

This dissertation is dedicated to my family as I could not have accomplished this without your unwavering support.

ACKNOWLEDGEMENTS

I would like to acknowledge Dr. J. Marshall Shepherd for giving me this incredible opportunity to pursue my Ph.D. Dr. Shepherd was my Introduction to Weather and Climate professor and I am so thankful that he has served as an incredible mentor and advocate since day one. I would also like to acknowledge my committee members Dr. Jace Weaver, Dr. Andrew Grundstein, and Dr. Jerry Shannon for their support and guidance during my time as a Ph.D. student at the University of Georgia. I am grateful for the hard work of Sarah Lips and Callum Lever whose initial research efforts provided a wealth of resources that supplemented this dissertation. Finally, this dissertation could not have been possible without the support from National Aeronautics and Space Administration (NASA) under Grant number NNX16AD87G The Energy-Water-Food Nexus Within The Backdrop of an Urbanized Globe: How Can GPM Help? NASA Precipitation Measurement Program as well as a grant awarded by the Georgia Water Resources Institute.

TABLE OF CONTENTS

Page

LIST OF TABLES

Page

LIST OF FIGURES

Page

CHAPTER 1

INRODUCTION AND LITERATURE REVIEW

1.1 Introduction

The Colorado Plateau is a major geological feature in the southwestern United States that is comprised of complex topography and boasts an extremely arid climate. The Colorado Plateau expands as far south and west as the Mogollon Rim in Arizona, as far north as the Uinta Mountains in Utah, and as far east as the western slopes of the Colorado Rockies. The Four Corners Region (FCR) is the intersection between the southeastern corner of Utah, southwestern corner of Colorado, northeastern corner of Arizona, and northwestern corner of New Mexico and is located on the Colorado Plateau. The FCR is defined in this study as the area between latitudes 33.4375ºN and 38.8125ºN and longitudes 105.9375ºW and 112.8125ºW (Figure 1.1). Notable geologic features in the FCR include portions of The Grand Canyon, the Mogollon Rim, and The Grand Staircase. Several high elevation mountain ranges are also located in the FCR. The Chuska Mountains reach 9,823 feet (2,994m) in elevation and straddle the Arizona-New Mexico border, the San Francisco Peaks in Arizona that reach up to 12,633 feet (3,851m), and the San Juan Mountains in southwestern Colorado that are located in the northeastern boundary where several peaks reach over 14,000 feet (4267m) in elevation (Figure 1.2).

In addition to the FCR's diverse geology and geography, the demographics of the FCR are particularly unique due to the high concentration of Native American reservations located within the region. The largest reservation is home to the Navajo Nation, who are a federally recognized tribe in the United States. Navajo traditionally refer to themselves as *Diné* which

translates to “The People” in the Native language [*Frankland et al.*, 2004]. The terms Navajo and *Diné* will be used interchangeably throughout this dissertation. The Navajo (*Diné*) reservation boasts a large population of 173,667 people and spans more than 27,000 square miles throughout parts of Arizona, New Mexico, Utah [*Navajo Epidemiology Center*, 2013]. The median income for households in the Navajo Nation is $27,389, which is well below the national average, and has a poverty rate of 38% [*Arizona Rural Policy Institute*, 2010].

One of the most pressing issues the Navajo Nation faces today is the inadequate supply of fresh, clean water resources for municipal and domestic water use [*Navajo Nation Department of Water Resources*, 2000]. Water infrastructure deficiencies as a result of minimal economic resources confounded by environmental and climatic factors have limited access to a clean water supply for many *Diné* families. Of significance is the environmental injustices involving groundwater contamination from poorly managed mining practices have reduced the security and availability of clean water sources and have contributed to public health issues on the Navajo reservation [*Hoover et al.*, 2017]. Extraction of natural resources such as coal, oil, and especially uranium is common on the reservation, and mining practices also utilize a substantial portion of the water resources on the reservation. Extractive mining industries have provided many Navajo with jobs but remain controversial as they have been found to result in severe deterioration of the environment through the contamination of local freshwater resources and stress water resources. A report by the *United States Environmental Protection Agency (U.S. EPA) Region IX* [2008] found that a significant portion of non-municipal water sources on the Navajo Nation contained levels of metal or radioactive materials that exceeded national standards. The public health impacts of arsenic, lead, and uranium concentrations found in unregulated water sources across

rural areas on the Navajo Nation have been widely studied [*Hoover et al.*, 2017; *Hoover et al.*, 2018; *Credo et al.,* 2019; *Erdei et al.*, 2019; *Ingram et al.*, 2020].

Though the Navajo have water rights under the 1908 *Winters Doctrine*, increased stress on the rivers and other regional water resources will continue as a result of both climate change and projected growing populations in the Southwest [*Parker*, 2010]. Currently, major sources of water to supply the Navajo Nation include the Colorado River, the Little Colorado River, the San Juan River, ephemeral streams, groundwater wells, alluvial aquifers, and surface reservoirs [*Nania et al.*, 2014]. Currently, livestock populations rely on roughly 7,500 stock ponds supplied by surface water runoff and 1,200 windmill powered livestock wells that tap into shallow alluvial aquifers for sources of water [*Navajo Department of Water Resources*, 2011]. Unfortunately, many of these critical water resources for livestock are already stressed and threatened. Studies of the Navajo Nation's hydroclimate, water resources, and clean water crisis have been conducted by *Nania et al.* [2014], *Cozzetto et al.* [2013], the *Navajo Department of Water Resources (NDWR)* [2003, 2011], and *Singer and Woods* [2017].

The current state of water scarcity on the reservation has forced many Navajo families to haul water from distant sources. It is estimated that up to 40% of families on the reservation live without potable water in their homes and many haul water from distant sources on a daily basis [*Navajo Nation Department of Water Resources*, 2000]. The water-hauling family's average one-way trip to haul water is roughly fourteen miles, where some logged longer round trips upwards of eighty miles [*Navajo Department of Water Resources*, 2003; *Nania et al.*, 2014]. Navajo families living in rural areas that haul water have to pay a higher cost for water due to greater transportation costs and smaller economies of scale [*United States Environmental Protection Agency*, 2001; *Cozzetto et al.*, 2013]. *Dornbusch and Associates* [2006] quantified the total cost

of water hauling that considered the economic cost of transportation and equipment as well as opportunity costs of time. The study found that families that haul water pay roughly $43,000 per acre foot for domestic water which is in stark contrast to the average $600 per acre foot that is typical for suburban water users [*Dornbusch and Associates*, 2006; *Navajo Department of Water Resources*, 2011]. These results show that Navajo water haulers that are often among some of the poorest individuals in the country are having to pay some of the most expensive prices for water in the United States. As a result of cost and equipment limitations for hauling water, per capita water consumption on the Navajo reservation ranges from 10 gallons per day for water haulers compared with the 100 gallons per day for those living in larger communities that have access to running water [*Singer and Woods*, 2017]. Efforts by the Navajo Water Project (https://www.navajowaterproject.org/), a program of the DigDeep to Water Project, to haul clean water and install home water systems are currently underway in Thoreau, New Mexico, Navajo Mountain in Utah, and Dilkon, Arizona.

Increasing access to water resources is critical for the Navajo's energy-water-food nexus (EWFN) and economic sectors. *Albrecht et al.* [2018] defines the energy, water, and food nexus (EWFN) as a framework used to assess the synergistic interaction between resource sectors and the effects on socioeconomics (Figure 1.2). Increased precipitation variability and drought conditions are expected to enhance the risk of a degradation in the synergistic relationships between the Navajo's EWFN. Energy sectors such as thermoelectric power will also suffer as a consequence of depleted water sources [*Nania et al.*, 2014]. The Navajo's economic sector will also be negatively impacted by climate change. Navajo rely upon water availability for dryland crops and farming as a source of food and economic income. Additionally, many Navajo keep livestock such as cattle, horses, and sheep for economic livelihood and enhance food security

[*Henderson*, 1989; *Nania et al.*, 2014]. Furthermore, livestock, specifically sheep and horses, are significant to Diné cultural traditional practices that [*McPherson*, 1998; *Benally*, 2011]. The potential changes in water supply as a result of regional climate change could have devastating consequences for the Navajo Nation. The expected increases in food, water, and energy prices due to climate change are anticipated to affect marginalized populations like the Navajo more than their wealthier counterparts [*Bohle et al.*, 1994; *Groisman et al.*, 2001; *Ivanic and Martin*, 2008]. *Shepherd et al.* [2016] note that the economy of food-water security risk is manifested by the following numbers from the *World Economic* [2011] Global Risks Report: global projections for a 50% increase in food demand, 30% increase in water demand, and 40% increase in energy demand by 2030. As demands for food, water, and energy increase with increasing populations and limited resources, vulnerable populations such as the Navajo will most likely to be subjected to limited access to resources. This results in augmented strains on socioeconomic issues already at play within native communities.

The overarching goal of this dissertation is to integrate satellite-based precipitation data from NASA in combination with water budget related data to examine the efficacy of available water monitoring tools, to assess spatial patterns of the water balance, and to further understand the water demands that relate to livestock on the Navajo Nation. This research ultimately seeks to address the impacts of hydroclimate on the Navajo EWFN. Precipitation estimates derived from satellites as well as an analysis of the water budget on the Navajo Nation aim to provide a better understanding of the Navajo's water scarcity crisis and to provide tools to enhance the monitoring of the precipitation input that will allow water managers to make more informed decisions. This dissertation will investigate the following objectives:

1) *Spatiotemporal trends in precipitation on the Navajo Nation utilizing satellite derived observations*: What are the precipitation patterns on the reservation? How well do space-borne satellite measurements from NASA's Integrated Multi-satellitE Retrievals for GPM (IMERG) V06 Final Run product perform in the region? Can IMERG V06 provide a high-resolution precipitation observation resource for local water managers in the region?
2) *A geospatial assessment of hydroclimate vulnerability using a simple water budget equation on the Navajo Nation*: Using satellite derived measurements of precipitation from NASA's IMERG V06 Final Run product and evaporation, runoff, and subsurface runoff data from the North American Land Data Assimilation System (NLDAS) Variable Infiltration Capacity (VIC) model, what is the water budget for the region and the reservation? What locations in the FCR and the Navajo Nation experience water shortage deficits or surpluses on a monthly and seasonal basis?
3) *Establishment of a novel precipitation per livestock (PPL) metric*: Using precipitation measurements from NASA'S IMERG V06 product and the Gridded Livestock of the World dataset, how much water from precipitation is available for the Navajo's livestock population? How does water stress fluctuate seasonally considering evapotranspiration and livestock consumption rates?

The research objectives outlined above will be explored in the following chapters of this dissertation. Each chapter is written as a completed manuscript to be submitted as a publication to scholarly journals. The introduction has provided background on the FCR and has highlighted the current water crisis situation on the Navajo reservation. The following sections in this introductory chapter provide a synopsis of the FCR's climate and hydroclimate, focusing

primarily on the influences of the North American Monsoon (NAM) system and dominant teleconnection patterns that drive precipitation regimes. The purpose of this section is to provide context about the climatic controls of precipitation that ultimately dictate the availability of surface water resources. Additionally, the following section will outline the potential future climate change scenarios as a result of anthropogenic greenhouse gas emissions that could impact the FCR's climate.

1.2 Literature Review

1.2.1 Climatology

The climate of the FCR is primarily driven by a large scale quasi-permanent subtropical high-pressure ridge, resulting in warm annual temperatures, frequently clear skies, and relatively low annual precipitation. Winter and summer temperatures tend to be extreme, while annual average temperatures range between 40 and 55ºF. Temperatures in the region are largely dependent upon elevation and latitude [*Garfin et al*., 2007]. Annual precipitation in the FCR is bimodal, with a peak occurring in winter from synoptic scale mid-latitude storm tracks originating in the Pacific and a second occurring during the summer from increased convective activity during the North American Monsoon (NAM). Decaying tropical storms occasionally contribute to the summer precipitation [*Hereford and Webb*, 1992]. The FCR receives roughly 12-13" of rainfall during the year primarily during the monsoon months, which are from July to mid-September [*Adams and Comrie*, 1997]. Snowfall amounts vary depending on elevation, but high elevation mountain ranges in these states typically receive 60" of snow on average while lower elevation, high desert regions can get up to 6" with low elevation deserts rarely receiving snow [*Sheppard et al.*, 2002]. According to the WMBWMI Section data, annual precipitation in

lower elevations on the Navajo reservation typically receive 15cm while higher elevations can receive up to 40cm [*Tulley-Cordova et al.*, 2018].

Between 30 and 50% of the annual precipitation occurs during the North American Monsoon (NAM) that brings rainfall to the southwestern United States from the beginning of July through mid-September [*Carleton et al.*, 1990; *Douglas et al.*, 1993; *Higgins et al.*, 1997; *Mitchell et al.*, 2002; *Sheppard et al.*, 2002]. *Higgins et al*. [1998] describe the onset of the NAM as a rapid change in regional weather patterns that change from hot and dry to cooler and rainy, noting that the exact date of NAM onset in the FCR is variable from year to year. The authors found that early (late) onset of monsoons in Arizona and New Mexico tend to have an increase (decrease) in precipitation compared to average monsoon seasons. In the presence of NAM, increased convection in the region from surface heating can produce severe thunderstorms, flooding, and mesoscale convective systems (MCS)s in favorable topographic regions [*Smith and Gall*, 1989; *Dunn and Horel*, 1994; *Maddox et al.*, 1995; *Adams and Comrie*, 1997; *Higgins et al.*, 2004; *Carrillo et al.*, 2016]. The NAM is centered over northwest Mexico, with the northern periphery of precipitation reaching the southwestern United States (Figure 1.4). Poleward displacement or weakening of the subtropical high can extend the boundary of moisture northward bringing sufficient moisture to a broad area across the region [*Watson et al*., 1994; *Adams and Comrie*, 1997].

The life cycle of the NAM is distinguished by the development, mature, and decay phases described by *Higgins et al.* [1997]. The authors cite several papers that describe key processes of the onset of precipitation in the region that include the generation of troughs in the desert Southwest [*Tang and Reiter*, 1984; *Rowson and Colucci*, 1992], the development of southerly low-level jets over the Gulf of California [*Carleton*, 1986; *Douglas*, 1995], the northward

displacements of the Bermuda and Pacific highs [*Carleton*, 1986, 1987], and the evolution of the monsoon boundary in Arizona [*Adang and Gall*, 1989]. Additionally, sea surface temperatures gradients and topography are of significance to the development phase of the NAM. *Adams and Comrie* [1997] explore the geographical and topographic features of the NAM that contribute to impacts over large areas of the southwestern United States and northwestern Mexico. To the west of the FCR is California's Pacific Coast, where average summertime sea surface temperatures (SSTs) at the middle and subtropical latitudes in the Pacific are relatively cool (<25ºC). Further south, average summertime SSTs in the Gulf of California and the tropical latitudes of the eastern Pacific are warmer (>28ºC). To the southeast is the Gulf of Mexico, which boasts relatively warm SSTs (>26ºC), while directly to the east is the Central Plains. Figure 1.3 shows the progression of SSTs leading up to, during, and at the termination of the NAM. The combination of atmospheric moisture from surrounding ocean sources and warm land surface temperatures are instrumental in establishing the mature phase of the NAM during late July and August. Both large-scale synoptic controls, such as the positioning of the subtropical ridge, and small-scale controls, such as elevation and extent of the inland penetration of moisture, are believed to be important mechanisms of precipitation variability with the NAM [*Carleton*, 1986; *Mock*, 1995; *Adams and Comrie*, 1997]. *Adams and Comrie* [1997] note the influence of elevation on precipitation variability citing instances of differing precipitation patterns on the Mogollon Rim and in the White Mountains in Arizona, where regions of higher elevation experience a much greater percentage of rainy days during the monsoon season than the lower desert regions as a result of increased convection. The decay phase of NAM occurring in September and even through early October is characterized as the "reverse of the onset phase, although changes tend to proceed at a slower rate" [*Higgins et al.*, 1997]. Ridging in the western

United States develops and causes the monsoon to retreat southward into Mexico where precipitation eventually subsides [*Higgins et al.*, 1997]. *Barlow et al.* [1997] note that the decay phase is difficult to define in regard to magnitude and spatiality of these changes, but the pattern is generally qualitatively agreed upon.

Certain configurations of the phases of ocean-atmosphere coupled teleconnection patterns such as El Niño-Southern Oscillation (ENSO), the Pacific Decadal Oscillation (PDO), and Atlantic Multidecadal Oscillation (AMO) have direct impacts on the interannual variability of precipitation in the FCR. The literature has shown that teleconnections may influence the timing and magnitude of the NAM system, control winter precipitation, and drive the onset of droughts. To this end, research has produced conflicting results over the direct impacts of ENSO on NAM variability. *Adams and Comrie* [1997] discuss these conflicting conclusions where the results of *Andrade and Sellers* [1988] show little correlation between ENSO and rainfall totals in the Arizona and New Mexico while *Harrington et al.* [1992] and *Hereford and Webb* [1992] find correlations in summer precipitation with warm phases of ENSO. PNA, which is closely tied to ENSO, can latitudinally shift the subtropical ridge [*Carleton et al.*, 1990]. PNA phases that produce northerly shifts in the ridge placement result in wetter summers while southerly shifts result in drier summers. Furthermore, wetter (drier) summers are associated with the meridional (zonal) phase of PNA and positive (negative) Pacific SST anomalies that amplify ridging over North American continent. *Tulley-Cordova et al.* [2018] also identified the increase in summer precipitation with the northward displacement of the subtropical ridge and concluded that summer monsoon precipitation is largely responsive to pressure patterns than climate modes. Several studies have investigated the impacts on the summer monsoon from deeper than average snowpacks in the region from strong PNA phases [*Carleton et al.*, 1990; *Gutzler and Preston*,

1997; *Higgins and Shi*, 2000; *Gutzler*, 2000; *Lo and Clark*, 2002]. In years with deeper than average snowpacks, more energy is required for melting and for evaporation of moist soils. These factors coupled with increased albedo from snow coverage result in a delayed and decreased warming of the land surface that ultimately play a role in determining the magnitude and establishment of the monsoon.

In general, winter precipitation tends to be wetter than average during El Niño phases and drier during La Niña phases of ENSO in the southwest [*Ropelewski and Halpert*, 1986; *Cayan and Webb*, 1992; *Cayan*, 1996; *Cayan et al.*, 1998; *Gutzler*, 2002]. *Cayan* [1996] found that during springs following an El Niño phase, positive SWE anomalies occur across the Four Corners region. Increased SWE can be beneficial for the supplying of water resources during springtime snowmelt that contribute to increased streamflow. *Tully-Cordova et al.* [2018] found that surface gauge observations of winter precipitation on the Navajo Nation are strongly correlated with PNA phases while moderate correlations were found with PDO.

Additionally, the region is highly prone to periods of prolonged warming and exceptional drought and have been identified in dendrochronology and palynology records [*Euler*, 1979; *Salzer*, 2000; *DeMenocal*, 2001; *Benson et al.,* 2006]. Of significance is the period of elevated aridity between 900 AD and 1300 AD where three episodes of prolonged multidecadal severe drought occurred centered around the years 1090, 1150, and 1280 AD. During this period, the Ancestral Puebloans occupied the region, constructing Great Houses and cliff dwellings that still remain today. However, by 1300 AD, the Ancestral Puebloans appeared to abandon the region. It is thought that the succession of the three most severe droughts on record for the FCR likely contributed to the abrupt abandonment by the civilization. *Benson et al.* [2007] compared tree-ring reconstructions of annual precipitation and soil moisture to study the cause of the persistent

and intense drought that occurred during the late 13th century that coincided with the Ancestral Puebloan abandonment of the FCR. The authors concluded that drought occurred as a result of a weakened or collapsed NAM system coupled with lower than average winter precipitation during a negative PDO phase that coincided with a positive AMO phase. Negative PDO phases can dampen the effects of El Niño while positive PDO phases can dampen the effects of La Niña, which play a role in drought and interannual precipitation variability in the southwest [*Sheppard et al.*, 2002].

1.2.2 Contextualizing the Impacts of Projected Regional Climate Change on Water Resources

Understanding the FCR's climate of the past and its effects on human life is important to contextualize the possibilities of climate change in the future and its implications for the population. The Four Corners region in the southwest is particularly interesting in terms of a region that has undergone changes in climate that have significantly influenced a society's ability to survive and thrive. The Ancestral Puebloans were a highly sophisticated society that occupied numerous locations across the Colorado Plateau from roughly 800 AD until their seemingly abrupt abandonment of the region by 1300 AD. There are many possible explanations for the fall of the civilization including social unrest and warfare, but it is likely that changes in climate were a significant contributing factor for their disappearance off the Colorado Plateau. The Ancestral Puebloan's diet consisted mostly of maize and therefore they were largely dependent upon the success of the crop. Maize is highly dependent upon wintertime precipitation for the generation and initial growth while the monsoon rains are needed to continue the flourishment of the crop as maize is sensitive to soil moisture [*Benson et al.*, 2007]. Right as the population of the civilization reached its peak, successions of severe decade long droughts occurred in the FCR

around the years 1090, 1150, and 1280 AD [*Cook et al.*, 2004]. The Ancestral Puebloans were likely unable to sustain their population due to the decreased productivity of their crops from severe and persistent droughts as a result of weakened monsoon systems and lower than average winter precipitation [*Benson et al.*, 2007]. It has been suggested that after the 26-year long drought around 1280 AD, they left the region in search of an environment more conducive for agricultural purposes [*deMenocal*, 2001].

The rise and fall of the Ancestral Puebloans should serve as an anecdote for modern society's vulnerability to climate change. Increased frequency of drought and variability in precipitation trends and patterns as a result of increased temperatures in combination with projected population increases in the region will threaten food and water security in the southwest. When hypothesizing the potential ramifications of climate change on the projected growing population in the southwest, it will be vital to remember the story of the Ancestral Puebloans and their vulnerability to the changes in climate of the region that likely contributed to the abandonment of their home on the Colorado Plateau.

Climate change is anticipated to increase water stress and disproportionately impact indigenous communities in the FCR such as the Navajo. Projections of future climate change scenarios as a result of anthropogenic greenhouse gas forcing show an increase in regional temperatures and increase in precipitation variability. As a result of regional climatic shifts, it is expected that the frequency, duration, and severity of droughts in the FCR is likely to occur with associated increased temperatures [*Cayan et al*., 2010; *MacDonald*, 2010; *Seager and Vecchi*, 2010]. Climate simulations from *Seager and Vecchi* [2010] suggest that the increased aridity in the region will be influenced by the poleward expansion of the wintertime storm track as a result of the planet warming from increased concentrations of greenhouse gases. Additionally, the

authors conclude that the region will experience decreases in wintertime precipitation due to the increased moisture divergence as a result of alterations to the mean atmospheric flow and diminished moisture convergence via transient eddies. *Cayan et al.* [2010] indicate that drought activity will increase by the end of the 21st century, particularly in the Colorado River Basin, resulting in depleted soil moisture and increase in water demand. Increased temperatures will result in increased evapotranspiration, resulting in enhanced aridity. In combination with reductions in annual precipitation, future climate change scenarios will reduce groundwater recharge [*Zekster et al.* 2005]. Decreased groundwater storage and recharge as a result of potential climatic change scenarios are expected to intensify the strains on already stressed water resources.

Some climatological studies on the Navajo Nation have also been conducted involving surface stations, climate datasets, and paleoclimate proxy datasets. A drought contingency plan from *Crimmins et al.* [2013] utilizes climatic precipitation data from Parameter-Elevation Regressions on Independent Slopes Model (PRISM) to assess drought conditions on the Navajo reservation. However, one of the limitations of their study is the spatial resolution of the climatology of precipitation for drought monitoring. The spatiotemporal scale is larger than that of short-term impacts of drought across the large acreage that the Navajo Nation spans. The need for accurate high spatiotemporal resolution precipitation observations for water resources is expressed in the conclusions of *Tulley-Cordova et al.* [2018]. The study used the Navajo Nation WMBWMI Section's surface station gauge network to conduct a precipitation climatology on the Navajo reservation. The authors assessed spatiotemporal precipitation patterns using statistical methods from a network of surface station observations on the reservation and identified regional patterns affected by teleconnections as well as onset and termination of the

monsoon precipitation. The study concluded that future changes in water resources as a result of deviation from climatic precipitation normals will be different in various regions of the reservation, suggesting some locations on the reservations will be impacted differently than others. The results of this study underscore the need for high spatiotemporal resolution precipitation observations in regions of complex terrain that are available to monitor shorter-term changes in precipitation as it relates to regional hydroclimate. It is evident from this section that the potential impacts of anthropogenic climate change could have significant ramifications for the Navajo Nation's water resources, as well as the hamper the synergy between EWFN sectors, resulting in increased vulnerability to climate change.

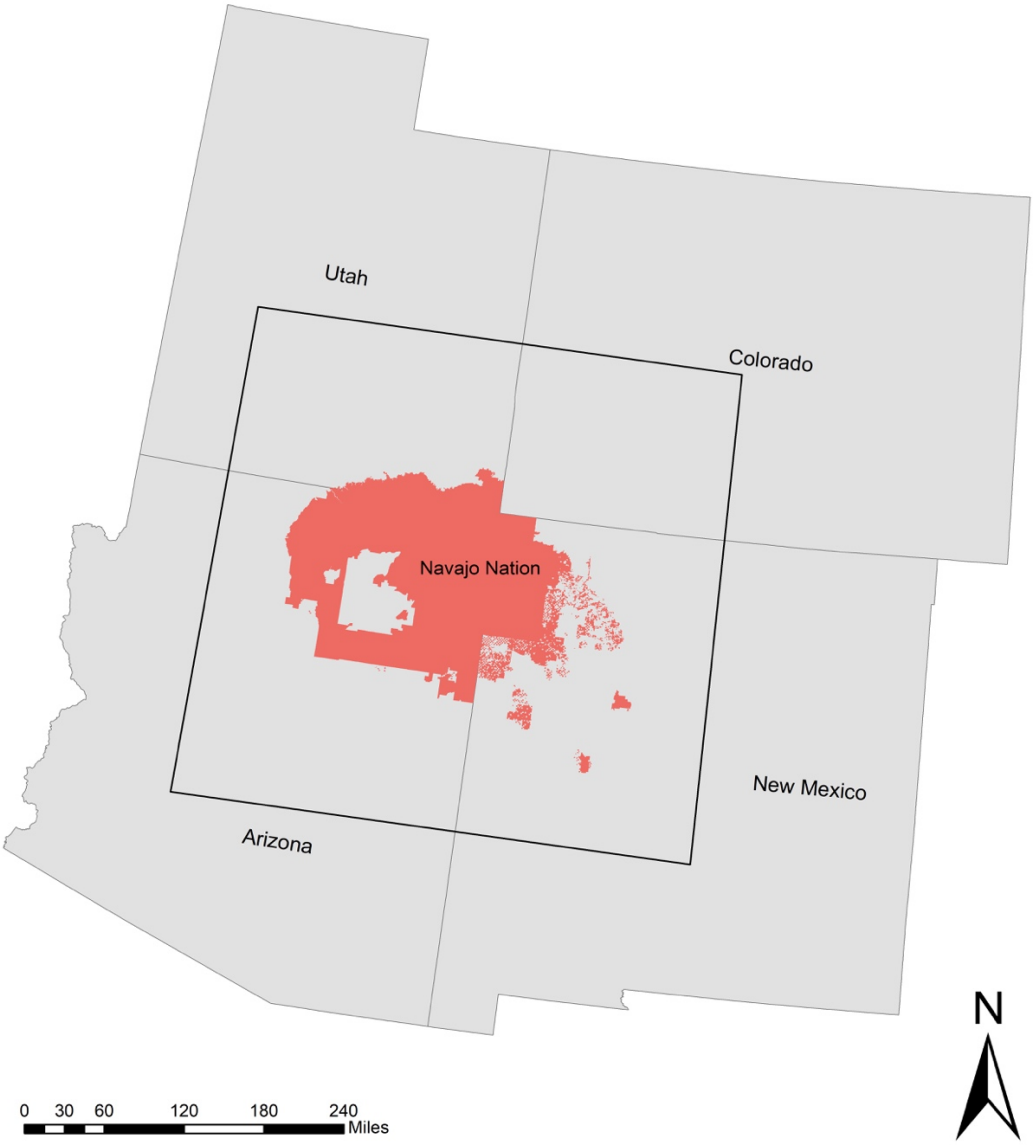

Figure 1.1. A map of the Navajo Nation and the Four Corners Region. The Navajo Nation is highlighted in coral while the proposed study region is bounded by the black box.

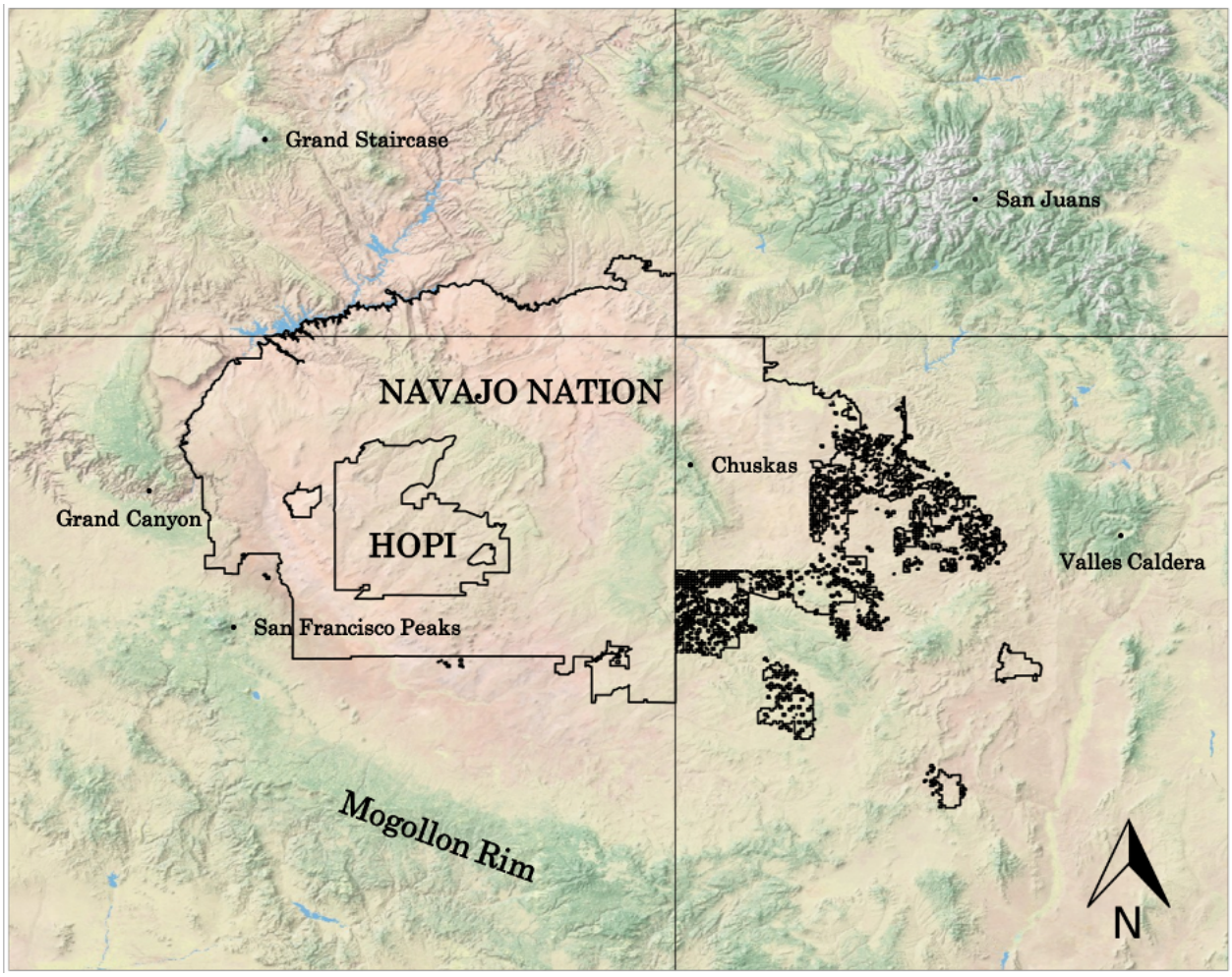

Figure 1.2. A physical map of the FCR that shows the defining geographic features in the study area. The Navajo Nation is outlined and shows the Hopi reservation, which is nestled in the southwestern sector of the Navajo Nation.

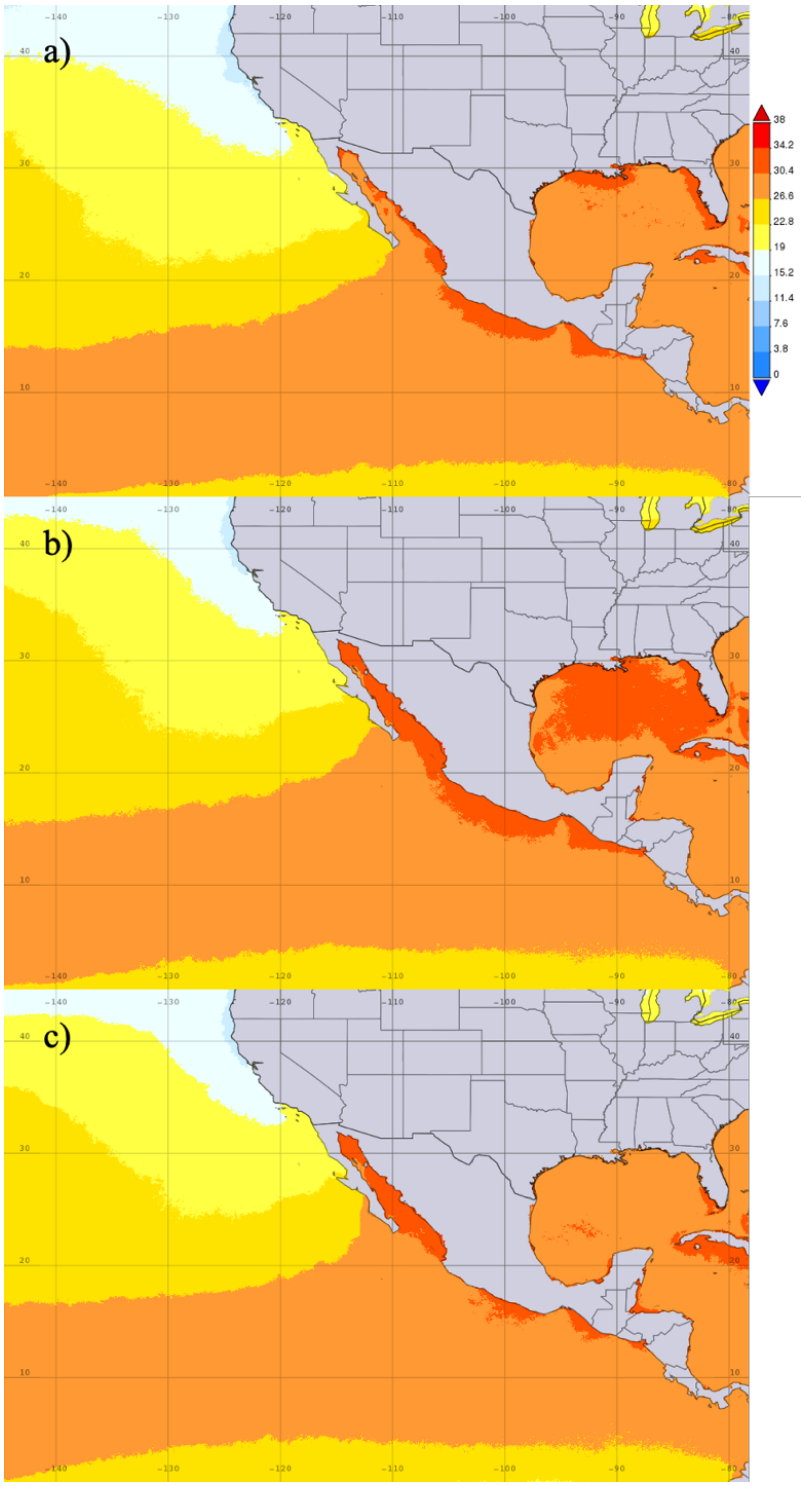

Figure 1.3a-c. Moderate-resolution Imaging Spectroradiometer (MODIS) Aqua 4km average SSTs at 11 µm from 2002 to 2018 for a. July, b. August, c. September. Analyses and visualizations were produced with the Giovanni online data system, developed and maintained by the NASA GES DISC. [*Retrieved from*: https://giovanni.gsfc.nasa.gov/giovanni/; *Acker and Leptoukh*, 2007].

Figure 1.4. A diagram of the atmospheric circulation during the North American Monsoon (NAM). Image adapted from *Crimmins* [2006] available at https://extension.arizona.edu/sites/extension.arizona.edu/files/pubs/az1417.pdf.

CHAPTER 2

QUANTIFYING THE EFFICACY OF A CONTEMPORARY GPM MERGED PRECIPITATION PRODUCT IN THE FOUR CORNERS REGION AND NAVAJO NATION[1]

[1] Long, K. A. and Shepherd, J. S. (2020). Quantifying the efficacy of a contemporary GPM merged precipitation product in the Four Corners Region and Navajo Nation. To be submitted to *Physical Geography*.

Abstract

The Four Corners Region (FCR) of the southwestern United States is topographically complex and arid, with a majority of the annual precipitation occurring during the summer monsoon season and winter months. The region is home to the Navajo reservation that spans roughly 27,500 square miles of desert landscape. Nearly 174,000 people live on the reservation where widespread water scarcity is a concern. Minimal water resources have left many Navajo (*Diné*) families with no access to clean running water in their homes and livestock populations surviving off of depleted surface water resources. Current efforts to monitor precipitation, a critical component for the replenishment of water resources, on the Navajo Nation and in the greater FCR include precipitation gauge observations at the surface that are sparse in spatial resolution. Furthermore, radar coverage in the FCR is insufficient, making hydrologic assessments for water resources difficult. The use of space-borne precipitation observations is believed to provide better spatial coverage of precipitation observations in the region. This research demonstrates, using NASA's IMERG V06 Final Run, that satellite-based rainfall estimates can be utilized in for hydroclimate analysis by stakeholders in the region. In an annual and seasonal analysis of IMERG V06 Final Run, the product is found to perform reasonably well in warmer and wetter months at low and mid-elevations (i.e. during the North American Monsoon) while performance diminishes during cooler months and in areas where the elevation exceeds 2500m. With knowledge of the behavior of the IMERG V06 Final Run product, water resource managers can have access to high-resolution precipitation observations to assess the state of water resources as well as drought conditions.

2.1 Introduction

Currently, one of the most pressing issues for the Navajo Nation is water scarcity. It is estimated that up to 40% of Navajo (*Diné*) families that live on the reservation do not have access to running water in their homes [*Navajo Nation Department of Water Resources*, 2000]. The threat to water security directly impacts the Navajo's energy-water-food nexus (EWFN) and influences community health, agricultural productivity, and economics. The nature of the indigenous socioeconomic issues and increasing water resource scarcity within the Four Corners Region (FCR) and the Navajo Nation underscores the need for high resolution spatiotemporal observations of precipitation for the region so that water resource management on local and regional levels may be accomplished. Accurate observations of precipitation are needed for climatological and hydrologic needs, especially as it relates to regional indigenous communities like the Navajo.

The FCR encompasses the Colorado Plateau, which is home to a large area of complex terrain including canyons, escarpments, and high-elevation mountain ranges (Figure 2.1). The Navajo reservation is nestled in the Four Corners Region (FCR) where the climate is largely driven by a large scale quasi-permanent subtropical high-pressure ridge, resulting in warm summer temperatures, cold winters, frequently clear skies, and low precipitation. The precipitation regime is bimodal, with a peak in late summer coinciding with the North American Monsoon system and a secondary peak in winter from the southerly shift of the mid-latitude storm track. Though many climatological studies in the region utilize surface observations from gauges as well as paleoclimate proxy datasets, the paucity of surface precipitation observations results in a decreased ability to represent accurate spatiotemporal trends, especially in areas of complex terrain. Although the surface stations from dense networks such as SNOTEL, the

Global Historical Climatology Network (GHCN) from NCDC, and from the Navajo Nation Water Monitoring Branch's Water Monitoring and Inventory (WMBWMI) provide several observations for surface precipitation observations in the region, direct measurements over a high spatiotemporal resolution are needed to enhance the understanding of short-term, fine-scale potential changes in precipitation for hydrologic purposes.

Limitations in gauge-based surface observations due to inhomogeneities related to poor spatial coverage, low temporal resolution, sensor type, observing practice, and observation errors are well understood [*Sevruk,* 1982; *Groisman et al.*, 1991; *Legates and DeLiberty*, 1993; *Peterson et al.*, 1998; *New et al.*, 2001]. Other systematic errors from ground-based precipitation gauges, especially in the southwest United States which covers large areas of complex terrain, include irregular sampling intervals, gauge calibration, undercatch, and evaporative losses [*Boushaki et al.*, 2009]. Additionally, snow-water equivalent (SWE) measurements from SNOTEL stations can also be limited by the manometer and pressure transducer systems as well as undercatch [*Serreze et al.*, 1999]. The current gauge networks that exist on the Navajo Nation are not uniformly distributed, and many gauges are clustered together in certain locations while large areas of the reservation lack any gauges at all. Surface gauges are also not homogenously distributed throughout areas of complex topography, which result in bias from station datasets (i.e. higher elevation stations tend to have greater precipitation than lower elevation stations due to orographic processes). Furthermore, some stations from the Water Monitoring Branch's Water Monitoring and Inventory (WMBWMI) gauge network are not automated due to limited cellular service and electrical infrastructure, contributing to sampling biases [*Tulley-Cordova et al.*, 2018].

Compacting the spatial resolution problem of the surface gauge networks is the inadequate coverage and hydrometeor detection issues of the National Weather Service's (NWS) Weather Surveillance Radar-1988 Doppler (WSR-88D) network. The NWS WSR-88D network of ground radars does not provide any radar coverage to the actual Four Corners state intersection in the region (Figure 2.2). Additionally, the locations throughout the region in which WSR-88D coverage are available may not provide the best estimates of precipitation. For example, the Z-R relationships used to detect precipitation in WSR-88D can be limited as they vary from radar to radar depending on geography and are influenced by storm type [*Ulbrich and Lee*, 1999; *Lee and Zawadzki*, 2005; *Prat and Barros*, 2009]. Furthermore, radar estimations of rainfall in the southwest can be restricted by evaporation of droplets between cloud base and surface and beam blockage from the local terrain [*Boushaki et al.*, 2009].

Space-borne precipitation estimates from satellite observations can provide high spatial coverage for precipitation observations globally, but the performance and accuracy of these estimates may differ regionally. Several studies have been performed in an effort to understand precipitation patterns and water resources on the Navajo Nation [*Navajo Nation Department of Water* Resources, 2003; *Garfin et al.*, 2007; *Crimmins et al.*, 2013; *Tulley-Cordova et al.*, 2018; *Tsinnajinnie et al.*, 2018], but to this end, none have evaluated the efficacy of NASA satellite-derived precipitation observations on the Navajo Nation or in the greater FCR, largely as a result of limited latitudinal coverage from previous satellite missions. The Tropical Rainfall Measuring Mission (TRMM) launched in 1997 was a joint effort between NASA and JAXA. TRMM's purpose was to observe precipitation at a high resolution between latitudes 36N-36S using a suite of onboard sensors including radar, the Visible and Infrared Scanners (VIIRS), and the TRMM Microwave Imager (TMI) [*Blumenfeld*, 2015]. Though TRMM provided valuable precipitation

estimates in the tropics, the satellite has since been replaced by NASA and JAXA's Global Precipitation Measurement (GPM) Mission, launched in February 2014. GPM's precipitation algorithm, Integrated Multi-SatellitE Retrievals for GPM (IMERG), broadens the global coverage of satellite-derived precipitation rates and has an improved spatiotemporal scale to provide estimates at every half hour on a 0.1º x 0.1º grid.

Several studies have evaluated IMERG and other remotely sensed precipitation product performances with ground-based observations from surface gauges and radar around the globe and in complex terrain. Many studies have found overestimations in low lying areas and underestimations with increasing elevation especially in cold climates [*Chen and Li*, 2016; *Behrangi et al.*, 2018; *Navarro et al.*, 2019; *Sharifi et al.*, 2019]. *Navarro et al.* [2019] have found that IMERG-F produced overestimations in low lying areas, but underestimated precipitation in the Alps during winter while the product performed reasonably well in complex terrain in the summer months. *Guo et al.* [2016] found that IMERG produces overestimations of light rainfall events in and arid region in China while *Sharifi et al.* [2019] found that overestimations are produced by IMERG in convective environments.

In the summer of 2019, NASA launched IMERG V06, which retrospectively extends the IMERG dataset to June 2000. IMERG V06 offers precipitation estimates in Early, Late, and Final runs which are available 4hrs, 14hrs, and 3.5months after observation respectively. Since IMERG V06's release, only a handful of studies have been published to validate the performance of the product. *Anjum et al.* [2019] found that there was no significant enhancement of performance from IMERG V05 to IMERG V06 over mainland China. *Maghsood et al.* [2020] found that at the country level in Iran, IMERG Final Run product is superior to the IMERG

Daily products. Additionally, the IMERG V06 Final Run is best suited for drought monitoring, hydrologic modeling, and agricultural forecasting [*Sungmin et al.*, 2017; *Maghsood et al.*, 2020].

This study only utilizes the Final Run of IMERG V06 and seeks to quantify the performance of the product throughout the FCR with special attention to the Navajo Nation to supplement the ongoing efforts by water managers in the region to monitor hydrology and drought. To this end, this is the first rigorous analysis of performance of a satellite-derived precipitation observation dataset that focuses primarily on the FCR and the Navajo Nation. Furthermore, this research is particularly motivated by current efforts between NASA and the Navajo Nation Department of Water Resources (NNDWR) to develop a Drought Severity Assessment Tool (DSAT). This tool utilizes Climate Hazards group InfraRed Precipitation with Stations data (CHIRPS), GPM, and TRMM data to produce a standardized precipitation index (SPI) [*Blumenfeld*, 2020]. Since drought and water monitoring projects are being developed for the Navajo Nation specifically utilizing NASA satellite precipitation observations, it is impactful to validate the efficacy of satellite-based products so that the monitoring of drought and regional hydrology can be as accurate as possible. In the following sections, an annual and seasonal statistical analysis of IMERG V06 Final Run using Parameter-elevation Regressions on Independent Slopes Model (PRISM) as a validation dataset will be conducted for the Navajo Nation and the greater FCR. Since this is a region of complex terrain, an elevational statistical analysis will also be performed at the annual and seasonal timescales to assess performance of the product at low (<1500m), mid-(>1500m and <2500m), and high (2500m) elevations. Verification of monthly and seasonal satellite-based precipitation estimates from IMERG V06 Final Run will be critical in providing a resource water resource management, especially as it relates to regional drought, hydrology, and

agricultural productivity. IMERG V06 Final Run will be interchangeably referred to as simply IMERG throughout this paper.

2.2 Data and Methods

2.2.1 IMERG V06 Final Run

To produce IMERG V06 Final Run observations, precipitation estimates from passive microwave (PMW) sensors in the GPM constellation are computed by the 2017 Goddard Profiling Algorithm (GPROF2017), gridded and intercalibrated to the GPM Ku Radar Radiometer Algorithm (CORRA), and merged into a half-hourly 0.1º x 0.1º field. The PMW estimates are then input into Climate Prediction Center Morphing-Kalman Filter (CMORPH-KF) Lagrangian time interpolation scheme and the Precipitation Estimation from Remotely Sensed Information using Artificial Neural Networks Cloud Classification System (PERSIANN-CCS) re-calibration schemes. The Final Run product uses both forward and backward morphing and includes a monthly gauge analysis adjusted with seasonal Global Precipitation Climatology Project (GPCP) Satellite-Gauge (SG) data. Precipitation phase is determined by humidity, surface temperature, and pressure where a probability of liquid precipitation phase is employed. Details on the handling of precipitation phase can be found in the IMERG Algorithm Theoretical Basis Document [*Huffman et al.*, 2019]. IMERG V06 Final Run data was downloaded from NASA's Giovanni online data portal which is developed and maintained by the NASA Goddard Earth Sciences (GES) Data and Information Services Center (DISC) [*Retrieved from*: https://giovanni.gsfc.nasa.gov/giovanni/; *Acker and Leptoukh*, 2007; *Huffman et al.*, 2019]. Monthly data from 2002 to 2018 were used to produce the IMERG V06 Final Run climatological analysis for this paper.

2.2.2 Parameter-elevation Regressions on Independent Slopes Model (PRISM)

The PRISM Climate Group at Oregon State provides national estimates of precipitation, as well as five other basic climate variables, on a 4km x 4km grid: http://prism.oregonstate.edu/. PRISM combines meteorological surface observations that are used in a regression analysis with a digital elevation model (DEM) in order to produce a model of monthly and annual climate analyses that accounts for orographic influence [*Daly et al.*, 1994]. Over 12,000 surface stations nation-wide sourced from networks such as NWS Cooperative Observer Program (COOP) and the United States Department of Agriculture (USDA) Natural Resource and Conservation Service (NSRC) Snow Telemetry (SNOTEL) and are used in the PRISM precipitation analysis [*Daly et al.*, 2008]. PRISM uses data from station networks and are ingested through a climatologically-aided interpolation (CAI) modeling technique that uses the 30-year long-term average as a first guess. Examples of PRISM's topographic and orographic considerations include the accounting of changes elevation, topographic facet orientation, topographic position, vertical atmospheric layer, and coastal proximity [*Daly et al.*, 2008].

While PRISM's strengths include its high spatial resolution and accounting of orographic influence, the dataset does present some limitations. For example, the paucity, inhomogeneity, and previously discussed deficiencies of surface gauge observations that PRISM uses introduce sources of error. This limitation may especially be exacerbated by the sparse surface observations in the Four Corners Region compared to other areas in the United States. The sparse distribution of observations means that PRISM is left to interpolate precipitation estimates over large areas. Despite these limitations, PRISM is a well-established dataset and is used in products such as the U.S. Drought Monitor (USDM). Furthermore, the dataset has been used to validate

satellite precipitation measurements before in studies of satellite performance in the United States [*Nesbitt and Anders,* 2009; *Hashemi et al.*, 2017]. In this paper, PRISM is believed to be the best dataset available for comparison of satellite-derived precipitation estiamtes and will serve as the objective dataset in which to validate IMERG V06 Final Run's patterns of precipitation. Monthly PRISM data from 2001 to 2018 were used to produce a climatological analysis to compare with the IMERG V06 Final Run product. While the IMERG V06 Final Run climatological precipitation considers the years 2002 to 2018 in this paper, it is believed that the data spans a long enough timeframe in which the discrepancies should be insignificant.

2.2.3 Methods

In order to quantify how IMERG V06 Final Run compares to PRISM in the FCR and on the Navajo Nation on monthly and seasonal time scales through the calculation of statistics to determine the strength of correlation (Pearson correlation coefficient and linear regression), mean bias error (MBE) calculated as 100 − (average PRISM/average IMERG) x 100%, and mean absolute error (MAE), which is simply the absolute difference between the PRISM and IMERG datasets. Seasonal maps are generated to visualize the geospatial patterns of precipitation, difference, and absolute error between the datasets. This is an important contribution as it reveals locations where the satellite either under or overestimates precipitation and identifies areas where large differences occur between IMERG and PRISM. Additionally, since the FCR is characterized by complex terrain, the same statistical evaluations of IMERG at different elevation regimes is performed. Topographic data from the United States Geological Survey (USGS) were resampled to 0.1º x 0.1º spatial resolution to show the average elevation for each grid cell [*United States Geological Survey*, 2014]. The statistical analysis is generated to

compare IMERG and PRISM climatological precipitation for low elevation (<1500m) grid cells (count = 480), mid-elevation (>1500m and <2500m) grid cells (count = 2814), and high elevation (>2500m) grid cells (count = 556) grid cells in the region (Figure 2.3) at monthly and seasonal temporal scales. In order to conduct the elevation performance analysis, the PRISM dataset was resampled to match the 0.1º x 0.1º spatial resolution of the IMERG dataset.

2.3 Results

2.3.1 Monthly and Seasonal Analysis

In the regional statistical analysis for all months and all elevations in Table 1.1, the months with the strongest Pearson correlation coefficients between IMERG and PRISM are June (R=0.856), May (R=0.817), and July (R=0.814) while the weakest are exhibited in January (R=0.617), March (R=0.646), and December (R=0.669). In the linear regression analysis from the scatter plots (Figure 2.4.a and Figure 2.4.e), the strongest coefficient of determination, R^2, are found in June (R^2=0.732), May (R^2=0.668), and July (R^2=0.663) where the weakest R^2 are found in January (R^2=0.381), March (R^2=0.418), and February and December that both share an R^2 value of 0.415. In the FCR, IMERG exhibits a higher mean monthly precipitation compared to PRISM in January, March, June, July, August, September, and October, and a lower mean monthly precipitation in February, April, May, November, and December. The MBE shows that the IMERG product produces the largest overestimates in January (19.602%) and June (18.822%) with the smallest overestimates produced in August (2.304%). IMERG produces the largest underestimation in December (-10.528%) and a small underestimation in February (-2.088%). January has the largest MAE (15.56mm) while the lowest MAEs occur during May (4.103mm).

In the monthly boxplot analysis for all elevations (Figure 2.5), the median, exhibited by solid line in middle of each box is consistently higher in IMERG than PRISM for all months except May. The IMERG dataset is skewed to lower precipitation values in many months, especially in December, January, February, April, May, and June. Generally speaking, the PRISM datasets exhibit more variability in the dataset than IMERG for most months, indicated by the larger spread in the IQR box. There is larger variability in both datasets July and August during monsoon season, suggesting a large spread in precipitation amounts. These months coincide with the North American Monsoon, which brings moisture to the Four Corners Region and generates convective storms where enhanced precipitation amounts can vary locally based on topography [*Hereford and Webb*, 1992; *Dunn and Horel*, 1994; *Adams and Comrie*, 1997; *Higgins et al.*, 1997; *Higgins et al.*, 1998; *Lo and Clark*, 2002; *Higgins et al.*, 2004; *Carrillo et al.*, 2016]. The variation in both datasets is smaller during drier months like May and June, where precipitation is minimal. The boxplots also reveal that PRISM has more outliers compared to IMERG in all months. The IMERG dataset exhibits no outliers in the cooler months of December, January, and February.

In the seasonal statistical analysis for all elevations (Table 2.2), the mean seasonal precipitation is larger in the IMERG dataset for all seasons except MAM, where IMERG exhibits a mean seasonal precipitation of 0.362mm less than PRISM. In the MBE analysis, IMERG overestimates the most in JJA by 4.393% followed by DJF (2.171%) and SON (1.688%). IMERG produces an underestimation in MAM by -1.879%. The largest mean average errors are found in DJF where the MAE is 9.452mm. JJA and SON exhibit similar MAE with 6.6mm and 6.643mm respectively. The smallest MAE is exhibited in MAM with 4.694mm.

The authors have chosen to qualitatively assess the seasonal spatial performance of the satellite dataset by showing the spatial patterns of precipitation of the IMERG V06 Final run and PRISM products, the spatial differences between PRISM and IMERG, and the scatter plot linear regression analysis in Figure 2.6.a-d. Paying attention to the Navajo Nation, IMERG (Figure 2.6.a) qualitatively produces higher precipitation across the reservation compared to PRISM (Figure 2.6.b), which shows lower precipitation amounts except in areas of complex terrain with higher elevation in the Chuska Mountains where it shows higher amounts. For the FCR, PRISM shows more precipitation variability than IMERG, which is likely attributed to the finer resolution and orographic considerations. PRISM also shows higher amounts in areas of higher elevation especially in San Juan Mountains to the northeast portion of the FCR and higher amounts along Mogollon Rim to the south of the Navajo reservation in all seasons. In particular during MAM, little precipitation is picked up along the Mogollon Rim in comparison to PRISM. These precipitation patterns are not as evident in the IMERG maps likely related to the coarse resolution of the dataset.

In the seasonal difference maps (Figure 2.6.c), each grid cell difference is calculated by taking the PRISM precipitation average and subtracting the IMERG precipitation average. If the difference is positive (negative), indicated by red (blue), this means that the PRISM precipitation average is greater than (less than) the IMERG precipitation average in that grid cell. This effectively shows the magnitude of the over (blue) or under (red) estimations occur. Large positive differences between PRISM and IMERG are evident in complex terrain especially in DJF, MAM, and SON, indicating that IMERG underestimates in these areas. For most of Navajo Nation, IMERG overestimates (blue) except in the Chuska Mountains, where the product underestimates (red). Generally speaking, the overestimations over the reservation and

throughout the FCR in blue are moderate especially in MAM, indicated by the lighter blue colors. Larger overestimations over the Navajo Nation are evident in DJF and JJA shows larger overestimations especially along the Mogollon Rim to the south of the reservation. The dark red grid cells during DJF, MAM, and SON, especially in the regions of high elevation terrain reveal that large magnitude of underestimations exhibited by IMERG. In the linear regression analysis from the scatter plots (Figure 2.6.d), the strongest coefficient of determination, R^2, is in JJA (R^2=0.665) and the weakest in DJF (R^2=0.436). IMERG has the strongest Pearson correlation coefficient with SON (R=0.903) and the weakest with DJF (R=0.66) (Table 2.2).

Figure 2.7 shows maps of the spatial distribution of the mean absolute difference between the two products. These maps are intended to qualitatively represent where IMERG precipitation observations can effectively be trusted based on the magnitude of error. In these map, the implementation of a red yellow green color scheme reveal where errors are smallest (green) suggesting that the precipitation observations can be trusted, where errors are moderate (yellow) suggesting that it may be appropriate to exercise caution when using the satellite product in these areas, and where errors are large (red) to show where the errors maybe too significant to use the product accurately. A threshold of 15mm was chosen because in a region where precipitation is low, 15mm of error in the satellite observations could lead to large over- or underestimations for water resource evaluation or drought monitoring. Focusing on the FCR, there are large errors greater than or equal to 15mm especially in areas of high complex terrain (i.e. San Juan Mountains). These errors are evident particularly in DJF, MAM, and SON. These errors are also apparent in JJA, however they are not as widespread as the rest of the seasons. In DJF and JJA there is an interesting cluster of errors along the Mogollon Rim to the south of the reservation. In this location, large errors greater than or equal to 15mm are present, however these errors do not

seem to be as apparent during MAM and SON seasons. Focusing within the boundaries of the Navajo reservation, these maps reveal that in all seasons, large errors are exhibited in the Chuska Mountains. For the rest of the reservation, in DJF, there are moderate to large errors in several broad areas including the central portion of the reservation, to the east and north of the Chuskas, as well as along the southern and southwestern boundary near the Mogollon Rim. In JJA and SON moderate to large errors also occur in these same areas. Generally speaking, in MAM, JJA and SON, there are more green pixels within the Navajo reservation boundaries, indicating that errors are relatively small. There are also several areas of green located within the reservation boundaries in DJF, however they are not as widespread as the other seasons. These maps indicate that for most of the year and in many areas within the Navajo reservation boundaries, there are either low to moderate errors in the satellite product. This suggests that the satellite can provide valuable and reliable information about the precipitation input for water resource management and drought monitoring, especially if users of the IMERG V06 Final Run product consider the limitations in specific locations.

In the seasonal boxplots (Figure 2.8), the median in the IMERG datasets is greater than the PRISM dataset for all seasons. The IMERG dataset is skewed to lower precipitation amounts in DJF and MAM, and SON while the dataset is skewed to higher precipitation amounts in JJA. IMERG produces less variability in for all seasons compared to PRISM and there is more spread in both datasets during DJF and JJA when there is more precipitation due to the regional bimodal precipitation regime compared to MAM and SON which are drier. IMERG has fewer outliers than PRISM for each season and exhibits no outliers in DJF while it exhibits the most in SON.

2.3.2 Low Elevation (<1500m)

In the monthly statistical analysis for low elevations (<1500m) (Table 2.3), Pearson correlation coefficients are strongest in June (R=0.891), July (R=0.88), and August (R=0.871) and are the weakest in April (R=0.555), October (R=0.663), and November (0.664). The strongest coefficient of determination from the linear regression analysis in the scatter plots (Figure 2.4.b and 2.4.f) is found in June (R^2=0.794), July (R^2=0.774), and August (R^2=0.759) and the weakest in April (R^2=0.308), October (R^2=0.439), and November (R^2=0.441). IMERG mean monthly precipitation is greater than PRISM mean monthly precipitation in all months. This is quantified by the MBE analysis showing overestimates in all months where the largest MBEs are found in June (29.367%), January (29.111%), and April (16.682%) and smallest MBEs in December (4.322%), February (4.769%), and July (12.725%). Mean absolute errors are considered to be small to moderate, where the largest MAEs are exhibited in January (9.585mm), August (8.529mm), and July (8.192mm) and the smallest are found in June (2.295mm), May (2.735mm), and April (3.287mm).

In the monthly boxplot analysis for low elevations (<150mm) (Figure 2.5), the median is higher in the IMERG data set compared to the PRISM data set for all months at low elevations, especially during the months of July, August, and January. This suggests that IMERG is skewed towards larger precipitation amounts during these months. There is large spread exhibited in the datasets during the start and midpoint of the monsoon season (July and August) the winter months as well of December, January, and February. There are fewer outliers in both data sets throughout all months at low elevations compared to all month at all elevations.

The seasonal statistical analysis shows that at low elevations (<1500m) (Table 2.4), IMERG has the strongest Pearson correlation coefficient with PRISM in JJA (R=0.881) and DJF (R=0.841) while SON displays the weakest correlations (R=0.652). Figure 2.9.a shows the

seasonal scatterplots and the regression analysis for low elevations and reveals that JJA and DJF have similar strong determinants of correlation (R^2=0.776 and R^2=0.708, respectively). Weaker R^2 values were exhibited in MAM (R^2=0.28) and SON (R^2=0.425). IMERG overestimated in all months at low elevations (<1500m) between 13-15%. The largest MAE was found in DJF (6.507mm) and the smallest MAE was found in MAM (3.432mm).

In the seasonal boxplot analysis for low elevations (<1500m) (Figure 2.8), the median is higher in IMERG for all seasons. In MAM and SON, the medians are skewed towards lower precipitation amounts in the IMERG dataset. There is similar considerable variability in the IQR in the datasets in JJA and DJF. There is smaller spread in IQR in the IMERG dataset compared to PRISM in MAM and SON. There are fewer outliers for both datasets. Outliers are exhibited in both datasets in MAM and SON.

2.3.3 Mid-Elevation (>1500m and <2500m)

In the monthly statistical analysis for mid-elevation (>1500m and <2500m) Table 2.5, Pearson correlation coefficients are strongest in July (R=0.844), August (R=0.837), and June (R=0.823) and weakest in March (R=0.596), November (R=0.618), and January (R=0.644). In the scatter plots and regression analysis (Figure 2.4.c and 2.4.g), the strongest determinant of correlation values are found in July (R^2=0.712), August (R^2=0.701), and June (R^2=0.677) and the weakest are found in March (R^2=0.355), November (R^2=0.382), and January (R^2=0.415). IMERG exhibits a higher mean in all months but December, and MBEs show that at mid-elevation, IMERG produces overestimates in all months but December. The largest overestimations are found in January (27.82%), June (20.322%), and March (12.525%) and a very small underestimate in December of -0.229%. Mean absolute errors are considered

moderate in all months at mid-elevations, where the largest MAEs occur in January (9.413mm), July (8.983mm), and August (8.42mm) and the smallest MAEs occur in May (2.953mm), April (4.327mm), and November (4.55mm).

In the monthly boxplot analysis at mid-elevations (Figure 2.5), there is not as much spread in IQR in cold wetter months (December, January, and February) compared to low elevations (<1500m). Increased variability is still found in July and August. IMERG exhibits less variability compared to the PRISM data set for most months especially in the drier months. Both data sets are in good agreement for most months except for January and February and even into March where the data sets are quite different. The median is higher in IMERG in all months except May, where they are similar. The median in many months, especially the drier months of April, May, and June shows that the IMERG data is skewed toward lower precipitation amounts. There are outliers present in all months except October in the IMERG dataset at mid-elevation.

In the seasonal analysis at mid-elevations (>1500m and <2500m) Table 2.6, the Pearson correlation coefficient is strongest for JJA (R=0.837) and weakest for SON (R=0.647). In the regression analysis in the scatterplots (Figure 2.9.b) the determinant of correlation is strongest in JJA (R^2=0.7) and weakest in SON (R^2=0.418). It is important to note that JJA performs the strongest in both correlation coefficients compared to the other three seasons that perform roughly the same. IMERG's mean precipitation is greater than the PRISM data set and the IMERG dataset overestimates for all seasons. The largest MBE is in DJF with 12.337% overestimation and the smallest overestimation is in JJA at 7.371%. The MAEs are small to moderate, where largest MAE is in DJF (7.443mm) and the smallest is in MAM (4.232mm).

In the seasonal boxplot analysis at mid-elevations (>1500m and <2500m) (Figure 2.8), the median is higher in the IMERG dataset compared to the PRISM dataset in all seasons. The

IMERG median indicates that the data is skewed to smaller precipitation amounts in DJF, MAM, and SON. There is more variability in wetter seasons such as DJF and JJA exhibited by wider IQRs in both datasets. Additionally, there are fewer outliers in each season in the IMERG dataset compared to the PRISM dataset.

2.3.4 High Elevation (>2500m)

At high elevations (>2500m), the monthly statistical analysis (Table 2.7) reveals that the strongest Pearson correlation coefficients are in August (R=0.746), July (R=0.693), and October (R=0.64) and the weakest in March (R=0.291), April (R=0.402), and December (R=0.46). In the scatter plots and regression analysis (Figure 2.4.d and Figure 2.4.h), the strongest determinants of correlation are found in August (R^2=0.556), July (R^2=0.48), and October (R^2=0.409) and the weakest in March (R^2=0.085), April (R^2=0.161), and December (R^2=0.212). IMERG mean precipitation is substantially smaller than PRISM for all months except June where IMERG mean precipitation is slightly greater. The MBEs reveal that IMERG produces significant underestimations for all months except June where the IMERG product overestimates by 10.398%. The largest underestimations are produced in December (-61.672%), February (-54.636%), and April (-53.468%). Large MAEs are exhibited in December (28.034mm), March (24.461mm), and February (23.101mm), with the smallest MAEs exhibited in June (3.347mm), followed by May (11.103mm) and August (12.591mm).

In the monthly boxplots analysis for high elevations (>2500m) (Figure 2.5), the IMERG IQR is smaller for all months compared to PRISM. The PRISM IQR is wider in winter and early spring, but not as wide during summer monsoon compared to other elevations. The IMERG dataset exhibits outliers in March, May, June, July, and August. In contrast to low and mid

elevations, IMERG exhibits substantially lower medians in all months except June, where IMERG exhibits a higher median. In contrast to low and mid-elevations, the median in the IMERG boxplots reveal a skew to higher precipitation amounts.

In the seasonal statistical analysis for high elevations (>2500m) (Table 2.8), the strongest Pearson correlation coefficient is in JJA (R=0.679) and the weakest is in MAM (R=0.395). The strongest determinant of correlation in the regression analysis in the scatter plots is in JJA (R^2=0.461) and the weakest is in MAM (R^2=0.156) (Figure 2.9.c). The mean precipitation in the IMERG dataset is substantially lower than the PRISM dataset and IMERG underestimates significantly at high elevations in the region. Large MBEs are found in all seasons, with the largest exhibited In DJF (-46.05%) and the smallest exhibited in JJA (-15.752%). Large MAEs are also found in most seasons, with the largest being in DJF (22.165mm), and the smallest MAE in JJA (8.985mm).

In the seasonal boxplot analysis for high elevations (>2500m) (Figure 2.8), the IMERG IQR is smaller for all seasons compared to PRISM, signaling less variability in the dataset. IMERG exhibits a wider IQR in DJF but shows a smaller IQR during JJA compared to other elevations. The IMERG dataset exhibits outliers only in JJA. The IMERG median is lower than PRISM for all seasons and indicates that the dataset is skewed towards higher precipitation amounts.

2.4 Discussion and Conclusion

This body of research seeks to quantify the performance of the newest satellite product from NASA, IMERG V06, in hopes of to provide insight on a new NASA precipitation observation resource. This study sheds light on IMERG V06 Final Run's performance at the monthly and seasonal timescales for all elevations, as well as an elevation analysis for low, mid-,

and high elevations. In the monthly analysis for all elevations, the strongest Pearson and determinants of correlation are in warm dry months of the May, June, and at the onset of the monsoon season in July. January, March, December, and February exhibit the weakest correlations. During these months, there is typically an abundance of frozen precipitation events. During March, the wintertime storm track begins to shift northward out of the region, and as warmer temperatures return, precipitation phase may be variable and light. There is no clear trend on whether the IMERG product over- or underestimates at the monthly time scale. However, it appears that IMERG typically overestimates during the warm monsoon season for all elevations. Mean average errors are modest except for January where the IMERG product exhibits a large MAE (>15mm). IMERG has the strongest correlations with the warm, dry months of May and June. Considering the performance of the IMERG V06 product's performance in the bimodal precipitation regime in the FCR, the relatively strong correlations in July and August, which coincide with the bulk of the monsoon season, suggests that the product performs quite well for liquid precipitation that falls in warm temperatures. In contrast, the wintertime precipitation during the cold months of December, January, February, and March, where frozen precipitation is common, IMERG does not perform as well. During these months, correlations are low compared to the rest of the year, and December and January exhibit large MAEs. This suggests that the IMERG product does not perform as well during cold winter months and may be related to the handling of precipitation phase in the IMERG algorithm. These results are not necessarily surprising given the handling of the precipitation phase in the algorithm. The passive microwave sensors do not directly measure whether the precipitation phase is liquid, mixed, or frozen, so estimates are derived using probabilities and other data [*Huffman et al.*, 2019]. Similar results have been found in an analysis of previous IMERG

products [*Chen and Li*, 2016; *Guo et al.*, 2016; *Behrangi et al*., 2018; *Navarro et al.*, 2019; *Sharifi et al.*, 2019]. These results suggest that the satellite product could be used in the monsoon season where the region experiences the highest amounts of rainfall. However, the satellite product may be limited in making any informed water resource management decisions during the winter months due to the decrease strength in correlations and larger over- or underestimates during these months. This limitation has important implications for water resource monitoring because winter precipitation drives snowpack conditions which are a crucial source of surface runoff, groundwater recharge, streamflow, and water supply [*Barnett et al.*, 2005; *Mote et al.*, 2005; *Hunter et al.*, 2006; *Li et al.*, 2017]. Furthermore, the spread between IMERG and PRISM with increasing precipitation amounts in all of the scatterplots for all months and seasons at all elevations indicate that there may be considerable discrepancies between datasets (Figure 2.4a-h, Figure 2.6a-d, Figure 2.9a-c). It is particularly evident in cooler months and seasons and in higher elevations. This could be attributed to issues related to PRISM's accounting of orographic influence as well as the IMERG algorithm handling of precipitation phase.

The seasonal analysis at all elevations shows that for all seasons there are stronger Pearson correlation coefficients but weaker determinants of correlation in the regression analysis compared to the monthly analysis. The MBE analysis reveals that IMERG overestimates for all seasons except MAM, where it underestimates. The moderate MAEs are also similar to the monthly analysis. Additionally, the difference maps in (Figure 2.6.c) show that for most of the Navajo Nation, IMERG performs reasonably well. The difference maps reveal that within the boundaries of the Navajo Nation, IMERG produces moderate overestimates for most areas in all seasons. Underestimations are primarily found in regions of high-elevation complex terrain. In the mean absolute error maps (Figure 2.7), DJF produces the most widespread moderate to large

differences in mean absolute errors. However, the absolute error maps reveal that in MAM, JJA, and SON, the product produces small to moderate errors for most areas that are not located in complex, high-elevation terrain, suggesting that IMERG can be used with high to moderate confidence throughout most of the year, except in DJF. These results suggest that at all elevations, the product produces superior performance in certain months compared to others. The analysis does not suggest that at all elevations, the seasonal timescale performs better or worse than the monthly timescale.

Since this is a region of complex terrain, it is critically important to highlight the strengths and limitations of the satellite product at low mid and high elevations. In the monthly analysis at low elevations (<1500m), the strongest correlated month between IMERG and the PRISM dataset is in June which is typically dry followed by July and August which is during the monsoon season. At low elevations the weakest correlations occur during April, October and November, which are months that are typically drier. Mean absolute errors are relatively modest in all months compared to mid- and high elevations. However, at low elevations IMERG produces overestimates for all months, where January and June exhibit large overestimations of almost 30%. The overestimations in January may be related to frozen precipitation. Although the driest month of the year, the overestimates in June may be a result of satellite detected droplets closer to the cloud base that ultimately evaporate before reaching the surface in the atmospheric column as they fall. Seasonally the strongest correlations are found in JJA and DJF, which are the seasons that experience the most precipitation. Very weak correlations especially found in the spring, when precipitation is low, are exhibited. Spring and fall correlations maybe weak as the wintertime storm track moves northward during the spring and the monsoon season ends during the fall. Precipitation during MAM and SON maybe light compared to other seasons.

Furthermore, as temperatures warm in the spring, evaporation of droplets from the cloud base may occur, resulting in weaker correlations between IMERG and PRISM. This also may occur at the end of summer and beginning of fall where temperatures may remain quite warm especially at lower elevations. Seasonally, overestimates and mean absolute errors are modest in all seasons at low elevations. These results suggest that at low elevations, the IMERG product performs quite well. There are moderate overestimations for all months and seasons at low elevations. The monthly timescale may offer better performance than the seasonal timescale, especially during the spring months (MAM).

In the monthly analysis at mid-elevation (>1500m and <2500m) the strongest correlations occurred during July and August which are during monsoon season. June which is dry is also highly correlated however July and August more strongly correlated. The weakest correlations are found in March and November which are typically dry however January also exhibits a relatively weak correlation. Again, this is a month in which there is substantial frozen precipitation. This suggests that mid elevation IMERG is able to pick up rainfall estimates quite well. Overestimates at mid-elevation are exhibited for all months but December, which has a very small underestimate. The largest overestimation is found in January where again this may be an issue related to the IMERG product handling of the precipitation phase. There is also substantial overestimate in June, which again may be related to evaporative loss. Absolute errors remain relatively modest and do not exhibit a significant difference compared to low elevations. Seasonally, the strongest correlations occurred during JJA and the weakest occurred during SON. The IMERG product again overestimates for all seasons, however, it is important to note that although DJ F exhibits the largest ever estimate in all of the seasons, all seasons experience a decrease in overestimation compared to lower elevations. The results suggest that the IMERG

product performs better at mid-elevations than at low elevations. These findings at mid elevation are important because most of this study region located in mid-elevation range. These results show that during the monsoon season, the IMERG product performs reasonably well at mid-elevation and could be used for water resource decisions and drought impacts for most of the FCR. These results also show the decreased performance in cooler months and seasons where frozen precipitation is abundant.

The monthly and seasonal analysis at high elevations (>2500m) show that IMERG performance decreases with increasing elevation and is the most significant limitation of the IMERG product in the region. The IMERG product exhibits a significant degradation in performance at elevation >2500m compared to low and mid-elevations throughout the FCR. Although August exhibits a relatively strong Pearson correlation coefficient, the regression analysis reveals that only moderate correlations are found for August July and October. More importantly, significantly weak correlations (R^2<0.25) are found in several months including March April and December. The IMERG product exhibits gross underestimations in all month except for the month of June where it overestimates by ~10%. Underestimations exceeding 50% are found in December, February, and April. In the high elevation statistical analysis, the mean absolute errors also increase substantially compared to low and mid-elevations. In the seasonal statistical analysis, JJA exhibit the strongest Pearson correlation coefficient, but the correlations are moderate at best. In the regression analysis JJA is the strongest of the seasons however the correlation relative to other elevations is not as strong. Additionally, MAM exhibits a weak correlation of only 0.156. The IMERG product exhibits underestimations for all seasons with the largest being roughly 46% in DJF. Mean absolute error also increases at high elevations compared to low and mid- elevations for all months and seasons. These results reveal the

significant limitation of the IMERG product in high elevation regions. The large and significant overestimation and absolute errors combined with weak correlations to the PRISM dataset suggest that the IMERG product would require significant improvement at higher elevations for the product to be used for accurate precipitation observations. These results are consistent in the literature where various satellite product measurements have been found to perform poorly at high elevations [*Chen and Li,* 2016; *Behrangi et al.*, 2018; *Navarro et al.,* 2019; *Sharifi et al.*, 2019]. However, the IMERG product in this region exhibit underestimations that are substantially larger compared to the results found in other research. These results are likely due to the fact that a higher elevations orographic effects can largely influence precipitation rates on a small spatial scale. Although the satellite has a relatively high resolution, the orographic effects that may influence precipitation rates maybe on such a small scale that cannot be detected by the satellite. The poor performance of the product at high elevations in this region suggest that this product cannot be used for any water resource management decisions in high elevation regions. This may have significant consequences, especially for the winter precipitation, where snowpack amounts are critical for annual water resources.

Although this research does not use the near real-time products from IMERG, it does use the gauge calibrated products that are available 3.5 months after observation that are considered to be more accurate than the real time product. The results in this paper primarily focused on errors that could arise from IMERG, but it is important to note that some of the errors may also be attributed to the PRISM dataset, which was used under the assumption that it is the best product for comparison. However, the PRISM dataset could introduce potential sources of error since it interpolates precipitation from a sparse network of station gauges. In summary, from these results, it appears that the IMERG V06 Final Run product can be used for short term water

resource decisions in warmer and wetter months at low and mid-elevations (i.e. during the North American Monsoon season) while caution should be exercised during cool months and in areas where the elevation exceeds 2500m. Generally, the product overestimates throughout the region and on the Navajo reservation with large underestimates in high-elevation regions. Over or under-estimates may vary significantly depending on location or season. In some scenarios, the monthly time scale, the IMERG V06 Final Run product may be considered more reliable than at the seasonal time scale. Overall, the IMERG V06 Final Run product performs reasonably well throughout the FCR and on the Navajo reservation and could be used in efforts to understand water resource management and to monitor drought.

Table 2.1. Statistical analysis for all months and all elevations.

	January	**February**	**March**	**April**	**May**	**June**
Mean IMERG (mm)	28.514	26.753	22.053	19.47	16.332	11.317
Mean PRISM (mm)	22.925	27.311	21.474	20.48	16.988	9.187
MAE (mm)	15.56	9.164	7.918	6.434	4.103	2.741
MBE (%)	19.602	-2.088	2.626	-5.186	-4.019	18.822
R	0.617	0.67	0.646	0.743	0.817	0.856
R^2	0.381	0.448	0.418	0.553	0.668	0.732
	July	**August**	**September**	**October**	**November**	**December**
Mean IMERG (mm)	47.651	49.553	39.207	31.193	19.642	30.169
Mean PRISM (mm)	46.156	48.411	37.834	30.183	20.505	33.345
MAE (mm)	9.595	9.036	7.715	6.923	6.389	10.427
MBE (%)	3.138	2.304	3.501	3.238	-4.393	-10.528
R	0.814	0.811	0.712	0.75	0.691	0.669
R^2	0.663	0.658	0.507	0.562	0.478	0.448

Table 2.2. Statistical analysis for all seasons and all elevations.

	DJF	MAM	JJA	SON
Mean IMERG (mm)	28.478	19.285	36.174	30.014
Mean PRISM (mm)	27.86	19.647	34.585	29.507
MAE (mm)	9.452	4.694	6.6	6.643
MBE (%)	2.171	-1.879	4.393	1.688
R	0.66	0.778	0.815	0.903
R^2	0.436	0.541	0.665	0.511

Table 2.3. Statistical analysis for all months at low elevations (<1500m).

	January	**February**	**March**	**April**	**May**	**June**
Mean IMERG (mm)	31.175	28.246	20.656	13.434	10.823	7.019
Mean PRISM (mm)	22.1	26.899	17.753	11.193	9.225	4.957
MAE (mm)	9.585	5.933	7.993	3.287	2.735	2.295
MBE (%)	29.111	4.769	14.055	16.682	14.764	29.367
R	0.833	0.832	0.807	0.555	0.768	0.891
R^2	0.695	0.692	0.651	0.308	0.589	0.794
	July	**August**	**September**	**October**	**November**	**December**
Mean IMERG (mm)	41.276	46.662	31.037	27.36	18.448	31.01
Mean PRISM (mm)	36.024	40.577	26.989	23.723	15.744	29.67
MAE (mm)	8.192	8.529	5.556	4.788	4.375	6.771
MBE (%)	12.725	13.04	13.044	13.291	14.654	4.322
R	0.88	0.871	0.752	0.663	0.664	0.83
R^2	0.774	0.759	0.565	0.439	0.441	0.69

Table 2.4. Statistical analysis for all seasons at low elevations (<1500m).

	DJF	MAM	JJA	SON
Mean IMERG (mm)	30.144	14.971	31.652	25.615
Mean PRISM (mm)	26.223	12.724	27.186	22.152
MAE (mm)	6.507	3.432	5.95	4.57
MBE (%)	13.007	15.011	14.109	13.518
R	0.841	0.529	0.881	0.652
R^2	0.708	0.28	0.776	0.425

Table 2.5. Statistical analysis for all months at mid-elevations (>1500m and <2500m).

	January	**February**	**March**	**April**	**May**	**June**
Mean IMERG (mm)	26.961	25.297	20.39	18.233	15.405	10.856
Mean PRISM (mm)	19.461	22.747	17.836	16.727	14.733	8.65
MAE (mm)	9.413	6.962	6.349	4.327	2.953	2.697
MBE (%)	27.82	10.081	12.525	8.257	4.36	20.322
R	0.644	0.713	0.596	0.707	0.793	0.823
R^2	0.415	0.508	0.355	0.5	0.629	0.677
	July	**August**	**September**	**October**	**November**	**December**
Mean IMERG (mm)	48.072	49.507	39.276	30.619	18.326	28.676
Mean PRISM (mm)	44.834	46.959	36.119	27.928	17.321	28.741
MAE (mm)	8.983	8.42	6.75	5.885	4.55	7.572
MBE (%)	6.736	5.147	8.039	8.788	5.488	-0.229
R	0.844	0.837	0.723	0.721	0.618	0.688
R^2	0.712	0.701	0.522	0.519	0.382	0.475

Table 2.6. Statistical analysis for all seasons at mid-elevations (>1500m and <2500m).

	DJF	MAM	JJA	SON
Mean IMERG (mm)	26.978	18.009	36.145	29.407
Mean PRISM (mm)	23.65	16.432	33.481	27.123
MAE (mm)	7.443	4.232	6.239	5.34
MBE (%)	12.337	8.756	7.371	7.769
R	0.695	0.666	0.837	0.647
R^2	0.482	0.444	0.7	0.418

Table 2.7. Statistical analysis for all months at high elevations (>2500m).

	January	**February**	**March**	**April**	**May**	**June**
Mean IMERG (mm)	34.075	32.83	31.677	30.945	25.777	17.364
Mean PRISM (mm)	41.168	50.767	43.098	47.49	35.101	15.558
MAE (mm)	16.998	23.101	24.461	19.814	11.103	3.347
MBE (%)	-20.816	-54.636	-36.057	-53.468	-36.171	10.398
R	0.48	0.464	0.291	0.402	0.57	0.501
R^2	0.23	0.215	0.085	0.161	0.325	0.251
	July	**August**	**September**	**October**	**November**	**December**
Mean IMERG (mm)	51.025	52.282	45.909	37.407	27.332	36.998
Mean PRISM (mm)	61.594	62.527	55.879	47.17	40.73	59.815
MAE (mm)	13.908	12.591	14.466	14.02	17.431	28.034
MBE (%)	-20.712	-19.596	-21.717	-26.1	-49.019	-61.672
R	0.693	0.746	0.61	0.64	0.506	0.46
R^2	0.48	0.556	0.372	0.409	0.256	0.212

Table 2.8. Statistical analysis for all seasons at high elevations (>2500m).

	DJF	MAM	JJA	SON
Mean IMERG (mm)	34.634	29.466	40.224	36.883
Mean PRISM (mm)	50.583	41.896	46.56	47.927
MAE (mm)	22.165	16.214	8.985	15.026
MBE (%)	-46.05	-42.185	-15.752	-29.943
R	0.473	0.395	0.679	0.591
R^2	0.224	0.156	0.461	0.35

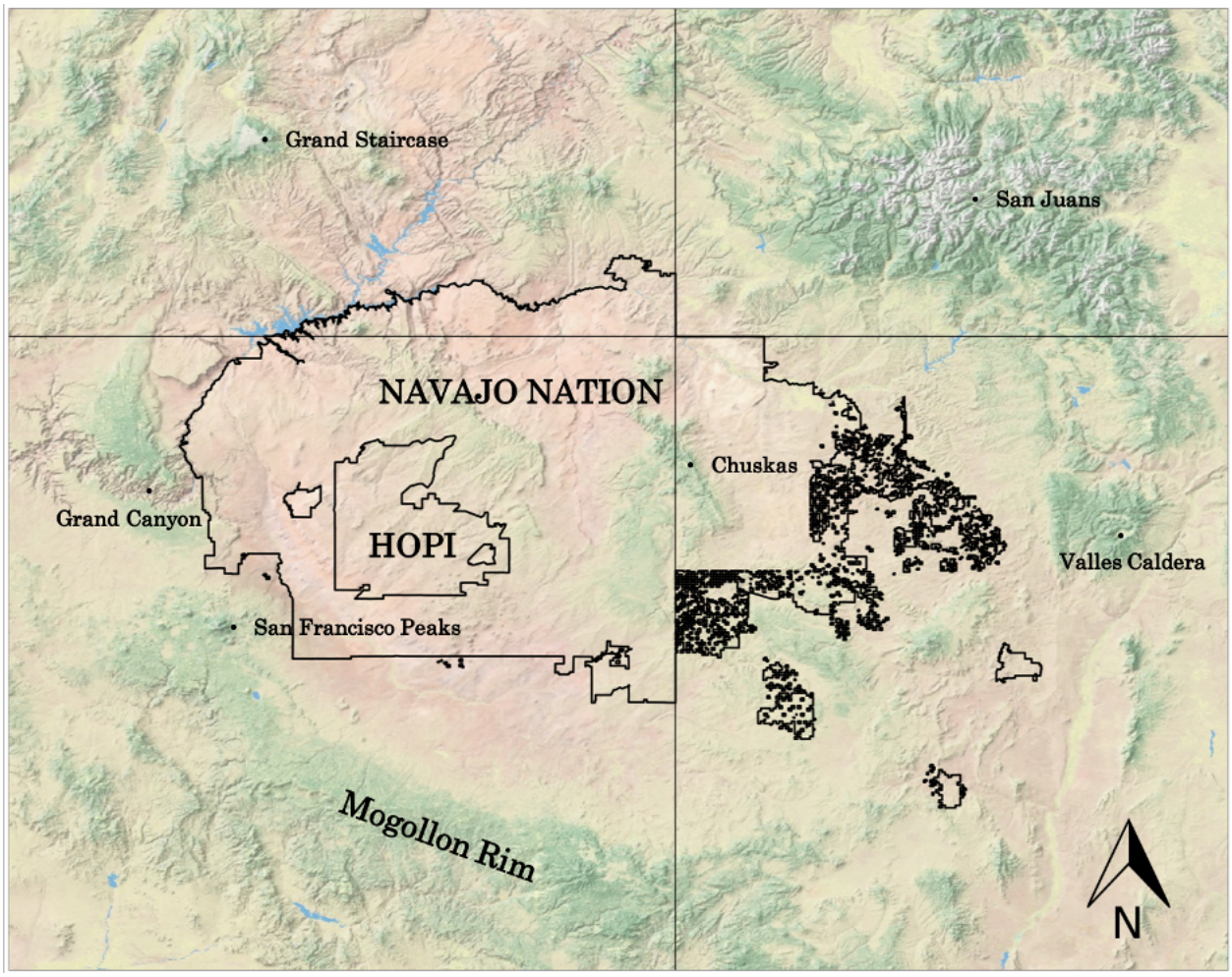

Figure 2.1. A physical map of the FCR that shows the defining geographic features in the study area. The Navajo Nation is outlined and shows the Hopi reservation, which is nestled in the southwestern sector of the Navajo Nation.

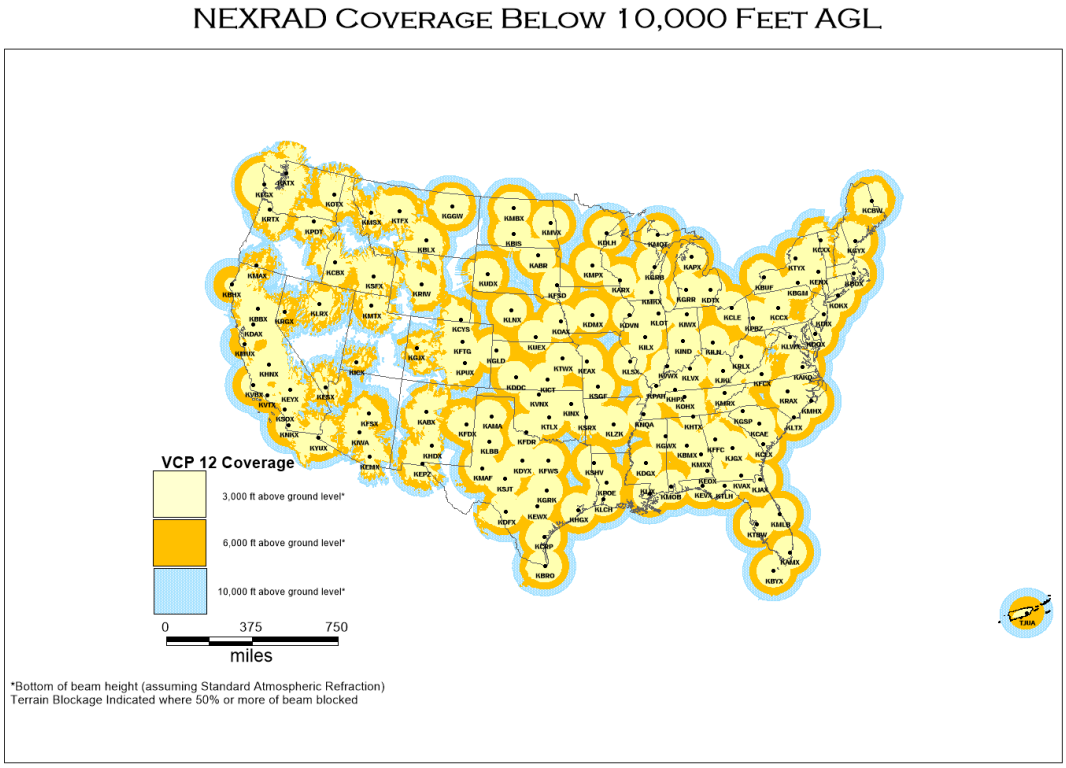

Figure 2.2. A map of the National Weather Service's WSR-88D NEXRAD radar coverage over the contiguous United States. Image reproduced from https://www.roc.noaa.gov/WSR88D/Maps.aspx with permission granted by the National Weather Service disclaimer: https://www.weather.gov/disclaimer.

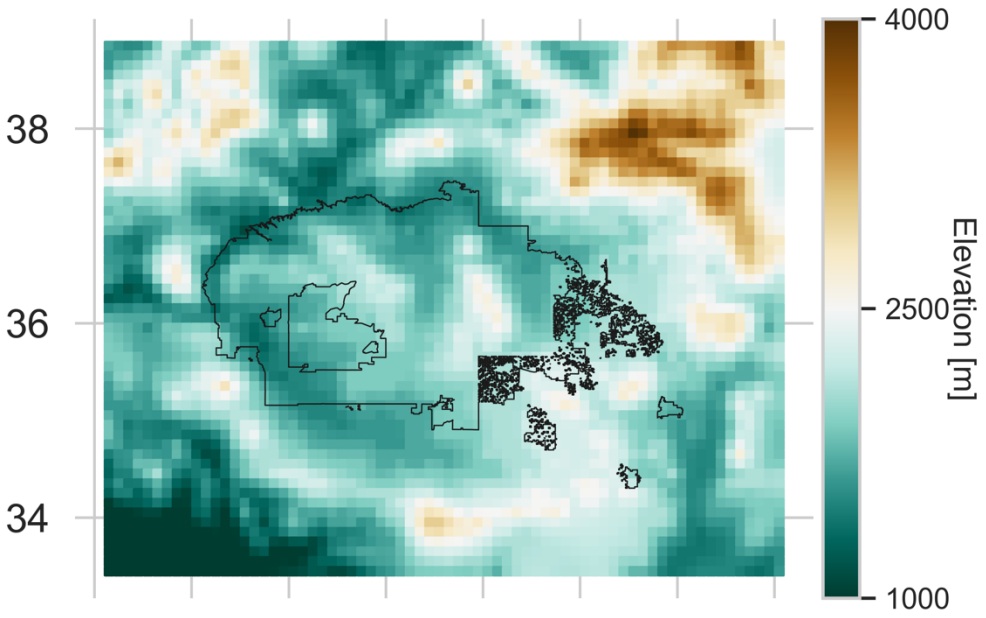

Figure 2.3. Average elevation in meters derived from USGS topographic data [*United States Geological Survey*, 2014] for each 0.1º x 0.1 grid cell in the study region.

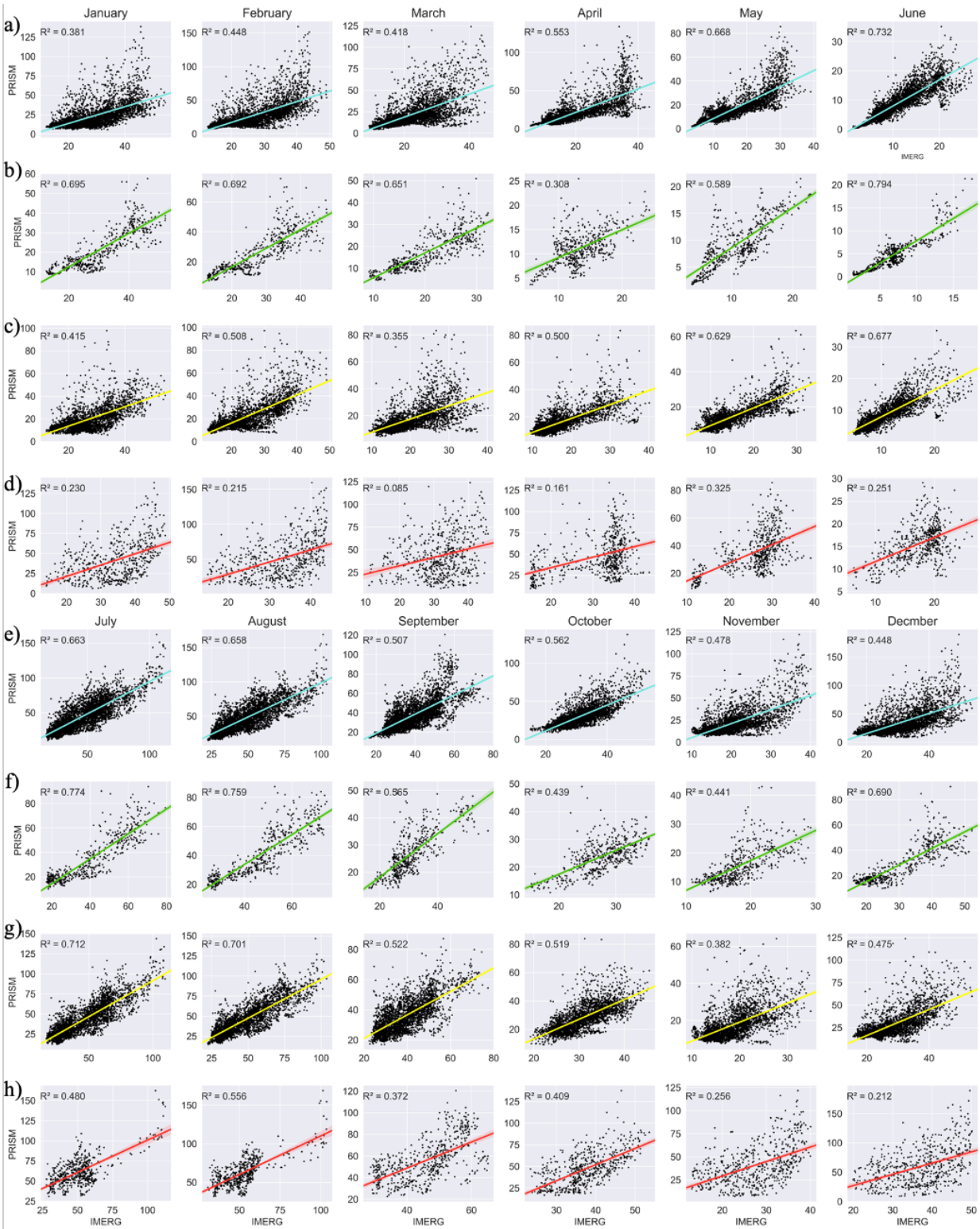

Figure 2.4a-h. Monthly scatter plots and linear regression analysis for all elevations (blue, a, e), low elevations (green, b, f), mid-elevations (yellow, c, g), and high elevations (red, d, h). The colored shading around the fit of the model represents the 95% confidence interval.

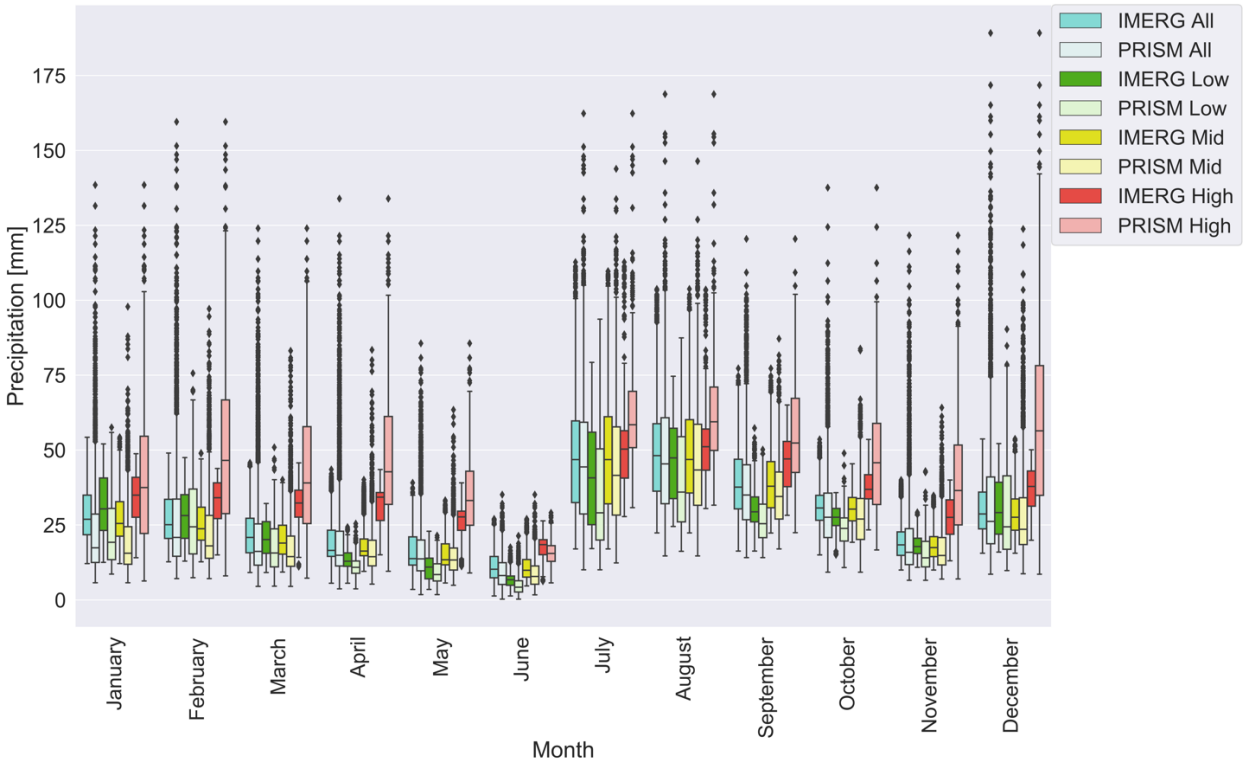

Figure 2.5. Monthly boxplots of IMERG and PRISM precipitation for all elevations (blue), low elevations (green), mid-elevations (yellow), and high elevations (red).

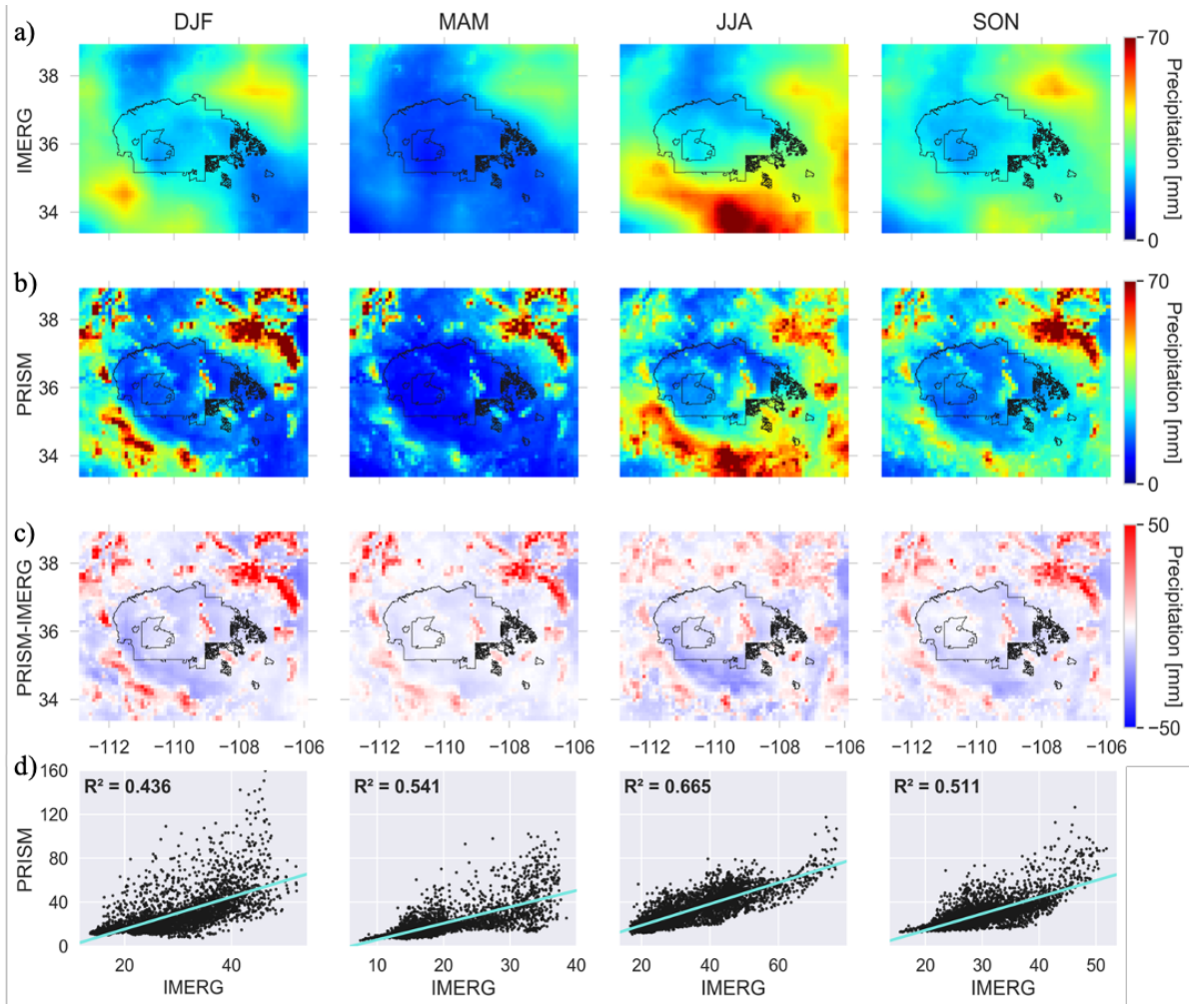

Figure 2.6a-d. a. Seasonal maps of the IMERG V06 Final Run precipitation [mm] for the Navajo Nation and FCR on a 0.1º x 0.1º grid. b. Seasonal maps of the PRISM precipitation [mm] for the Navajo Nation and FCR on a 0.1º x 0.1º grid. c. Seasonal maps of the difference between PRISM and IMERG V06 Final run [mm] for the Navajo Nation and FCR on a 0.1º x 0.1º grid. d. Seasonal scatter plots and linear regression analyses for all elevations in the study region. The blue shading around the fit of the model represents the 95% confidence interval.

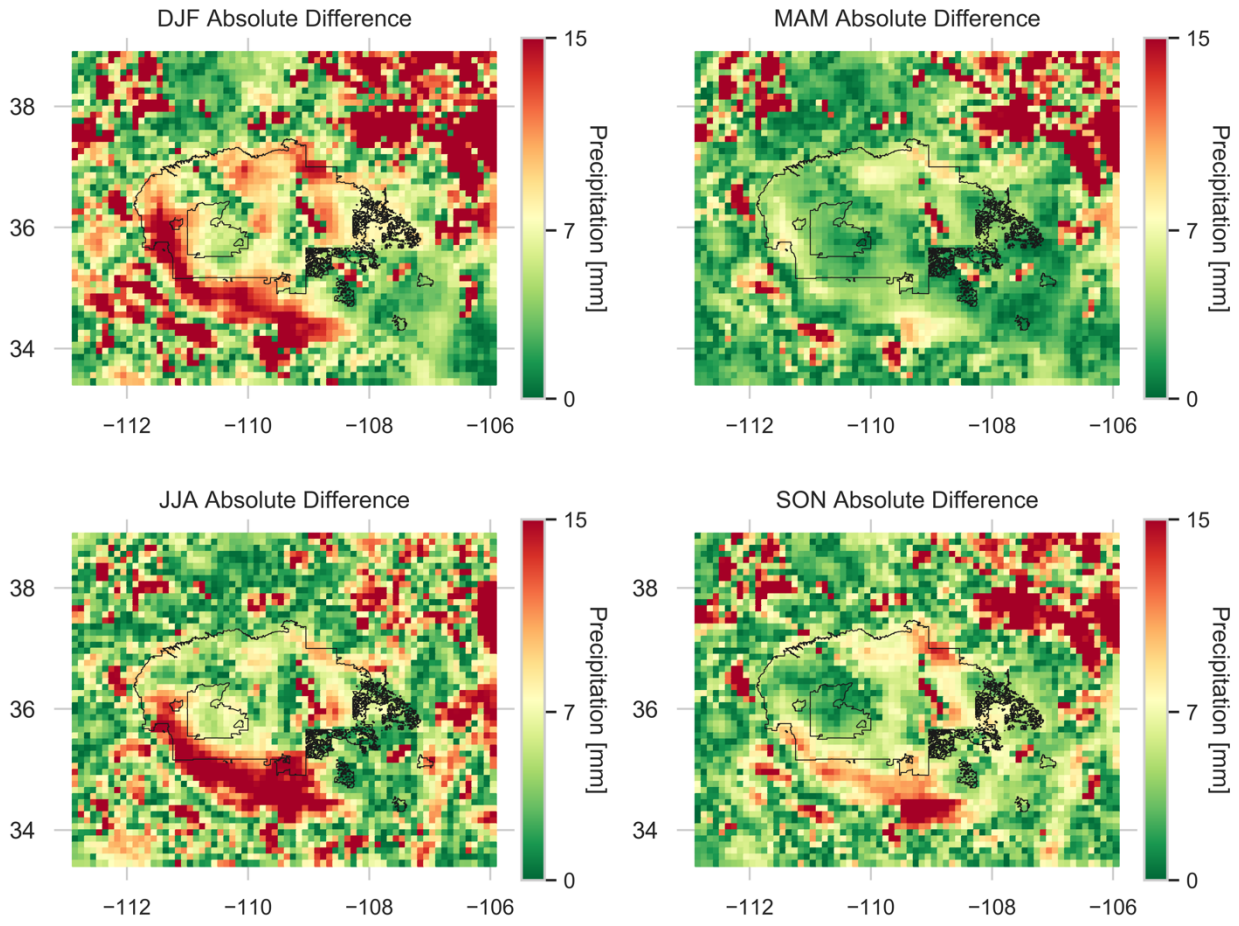

Figure 2.7. Seasonal maps of the mean absolute difference between PRISM and IMERG V06 Final Run on a 0.1º x 0.1º grid.

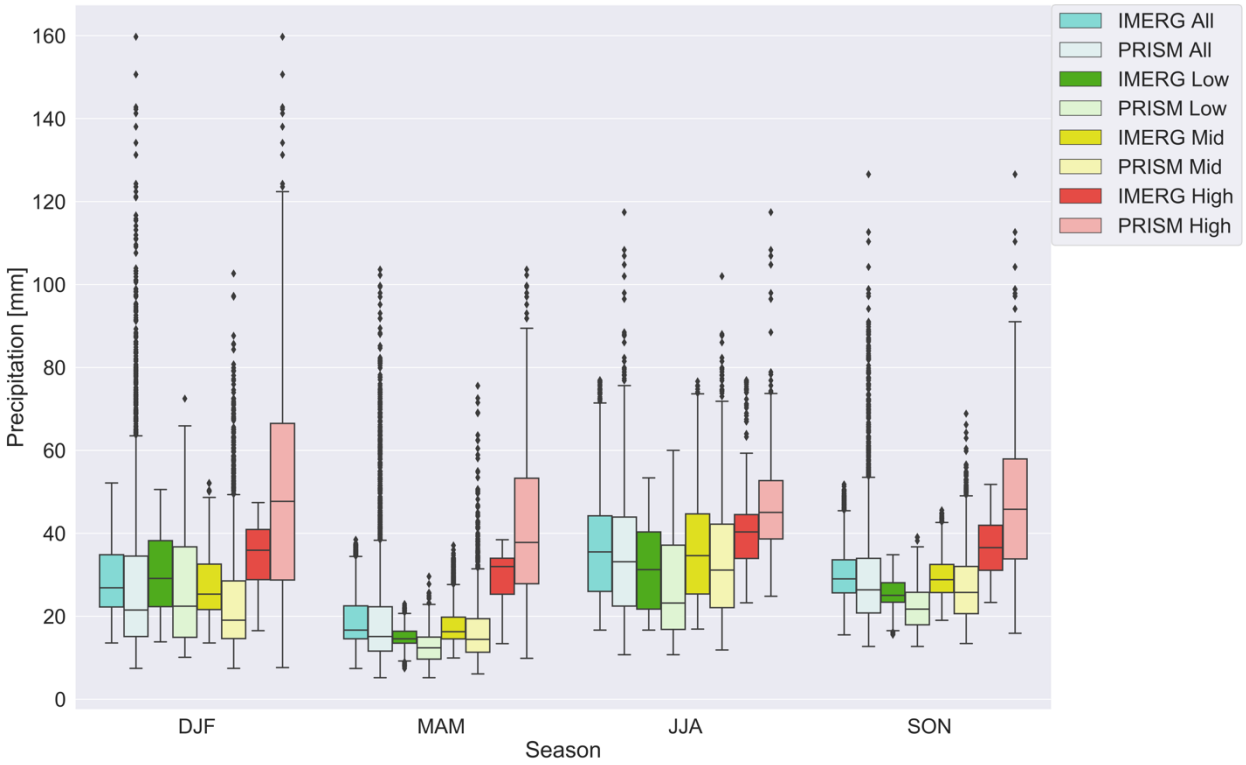

Figure 2.8. Seasonal boxplots of IMERG V06 Final Run and PRISM precipitation for all elevations (blue), low elevations (green), mid-elevations (yellow), and high elevations (red).

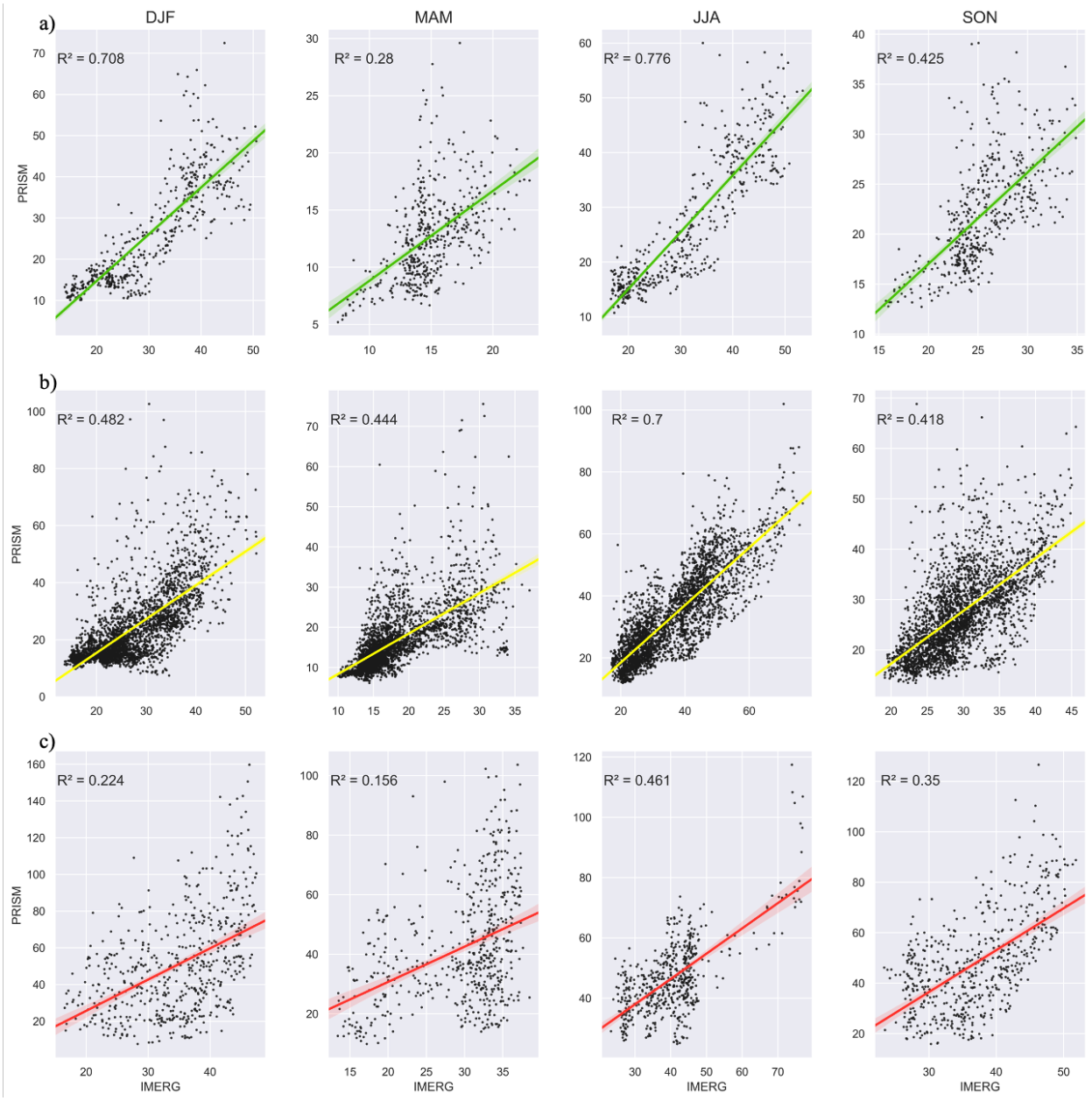

Figure 2.9a-c. Seasonal scatter plots and linear regression analysis for low elevations (a.), mid-elevations (b.), and high elevations (c.). The shading around the fit of the model represents the 95% confidence interval.

CHAPTER 3

A GEOSPATIAL WATER BUDGET ANALYSIS OF THE FOUR CORNERS REGION AND THE NAVAJO NATION[2]

[2] Long, K. A. and Shepherd, J. S. (2020). A Geospatial Water Budget Analysis of the Four Corners Region and Navajo Nation. To be submitted to *Journal of Arid Environments.*

Abstract

In the natural water cycle, precipitation is the most critical input for surface freshwater resources. The Navajo Nation located in the Four Corners Region (FCR) is currently struggling with a water security crisis, which is expected to be exacerbated by future climate change scenarios that result in hydroclimate variability. There is a need to enhance the understanding of regional hydroclimate on a detailed spatial scale in order to identify locations that experience large deficits or surplus in surface water. This research establishes a geospatial water budget analysis derived from hydroclimatic data. This research employs NASA's IMERG V06 Final Run precipitation observations and NLDAS-2 total evapotranspiration and runoff data for the Navajo Nation and FCR on a 0.1º x 0. 1º grid. An annual water budget analysis, a spatial analysis of seasonal total evapotranspiration and runoff, and a monthly and seasonal spatial analysis of water storage (ΔS) is performed. This novel spatial water budget analysis using space-borne precipitation measurements reveals that trends in hydrology on the Navajo Nation and in the FCR are largely a function of vegetation coverage and type, elevation, and season. This research is done to provide the Navajo with a better understanding of the natural water cycle as it relates to their water resources and hydroclimate. It also sheds light on areas that may be impacted significantly in future climate change scenarios where precipitation variability and increased temperatures will alter regional hydroclimate.

3.1 Introduction

Precipitation is the crucial primary input of freshwater in the natural water cycle. The amount of precipitation drives surface and groundwater reservoir recharge and influences agricultural productivity. Surface water is critical to the energy-water-food nexus (EWFN), where surface water withdrawals are utilized primarily for drinking-water, public use, irrigation, and thermo-electric power (Figure 3.1). According to the United States Geological Survey (USGS), roughly 74% of all water used in the United States in 2015 came from surface water resources, which are largely dependent upon precipitation input [*Dieter et al.*, 2017].

Thus, variability in precipitation can have significant impacts on water resources and hydroclimate of a region. In the arid Four Corners Region (FCR) of the southwestern United States, precipitation is bimodal, with a peak in winter precipitation usually falling as snow, especially in regions of high elevation, and a second peak in the summer months of July, August, and September, corresponding with the North American Monsoon (NAM) system. The two peaks are separated by a warm dry season, typically between March and June, after the winter storm track begins to migrate poleward and temperatures rise. NAM and wintertime synoptic-scale driven precipitation in the region is also largely influenced by teleconnections such as El Nino Southern Oscillation (ENSO) and the Pacific Decadal Oscillation (PDO). Teleconnection driven precipitation variability is well documented in the literature [*Carleton et al.*, 1990; *Hereford and Webb*, 1992; *Harrington et al.*, 1992; *Woodhouse and Meko*, 1997; *Tully-Cordova et al.*, 2018]. Additionally, the region is highly prone to periods of exceptional warming and prolonged drought. Severe droughts persisting over long time periods have also been identified in dendrochronology and other paleoclimate proxy records, as well as Palmer Drought Severity Index (PDSI) reconstructions [*Cook et al.*, 2004; *Salzer and Kipfmueller*, 2005; *Benson et al.*, 2007; *MacDonald*, 2010).

Thy hydrology in semi-arid regions is characterized by the sporadic, small-scale precipitation, high evaporation rates, low transpiration rates, low surface runoff, and minimal infiltration of soils. The generally sparse vegetation seen in the NDVI image from MODIS-Terra (Figure 3.2) means that the soil is the first point of contact for rainfall, and thus rainfall-runoff processes are determined by soil property. Hydrophobic soils, sand dunes, and exposed surface rock are common in the FCR and can largely influence runoff [*Pilgrim et al.*, 1988]. Sand dunes alone cover a third of the Navajo Reservation [*Redsteer et al.*, 2013]. The scattered nature of vegetation leaves soils vulnerable to soil crusting, which can lead to a large reduction in infiltration [*Morin and Benyamini*, 1977]. Additionally, bare soils can result in enhanced evaporation from the surface since there is no major pathway hinderance between the surface and atmosphere [*Pilgrim et al.*, 1988]. Despite a large fraction of bare surface and exposed rock, there are a number of diverse species of vegetation that are elevation dependent that are be found in the region. Grass-shrub exists at altitudes below 1650m mainly that are predominantly sparse grassland-browse types of vegetation, pinyon-juniper forests that reside between 1650m and 2300m and are dominated by woodland-browse species, and pine forest at higher altitudes above 2300m [*El-Vilaly et al.*, 2018]. The Navajo reservation is home to 1 million acres of ponderosa pine and mixed conifer forest as well as over 4.8 million acres of pinyon-juniper woodlands. Large pinyon-juniper forests can be problematic for water yields since they have high evapotranspiration rates even in instances of low precipitation amounts and have been found to promote hydrophobic soils [*Ffolliott and Stropki*, 2008; *Robinson et al.*, 2010]. Furthermore, vegetation that does exist in semi-arid regions have adapted water retention mechanisms and have developed deep or expansive rooting systems that allow them to survive prolonged periods without water. Although vegetation does exist in arid and semi-arid regions, evaporation from

bare soils is greater than transpiration from plants, leaving evaporation as the largest driver of hydrology, which is dependent upon water availability [*Camacho Suarez et al.*, 2015]. As soils dry, soil temperature gradient largely affects evaporation rates [*Rose*, 1968]. Runoff is influenced by the variable spatiotemporal nature of precipitation, enhanced evaporation rates particularly in characteristic warm summertime temperatures, soil composition, groundwater resources, and antecedent precipitation that impacts surface runoff processes [*Wheater et al.*, 2002; *Blöschl et al.*, 2013; *Hrarchowitz et al.*, 2011; *Camacho Suarez et al.*, 2015].

The Navajo Nation settled in the Four Corners Region of the southwestern United States is currently facing a water scarcity crisis. The Navajo (*Diné*) rely on both surface water and groundwater resources to meet domestic, agricultural, and industrial water demands [*Nania et al.*, 2014]. Surface water reservoirs are particularly significant for the livestock water supply [*Navajo Department of Water Resources*, 2011]. The Navajo claim water rights to the Colorado River, the Little Colorado River, and the San Juan River, through the *Winter's Doctrine*, but climate change and hydrologic variability threaten the supply of water from these resources that serve a region that is already in high demand [*Nania et al.*, 2014]. Thus, the need to understand the spatial trends of the water budget in the FCR and on the Navajo Nation becomes increasingly important in the context of increased temperatures driven by anthropogenic climate change. In the FCR, hydroclimatic change forced by anthropogenic greenhouse gas emissions include declines in snowpack where increased temperatures produce earlier snowmelt and result in more winter precipitation falling as rain [*Redsteer et al.*, 2011; *Cayan et al.*, 2013; *Gershunov et al.*, 2013]. Reduced snowpack results in decreased river discharges from the Upper Colorado River and Rio Grande [*Hoerling et al.*, 2013], which will place strains on already stressed regional water resources. *Mote et al.* [2005] found that over the last century, the snow-water equivalent

(SWE) in the western United States in general has decreased. This is significant because the snowpack is a crucial source of surface runoff, groundwater recharge, and water supply [*Barnett et al.*, 2005; *Mote et al.*, 2005; *Hunter et al.*, 2006; *Li et al.*, 2017]. Winter precipitation can account for 50 to 70% of the annual precipitation in mountainous areas throughout the western region [*Hunter et al.*, 2006]. In particular, this has important implications for the Colorado River Basin because changes in wintertime precipitation as well as increased temperatures will result in decreases in SWE in the snowpack and earlier snowmelt, affecting the timing of peak streamflows for the Colorado River [*Hamlet et al.*, 2005]. *Seager et al.* [2013] conducted a study using the Coupled Model Intercomparison Project Five (CMIP5) and found that increased temperatures as a result of greenhouse gas emissions are projected to cause the net flux of water substance at the surface (P-E) in the southwestern United States to decrease. The authors note that a decrease in P-E would result in declining surface water reservoirs, contributing to decreased surface water availability. Furthermore, the expected increase in temperatures superimposed with the frequency and magnitude of long-term severe droughts are likely to exacerbate surface water security issues, resulting in significant consequences for the region's indigenous populations, including the Navajo. In general, climate model simulations indicate that the southwestern region is expected to experience increased aridity and droughts will become more severe and prolonged [*MacDonald*, 2010]. Climate simulations from *Seager and Vecchi* [2010] suggest that the increased aridity in the region will be a result of the poleward expansion of the subtropical high-pressure as a result of the planet warming from increased concentrations of greenhouse gases. Additionally, the authors conclude that the region will experience decreases in wintertime precipitation due to the increased moisture divergence as a result of changes in mean atmospheric flow and reduced moisture convergence via transient eddies. *Cayan et al.*

[2010] indicate that drought activity will increase by the end of the 21st century, particularly in the Colorado River Basin, resulting in depleted soil moisture and increase in water demand. These prolonged periods of drought are expected to contribute to increased aridity across the region.

Today, the Navajo Nation has already experienced the direct impacts of hydroclimatic change that include observed declines in snowpack, significant changes in surface water features, and decreasing water quality. According to an analysis of observations of surface water features and streamflows by *Redsteer et al.* [2011], over 30 major surface water features have become either dry year-round or ephemeral since the 1920's. Higher temperatures have resulted in a decreased snowpack, earlier onset of snowmelt, and increased aridity from higher evapotranspiration rates coupled with a long-term decrease in precipitation [*Maurer et al.*, 2007; *Barnett et al.*, 2008; *Bonfils et al.,* 2008; *Pierce et al.,* 2008; *Hidalgo et al.*, 2009; *Redsteer et al.*, 2011]. These factors are likely the forcing mechanisms of perennial streamflow disappearance over the last century [*Redsteer et al.*, 2011]. Additionally, *Redsteer et al.* [2011] have documented an appreciable decline in water quality, finding that many wells have become increasingly saline as a result of overuse and lack of recharge.

The current situation regarding water resources in the reservation underscore the need for a geospatial water balance analysis. A spatial water budget analysis would not only provide the Navajo with a better understanding of the spatiotemporal patterns of the water budget but may also help identifying key areas that may be critically impacted by future climate change scenarios. For example, it is likely that temperatures will increase as a result of anthropogenic greenhouse gas forcing. An increase in temperatures will enhance evaporation rates that will deplete surface water storage reservoirs. This information could enhance the decision-making

process for local water resource managers if they know when and where areas experience water storage deficits on average.

In the following sections, an analysis of the annual water budget for the greater FCR is done using the water mass balance equation (1) on a monthly basis. Then, total evapotranspiration (TET), surface runoff (non-infiltrating), and subsurface runoff from NLDAS-2 are used to map the seasonal averages from 2001-2018 for the FCR with special attention to the Navajo Nation. These averages are then used to map the spatial trends of the storage residual, ΔS, calculated by equation (1), which is a modified natural water balance equation from *Welty* [2009], for surface storage, in order to assess the availability of water in the FCR and Navajo Nation on a monthly and seasonal basis. The intention of this study is to primarily focus on the broader picture with regards to the surface water budget and to identify areas of water storage surplus and deficit on a monthly and seasonal scale. The study considers data from 2001-2018, due to limitations in the time span for the IMERG V06 dataset. These results will be useful to indicate areas of concern where water scarcity will increase from drought conditions during critical parts of the year that are expected to place strain on water resources. Furthermore, this is the first in depth geospatial water budget analysis of the FCR and the Navajo Nation to include NASA's satellite-based IMERG V06 Final Run precipitation observations. The use of satellite-derived precipitation estimates will provide a quantification of the water balance at a high spatial resolution.

$$\text{Precipitation} - \text{Runoff} - \text{Evapotranspiration} = \Delta\text{Storage} \quad (1)$$

3.2 Data and Methods

The first phase of the multi-institution North American Land Data Assimilation System (NLDAS-1) was established in 2000 and was implemented through 2005 [*Mitchell et al.*, 2004]. Phase 1 was run for a 3-year period between October 1996 and September 1999, where the main objectives were to determine the NLDAS configuration with selected land surface models (LSMs) and surface forcing data [*Xia et al.*, 2012; *Mocko*, 2012]. NLDAS Phase 2 (NLDAS-2) has the same general configuration as NLDAS-1 but has been upgraded to include a longer time span of forcing data from January 1979 and updated LSMs [*Xia et al.* 2012]. Information on the forcing data for NLDAS-2 can be found in *Rui and Mocko* [2014]. Noah, Mosaic, Sacramento Soil Moisture Accounting Model (SAC), and Variable Infiltration Capacity Model (VIC) are the four land surface models (LSMs) make up the operational version of NLDAS-2. The LSMs are capable of simulating the surface water balance and the surface energy balance but do not account for influences of groundwater or irrigation processes on evapotranspiration (ET) [*Xia et al.*, 2012]. The primary purpose of NLDAS-2 is to provide information for the land surface modeling and water management communities and supports the U.S. Drought Monitor analysis [*Xia et al*. 2016].

This study utilizes data from the VIC LSM in NLDAS-2. NLDAS-2 data was downloaded from NASA's Giovanni data portal, which is developed and maintained by the NASA Goddard Earth Sciences (GES) Data and Information Services Center (DISC) [*Retrieved from*: https://giovanni.gsfc.nasa.gov/giovanni/; *Acker and Leptoukh*, 2007; *Mocko*, 2012; *Xia et al.*, 2012]. The spatial resolution of the dataset is 0.125º x 0.125º and the temporal scale comes as either hourly or monthly. This study employs the monthly VIC NLDAS-2 dataset for TET, surface runoff (non-infiltrating), and subsurface runoff. The VIC model incorporates a two-layer soil column where the upper soil zone represents the soil column's dynamic behavior that

responds to rainfall and the lower layer represents the slow dynamics of between-storm soil moisture behavior [*Liang et al.*, 1994; *Liang et al.*, 1996]. The lower layer responds to rainfall only when the upper layer is wetted, allowing the model to separate subsurface base flow from the storm direct runoff [*Liang et al.*, 1994]. VIC uses a variable infiltration capacity scheme that is based on the Xinanjiang model [*Zhao*, 1980] where direct surface runoff is calculated by the grid fraction for which precipitation exceeds the point infiltration capacity of the soil when added to the soil moisture storage from the previous time step [*Wood et al.*, 1997]. Gravity-driven drainage is assumed for flow between the upper layer and lower layers following *Brooks and Corey* [1964] and nonlinear drainage based on the Arno model conceptualization [*Francini and Pacciani*, 1991] is used to determine drainage from the lower layer. To model evapotranspiration, VIC accounts for three types of evaporation including evaporation from the canopy layer and transpiration from each vegetation class and evaporation from bare soil [*Liang et al.*, 1994]. Total evapotranspiration is then computed as the sum of these three components, which are weighted based on areal surface cover fractions [*Liang et al.*, 1994]. Surface potential evaporation is based on the Penman-Montieth equation with the canopy resistance at zero and VIC considers architectural and aerodynamic resistance [*Liang et al.*, 1994]. Soil moisture and rooting depth influence transpiration [*Liang et al.*, 1994]. Evaporation and transpiration are thus dependent upon vegetation class where fraction of roots for the upper and lower soil column zones are assigned for each land cover type. The layers within the root zone and the top layer can lose moisture to evapotranspiration following the Arno formulation [*Francini and Pacciani*, 1991; *University of Washington Computational Hydrology Group*, 2016]. Therefore, moisture can be transpired from either or both of the model layers contingent upon specified root fraction

and soil moisture can move upward from the lower layer to the upper layer when there is a sufficient moisture gradient as a result of surface drying [*Wood et al.*, 1997].

The justification for the use of the VIC LSM in NLDAS-2 is due to the enhanced skill in modeling runoff in arid regions of complex terrain compared to the other LSMs. In a study by *Xia et al.* [2016] that evaluated performance of the four LSMs in NLDAS-2 on a River Forecast Center basin scale, VIC's runoff performs better in the CBRFC compared to the other LSMs. These findings by *Xia et al.* [2016] are consistent with other NLDAS research performed in the western United States [*Xia et al.*, 2012]. The superior performance in runoff compared to the other LSMs in the region is likely due to the elevation band-type approach to snowpack modeling that allows for more accurate timing of snowmelt [*Nijssen et al.*, 2001; *Lohmann et al.*, 2004]. Additionally, *Xia et al.* [2016] found that for the Colorado Basin RFC (CBRFC) VIC corresponds well with FLUXNET ET but tends to overestimate ET in the summer months where temperatures are warm. Although the *Xia et al.* [2016] found that the Noah LSM provides slightly more robust correlations with evapotranspiration in the CBRFC, it was not chosen for this study due to the early onset of runoff. Peak Noah LSM runoff in the CBRFC was ~1-2 months early compared to USGS observations [*Xia et al.* 2016]. Despite the fact that the runoff term is small on average for the FCR and the Navajo Nation compared to evapotranspiration and precipitation, it is actually a significant component of the water balance in areas of high elevation throughout the region, especially where snowpack is present. Since part of this study aims to quantify the residual storage term of equation (1) for the FCR and the Navajo Nation where areas of high elevation are present, VIC is believed to be the best LSM for our study region. It is important to note that since the LSMs in NLDAS-2 do not account for the influences of evapotranspiration from groundwater and irrigation processes, this may have some implications

for the Navajo Nation. Currently, the Navajo Indian Irrigation Project (NIIP) has rights to irrigate ~10,630 acres of land, and nearly 90 smaller irrigation projects operate on the reservation [*Nania et al.*, 2014]. Many of these irrigation projects supply water for agricultural purposes, which may influence local evapotranspiration rates.

Monthly precipitation data from IMERG V06 Final Run [*Retrieved from*: https://giovanni.gsfc.nasa.gov/giovanni/; *Acker and Leptoukh*, 2007; *Huffman et al.*, 2019]. A detailed analysis of the performance of the IMERG product can be found in Chapter 2 of this dissertation. While the strengths of the dataset include a high spatial resolution precipitation data resource that performs quite well during the summer and at low (<1500m) to mid-elevations (>1500m and <2500m), the product is limited due to significant underestimations during the cold winter months and at high elevations exceeding 2500m. The shortcomings of the IMERG product in the winter and in regions of elevated complex terrain may introduce some limitations in the results of this research. It is important to note that the primary goal of this research is to provide an initial quantification of the water balance at a high spatial resolution to shed light on the temporal evolution of the water balance throughout the year. IMERG V06 Final Run was upscaled in ArcMap to 0.125º x 0.125º to match the NLDAS-2 resolution for the monthly averages of TET, surface runoff (non-infiltrating), and subsurface runoff in order to create the water budget analysis. An evaluation of the annual water budget was conducted using the monthly data from 2001-2018. Seasonal maps of TET, surface runoff (non-infiltrating), and subsurface runoff are created in order to reveal the spatial trends of each water budget component in the FCR and on the Navajo reservation. Then, using equation (1), the storage residual was calculated for each grid cell to analyze the region for storage surplus and deficits on a monthly and seasonal basis.

3.3 Results

3.3 The Annual Water Budget

The annual water budget is assessed by taking the average of precipitation, TET, surface runoff (non-infiltrating), and subsurface runoff of all grid cells in the FCR for each month (Figure 3.3). As expected, the precipitation from IMERG V06 Final Run shows the bimodal distribution of precipitation throughout the year. There is a peak in precipitation in December around 30mm from the winter storm track and precipitation slowly declines throughout the rest of the winter and spring. Precipitation reaches a minimum in June, where the average precipitation is 10mm throughout the FCR. The onset of the North American Monsoon system is distinguishable by the sudden increase in precipitation in July to the maximum peak of precipitation in August at just over 50mm. The termination of the NAM is much more gradual, where precipitation slowly declines to 20mm by November before the mid-latitude storm track reaches further south again for the winter.

Total evapotranspiration for the region is at a minimum in winter when temperatures are much cooler throughout the region. As temperatures warm during the spring and snowmelt is initiated, the total evapotranspiration increases at a steady rate from March through May. Then, the rate of evapotranspiration slows between May and June despite increased temperatures. This is due to the drier upper layers of the soil column as a result of the springtime snowmelt termination and coincides with the annual precipitation minimum. Additionally, the decrease in TET could be contributed to the variety of plant species in the region that have adapted so that they transpire less in warm temperatures to retain moisture during periods of dry weather and extreme temperatures. The rate of evapotranspiration then increases from June to July as a result of the increased precipitation from the NAM system. The increase in TET is likely contributed

more to evaporation of precipitation from high temperatures than transpiration. Looking at the runoff curves, the surface runoff increases slightly and subsurface runoff decreases slightly during this time on average throughout the region suggesting that soils are not being infiltrated by precipitation and instead are being evaporated. The rate of evapotranspiration decreases slightly between July and August and declines rapidly from September into the fall and winter months coinciding with the termination of NAM and cooler temperatures.

On average, surface and subsurface runoff in the region are relatively small terms in the FCR. These terms are significantly more important in areas of high terrain, and this is discussed at length in a later section of this paper. On average for the FCR, surface runoff (non-infiltrating) is ~0mm in the winter months, increasing marginally in the spring months due to snowmelt in higher elevations. Surface runoff increases to ~3mm by July and stays steady throughout the NAM season, where surface runoff begins to decline after September. These results are interesting as they show that even during the monsoon season, the runoff term is small, indicating that much of the precipitation that falls is evaporated. Small runoff amounts are likely exacerbated in areas of lower elevation where the distance of the atmospheric column between cloud base and the surface are larger, allowing for sufficient time for evaporation of droplets before reaching the surface, especially in sufficiently warm temperatures. The subsurface runoff, which is the water that infiltrates the soil and enters the vadose zone that flows laterally to streams, has an opposing trend compared to the non-infiltrating surface runoff. Subsurface runoff has the highest values in the spring months, indicating that the moisture from snowmelt has saturated deep into the soil column. The minimum for subsurface runoff is reached in July and sustained through August, where it only slightly increases in September. This trend is likely a result of high temperatures evaporating precipitation and increased surface runoff due to soil

type, especially during periods of heavy precipitation during the monsoon before it is able to infiltrate the soil.

The storage term, ΔS, for the region generally reflects the pattern of precipitation. The storage term shows a surplus of water available in the winter months. This surplus of water is stored in the snowpack in high elevation regions and is a result of low evapotranspiration rates and runoff. As snow begins to melt, total evapotranspiration rates increase, and the region is dominated by dry conditions, the storage term declines rapidly from February to March, where ΔS reaches 0mm. Then, large deficits occur from April reaching a maximum deficit in June, where precipitation is at a minimum and TET rates are sufficiently high in late spring, likely due to sufficient soil moisture from springtime snowmelt. The rapid increase in the storage term from June to July signals the onset of the NAM where precipitation is frequent and ΔS is able to recover from the large deficit accrued during the spring dry season despite enhanced TET rates during the summer. ΔS continues to recover until October, when it levels off during the period of dry conditions between NAM termination and the southerly shift of the winter-time mid-latitude storm track.

These results reaffirm that the FCR ΔS is primarily governed by total evapotranspiration processes that are dependent upon water availability, which is driven by precipitation inputs. On average for the entire region, the surface runoff and subsurface runoff essentially cancel each other out and become negligible for most of the region. However, it is again important to emphasize that the runoff terms become increasingly important in areas of complex terrain, as shown by the spatial trends in the maps of each component in the next section. Additionally, the precipitation amounts can largely vary in complex terrain, where some areas of high elevation experience increased local precipitation amounts due to orographic enhancement. Precipitation

from the winter storm track is the most significant input of precipitation while precipitation from the NAM system provides replenishment from the dry spring months for ΔS. As a result, the annual ΔS trend generally follows the annual precipitation trend. However, the high total evapotranspiration rates prevent ΔS from peaking during the NAM months despite the large increase in precipitation. Instead the peak in ΔS is in the winter, signaling that winter precipitation is the most important for water resources in the FCR, which is consistent with the literature. More significantly, the wintertime snowpack is significant for ΔS. If the snowpack declines, or SWE levels decrease throughout the FCR, total evapotranspiration will be impacted as a result of earlier snowmelt and changes in soil moisture, making it more difficult for the storage term to recover during the subsequent NAM season. This effect is especially exacerbated if favorable modes of teleconnections are present that may influence variability in NAM timing and magnitude of precipitation or driving drought conditions.

3.3.2 Spatial Trends of Seasonal Water Budget Components

An extensive analysis of the monthly and seasonal spatial precipitation trends in the region are highlighted in Chapter 2 of this dissertation, and thus, this discussion of results primarily focuses on the spatial trends of total evapotranspiration and runoff components. In Figure 3.4, total evapotranspiration rates across the region are low in DJF as a result of cool temperatures and low soil moisture. TET rates increase in MAM as spring snowmelt occurs, moistening soils deep within the column. Rates of total evapotranspiration reach their peak in JJA as a result of increased temperatures and the onset of the NAM. By SON, total evapotranspiration rates begin to decrease throughout the FCR as NAM precipitation terminates and cooler temperatures settle in the region. The spatial trends of total evapotranspiration reveal

a relationship with elevation which is closely linked to vegetation type present. To the southwest of the Navajo Nation lies the Mogollon Rim, which is home to the Kaibab, Coconino, Apache, and Sitgreaves National Forests. These forests are abundant with ponderosa and pinyon pine trees, junipers, bushgrass, and Douglas-firs and the distribution of these plant species are elevation dependent [*Fairweather et al.*, 2007]. To the northwest of the Navajo Nation lies the San Juan Mountains, a region of high-elevation mountains. Here, vegetation can be divided into four ecological zones based on elevation known as the alpine (>3500m), subalpine (>2800m and <3500m), upper montane (>2300m and <2800m), and lower-montane foothill (<2300m) [*Neely et al.,* 2001]. The alpine zone is located above the tree line, where vegetation is dominated by shrubs and wet meadows. The subalpine zone contains bristlecone pine, spruce-fir, and riparian shrubland. The upper montane zone is distinguished by aspen groves, lodgepole pine forests, montane grasslands, and mixed conifer forests. The lower montane foothills are characterized by Douglas-fir, ponderosa pine, pinyon-juniper woodlands, and intermontane-foothill grasslands. High elevation areas where snowpack is present through the winter, especially in the San Juan's, vegetation type influences transpiration rates. Focusing on the Mogollon Rim and San Juan Mountains in the maps, total evapotranspiration rates are higher than surrounding areas in MAM, JJA, and SON (Figure 3.4), where rates increase as a function of the increased vegetation in the area (Figure 3.2). Transpiration rates may be higher at high elevations due to substantial soil moisture available throughout the column from snowmelt. JJA has high TET across the entire region, even in areas where vegetation is not present, suggesting that the TET maximum during the summer is largely driven by evaporative processes, consistent with the literature.

Figure 3.5 shows that the surface runoff component for the region is low for most of the region in DJF and SON. In DJF, most of the precipitation falls as snow at higher elevations and

runoff values are low during this season as a result of cool temperatures preventing snowmelt. SON's low surface runoff is contributed to the low precipitation typical of the region during October and November. The largest surface runoff values in MAM occur in areas of higher terrain such as the San Juan Mountains where snowmelt is initiated in due to warming springtime temperatures. The San Juan's also have the largest surface runoff values in JJA, likely attributed to locally higher rainfall amounts from orographic enhancement during the NAM and cooler temperature at elevation, which inhibit evaporation rates. Interestingly, the surface runoff for the entirety of the Navajo reservation is low even in the isolated areas of higher terrain such as the Chuska Mountains year-round. This suggests that soils on the Navajo reservation are not infiltrated by runoff from snowmelt in high elevations or from precipitation during the monsoon season and instead are evaporated. Slightly higher amounts of runoff surrounding the Navajo reservation coincide with higher amounts of vegetation seen in the NDVI. Overall, surface runoff throughout the year is negligible on the Navajo reservation throughout the year, again indicating that evaporative processes are the most significant driver of hydrology within the boundaries of the reservation.

Figure 3.6 shows that the subsurface runoff for the region is minimal in the winter months, where higher values can be seen in areas of higher terrain and more dense vegetation (Figure 3.2). In the spring, positive values of subsurface runoff are found in the San Juan's and other areas of higher terrain attributed to snowmelt. Large positive values remain throughout the summer months in high terrain, which is also likely attributed to snowmelt and increased rainfall in complex terrain during the monsoon season. Interestingly, on the Navajo reservation and just to the southeast of the reservation boundaries, negative values are found. The areas with negative values continue to increase to a peak in JJA and become less negative during the fall. Negative

subsurface values arise in VIC NLDAS-2 most likely as a result of the moisture moving from the lower to upper layers of the soil column during periods of excessive surface drying. Subsurface runoff loss is a function of land cover type, root depth, and high total evapotranspiration rates in these areas as a result of low soil moisture at the surface and in the upper layers of the soil column in VIC. This may be exacerbated by low soil moisture content at lower levels of the soil column towards the end of the summer. This conclusion is supported by the low surface runoff values indicating that soils may not be infiltrated by monsoon precipitation and are instead evaporated.

3.3.3 Spatial Analysis of ΔS

Figure 3.7 shows the monthly spatial trends of ΔS in the FCR. In January and February, ΔS is positive for mostly the entire area, with higher storage values in areas of higher terrain. However, storage begins to become more negative the south of the reservation in spots along the Mogollon Rim in February. By March, as the wintertime storm track migrates northward out of the region, the storage term begins to become more negative, especially in regions south of the reservation. By April, much of the region's storage of water has dipped below 0mm as a result of shifting storm tracks and initiation of snowmelt, leading to runoff. By May, the region's storage term becomes largely negative as the dry season sets in and temperatures begin to increase, resulting in increased TET. This lasts through June. ΔS is most negative in regions of complex terrain and areas that have more vegetation, such as the San Juan Mountains, Chuska Mountains, and the Mogollon Rim as a result of higher evapotranspiration rates from vegetation and higher runoff. The onset of the North American Monsoon in July is evident in the ΔS maps. The storage term in the southern portions of the study region and the southern part of the reservation become

more positive when the NAM drifts northward in July. The northern part of the study region still shows negative storage likely as a result of the NAM precipitation not stretching far enough northward at this time. The storage is still negative in these areas in August, but there is some relief provided by the monsoon. Storage does not become replenished on the Navajo reservation until September however regions of complex terrain and vegetated areas still show negative storage. This is likely a result of evapotranspiration still being high due to the warm temperatures and transpiration of higher elevation vegetation, especially in pinyon-juniper forested areas. As temperatures begin to cool by October, storage increases due to the decrease in evapotranspiration coinciding with a decrease in precipitation. Increase in storage continues through November as temperatures decrease and December when the winter storm track returns to the area.

These patterns are also evident in the seasonal analysis of ΔS (Figure 3.8). In the winter, there is a surplus of water due to increase in precipitation from wintertime storm track and low evapotranspiration rates. As the storm track shifts north, snowmelt increases, and temperatures warm during the spring, evapotranspiration rates increase, resulting in storage deficits throughout the region, where the largest deficits are in high elevation. During the summer months, large deficits are found the in the north likely due to the extent of NAM precipitation not reaching these areas. Evaporation rates are higher due to higher temperatures contributing to increase in total evapotranspiration in the region. Further to the south, storage is in surplus likely due to increased rainfall from the NAM.

3.4 Discussion and Conclusion

This geospatial study of the water balance in the FCR and on the Navajo Nation using IMERG Final Run and VIC NLDAS-2 data demonstrates that the region is primarily dominated by evaporative processes, which are largely dependent upon water availability, which is driven by precipitation inputs. Elevation and vegetation play a role in the FCR's runoff and total evapotranspiration regimes, while evaporation is more important in the generally barren landscape across the Navajo Nation. In the fall, the storage begins to recover due to decrease in temperatures that drive the evaporation rates. Runoff terms are small, but may be important locally, especially in areas of high elevation. Winter precipitation is the most important precipitation input for water supply, indicated by the ΔS trends, while the NAM is critical for replenishment of ΔS, especially in the southern portion of the study area, after the warm and dry spring and early summer months. However, it is important to note that the IMERG product may produce large underestimates of precipitation in the winter and in areas of high elevation (>2500m) that may present a limitation in the accuracy of this water balance analysis.

The results of this study are intended to gain a better understanding of the water balance spatial trends throughout the FCR and Navajo Nation in order to understand the impacts of hydroclimate variability as it relates to Navajo surface water resources. This is the first known spatial water balance analysis of the region with a special focus on the Navajo Nation utilizing satellite-derived precipitation measurements. The conclusions from this study reveal spatiality of the widespread ΔS deficits particularly in the spring and summer months that limit water availability in the region and on the Navajo Nation. This study highlights regional and local deficits and surpluses of ΔS that have been found to be largely governed by evapotranspiration rates, which are dependent upon moisture availability from precipitation, throughout the year.

The results of this study underscore the gravity of potential future water resource impacts that would increase the Navajo's vulnerability to future climate change.

Additionally, this work further demonstrates the significance of precipitation variability (natural or anthropogenically forced) and the impacts of increased temperatures as a result of anthropogenic greenhouse gas emissions could have for the region's hydrology. Natural interannual precipitation variability from certain configurations of teleconnection modes that weaken the monsoon and promote drier winter conditions could lead to significant water resource impacts in the FCR and on the Navajo reservation. In particular, diminishes in wintertime precipitation, which is the most critical season for the annual water supply, could be devastating. The natural cycles of precipitation in the region superimposed with the projected impacts of anthropogenic climate change, especially related to increased temperatures, will also contribute to the continued depletion of surface water resources that the Navajo rely on. An increase in summer temperatures will drive already high evapotranspiration rates during the monsoon season, which would lead to a diminishment in replenishment of surface water reservoirs. Variability in hydroclimate will lead to an alteration of the annual changes in ΔS, enhancing storage deficits while simultaneously reducing storage surpluses in certain areas.

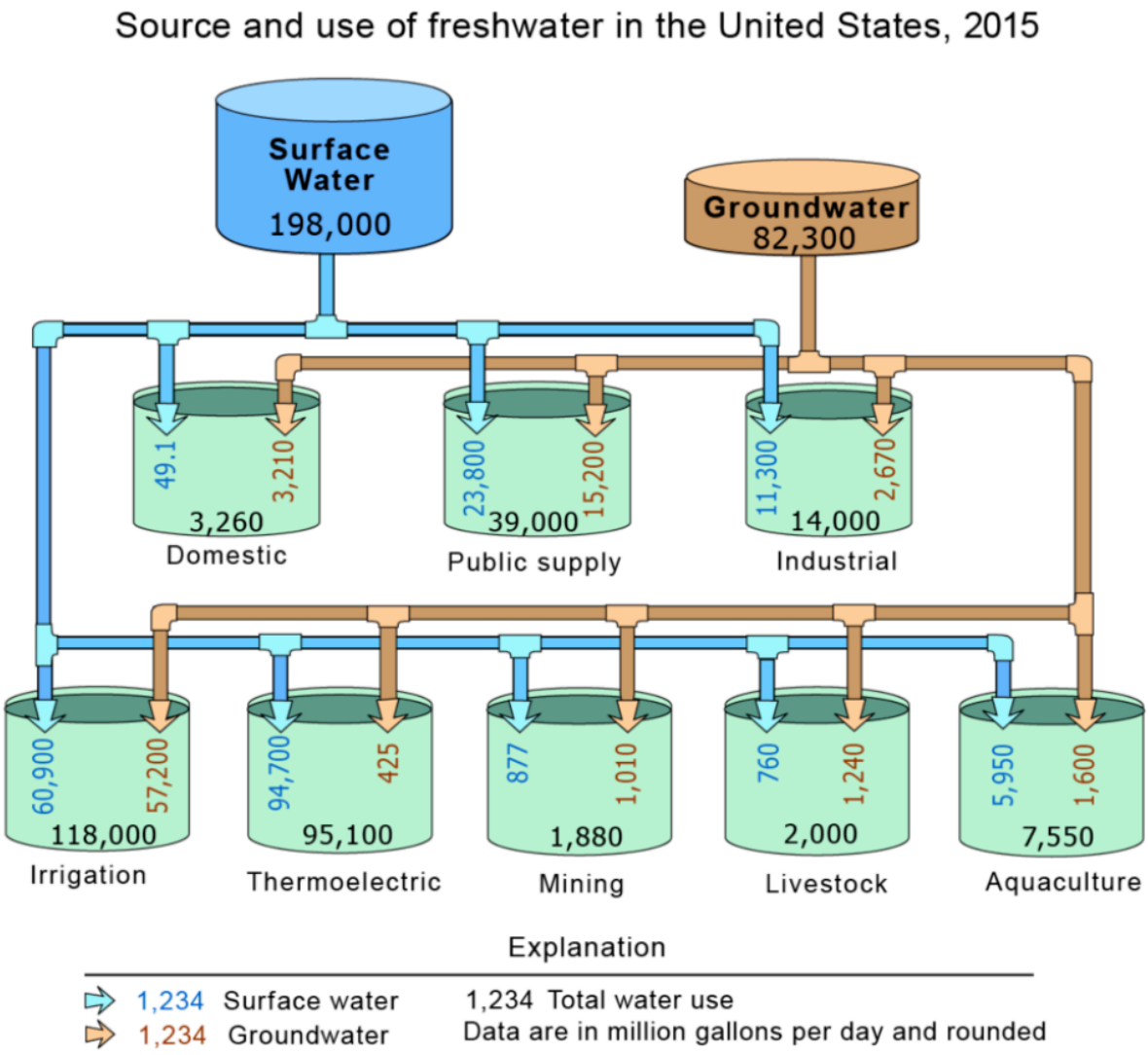

Figure 3.1. USGS schematic of freshwater sources and uses for 2015 in Mgal/day. Image reproduced from https://www.usgs.gov/media/images/source-and-use-water-us-2015.

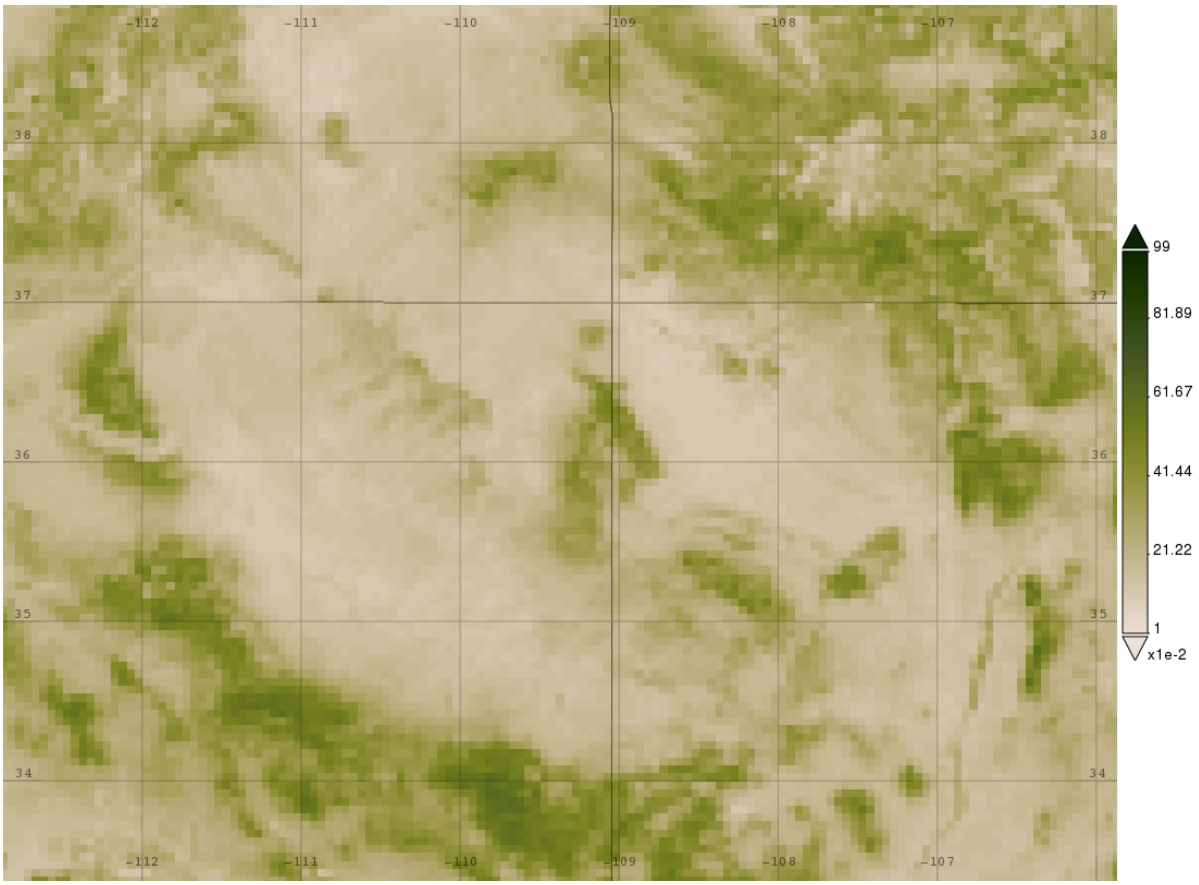

Figure 3.2. Time averaged monthly NDVI from 2001 to 2018 of the FCR from MODIS-Terra on a 0.05º x 0.05º grid. Analyses and visualizations were produced with the Giovanni online data system, developed and maintained by the NASA GES DISC. [*Retrieved from*: https://giovanni.gsfc.nasa.gov/giovanni/; *Acker and Leptoukh*, 2007].

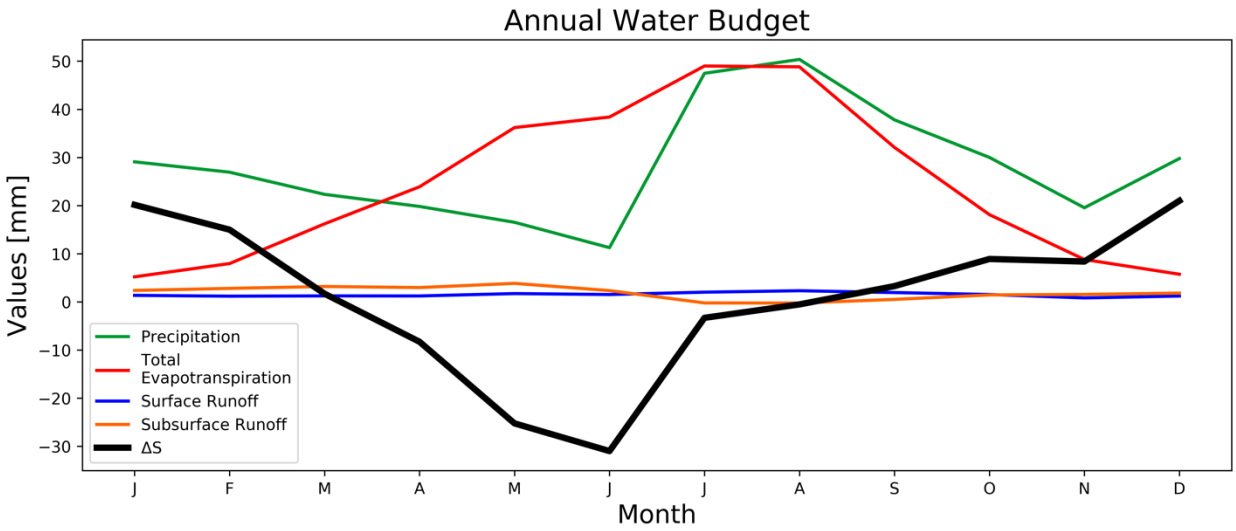

Figure 3.3. The average annual water budget for the FCR. The green line represents precipitation, while the red represents total evapotranspiration, and blue and orange represent surface and subsurface runoff, respectively. The bold black line represents ΔS, which is computed from equation (1).

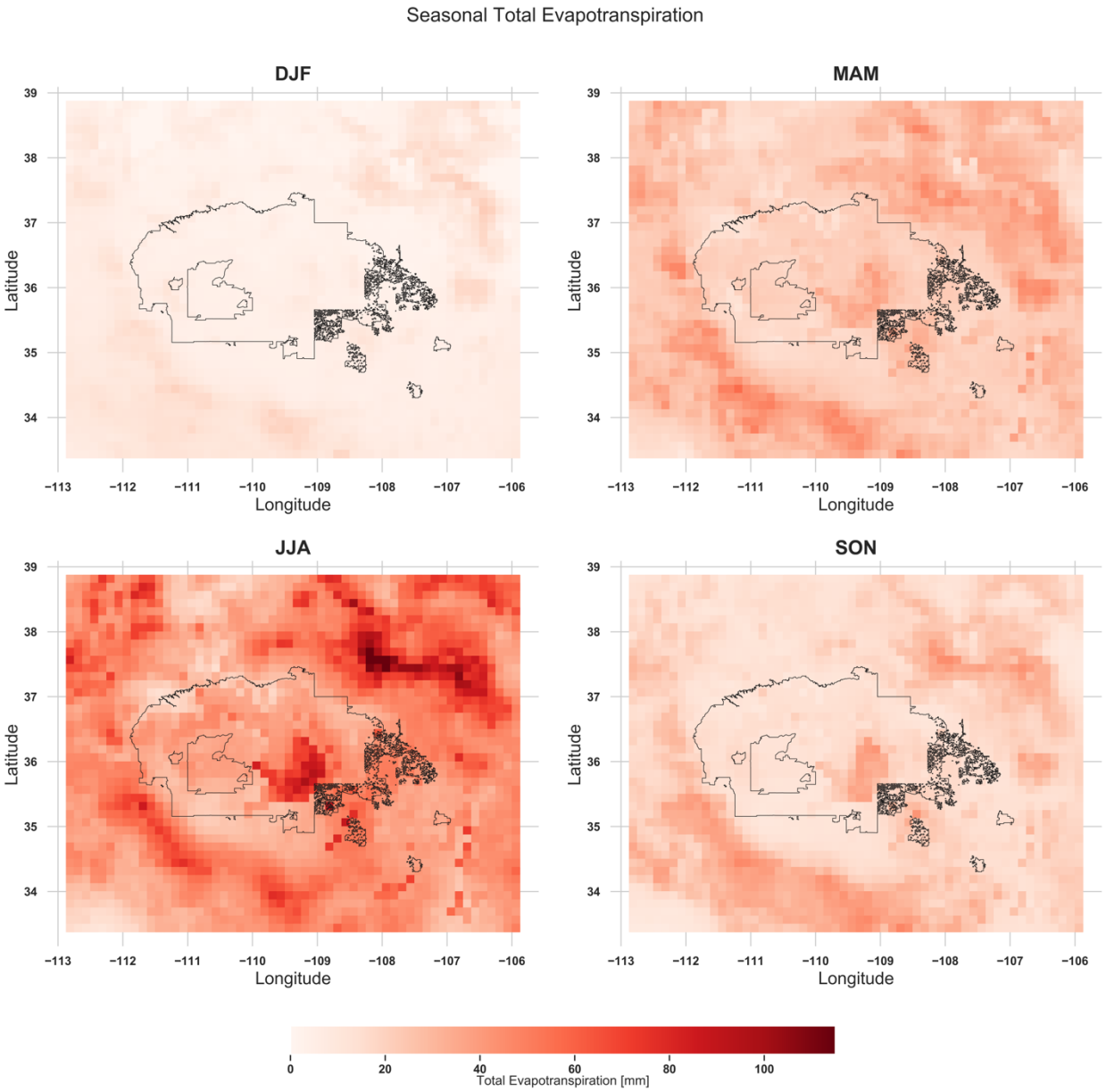

Figure 3.4. NLDAS-2 total evapotranspiration by season for the Navajo Nation and FCR on a 0.125º x 0.125º grid.

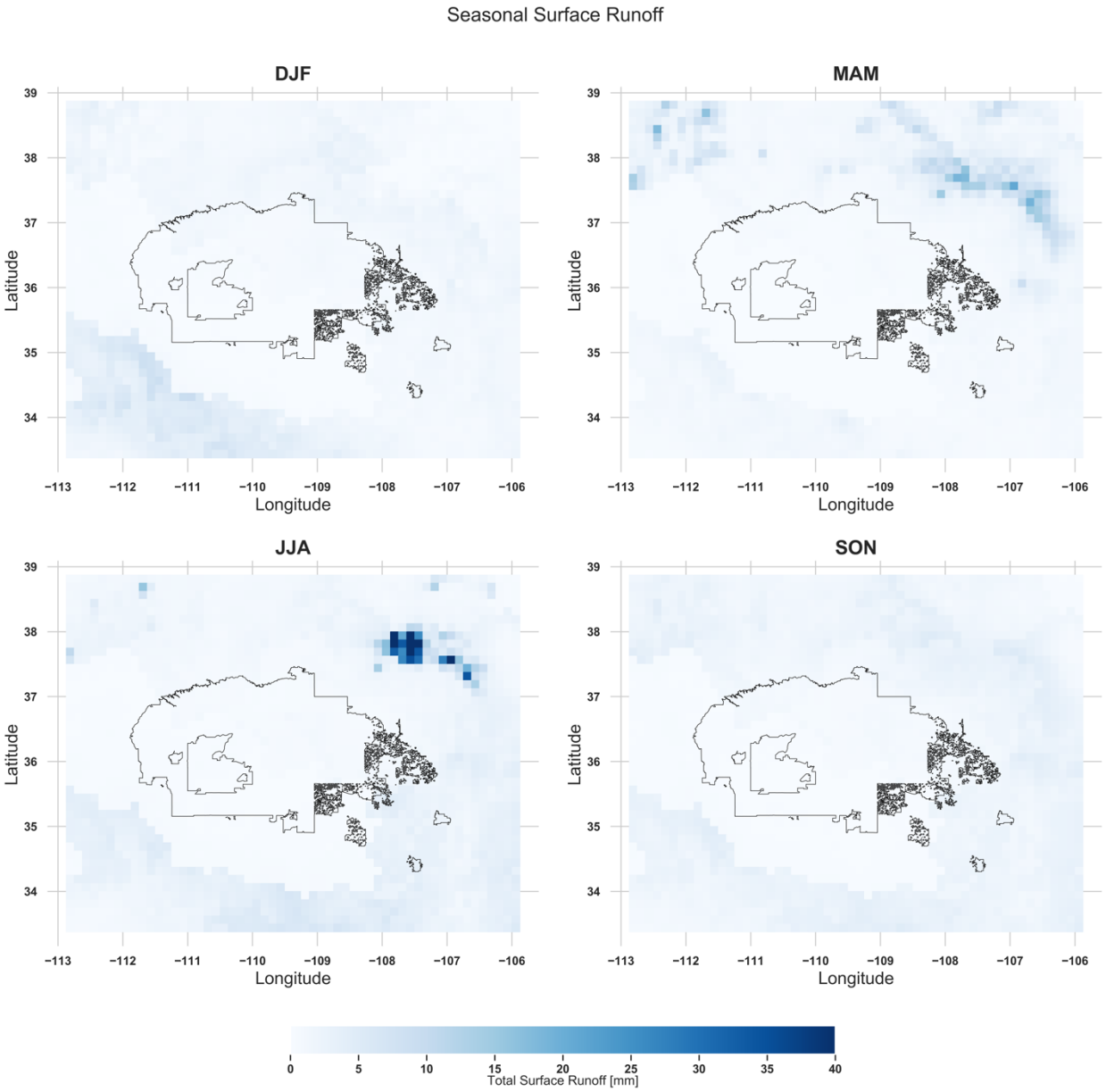

Figure 3.5. NLDAS-2 surface runoff by season for the Navajo Nation and FCR on a 0.125º x 0.125º grid.

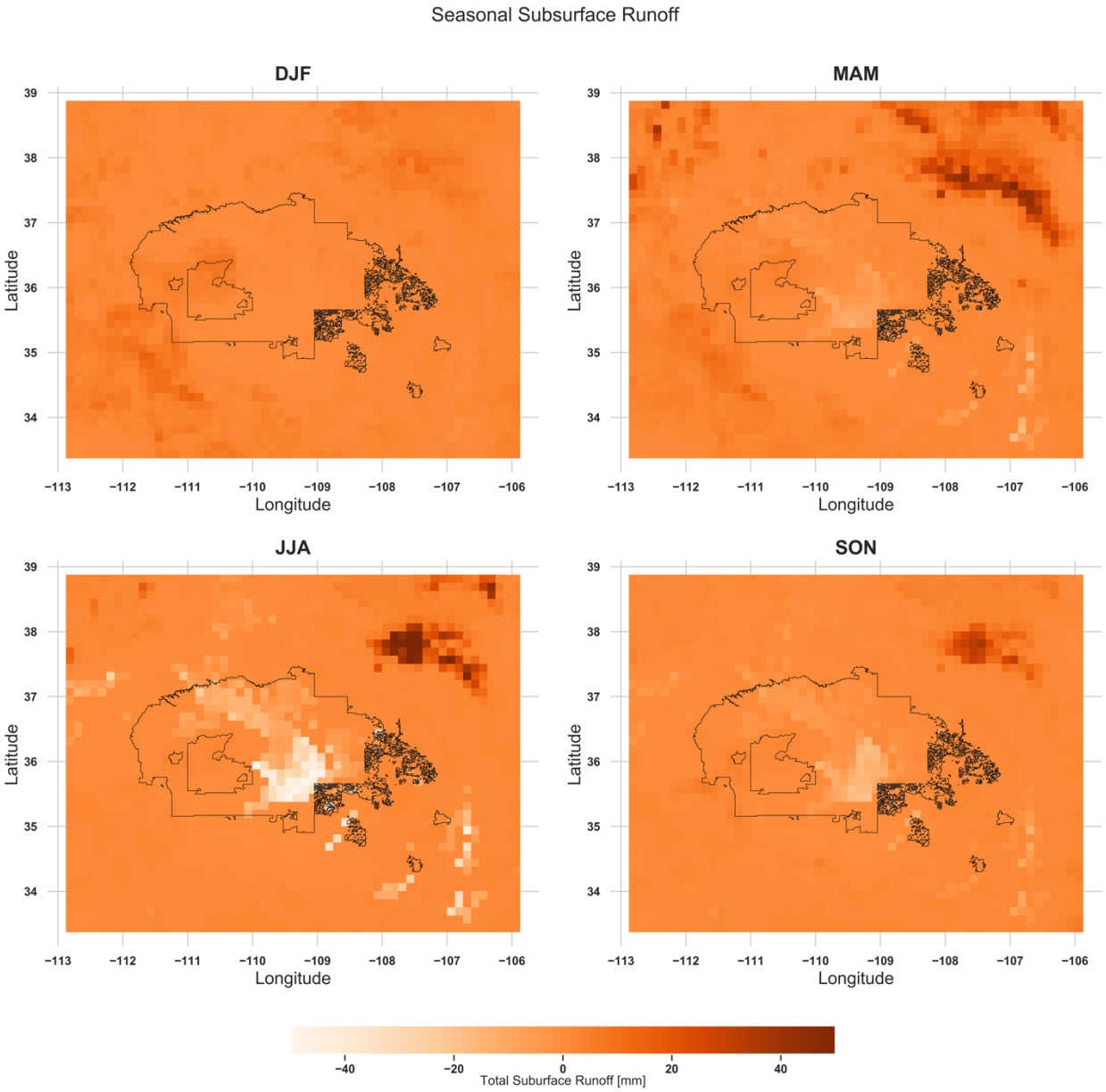

Figure 3.6. NLDAS-2 subsurface runoff by season for the Navajo Nation and FCR on a 0.125º x 0.125º grid.

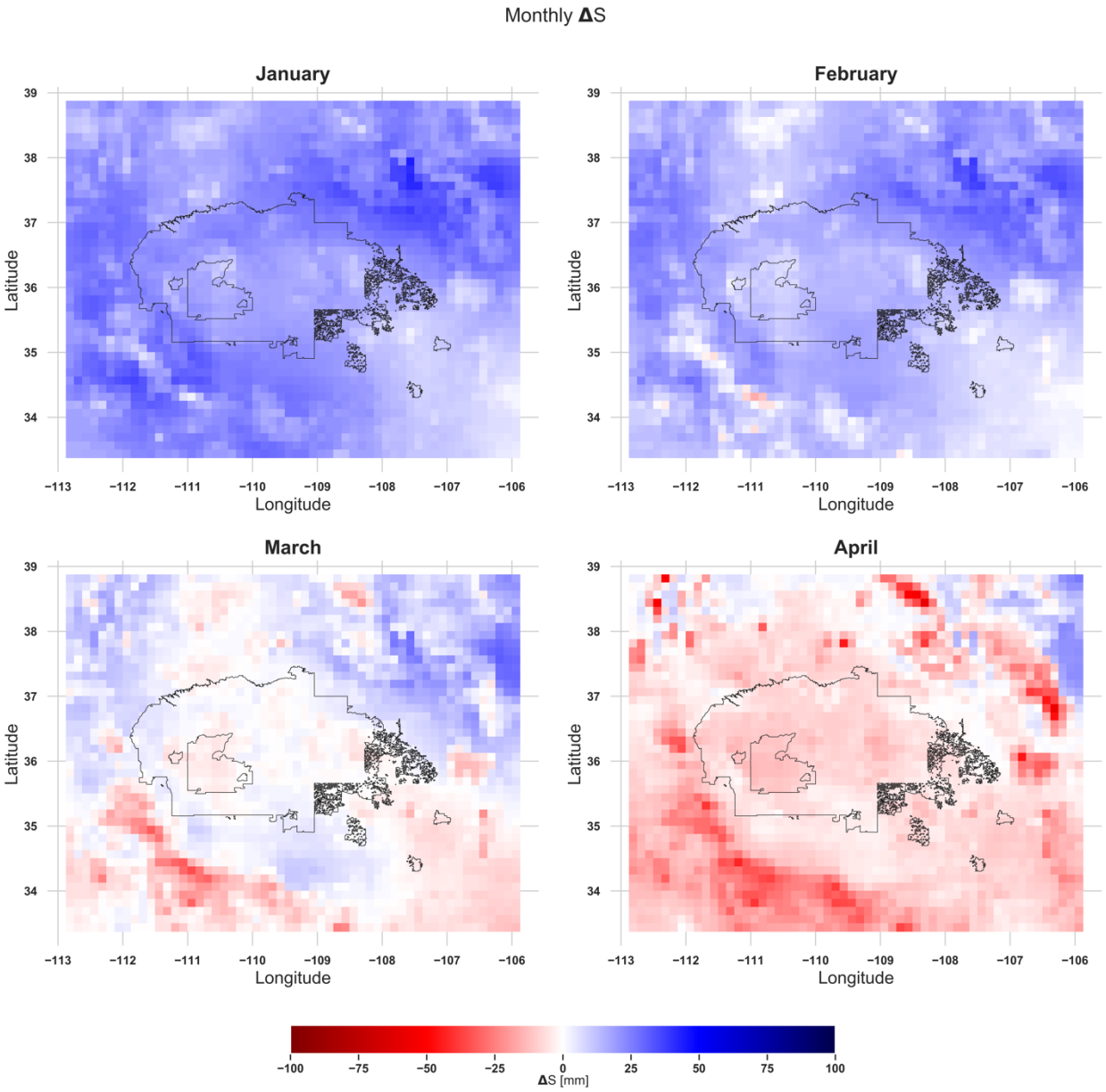

Figure 3.7. ΔS by month for the Navajo Nation and the FCR on a 0.125º x 0.125º grid.

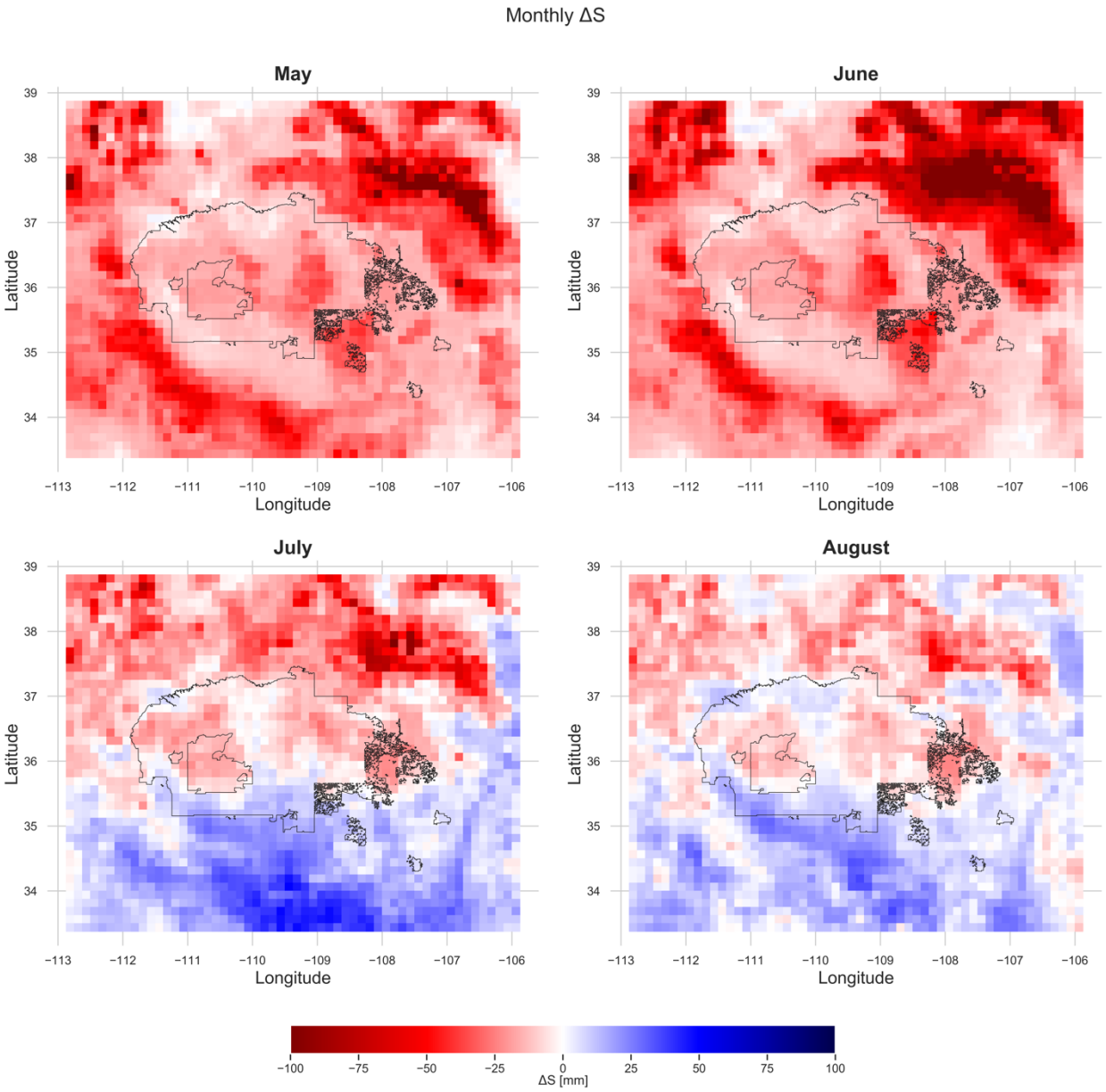

Figure 3.7. (continued).

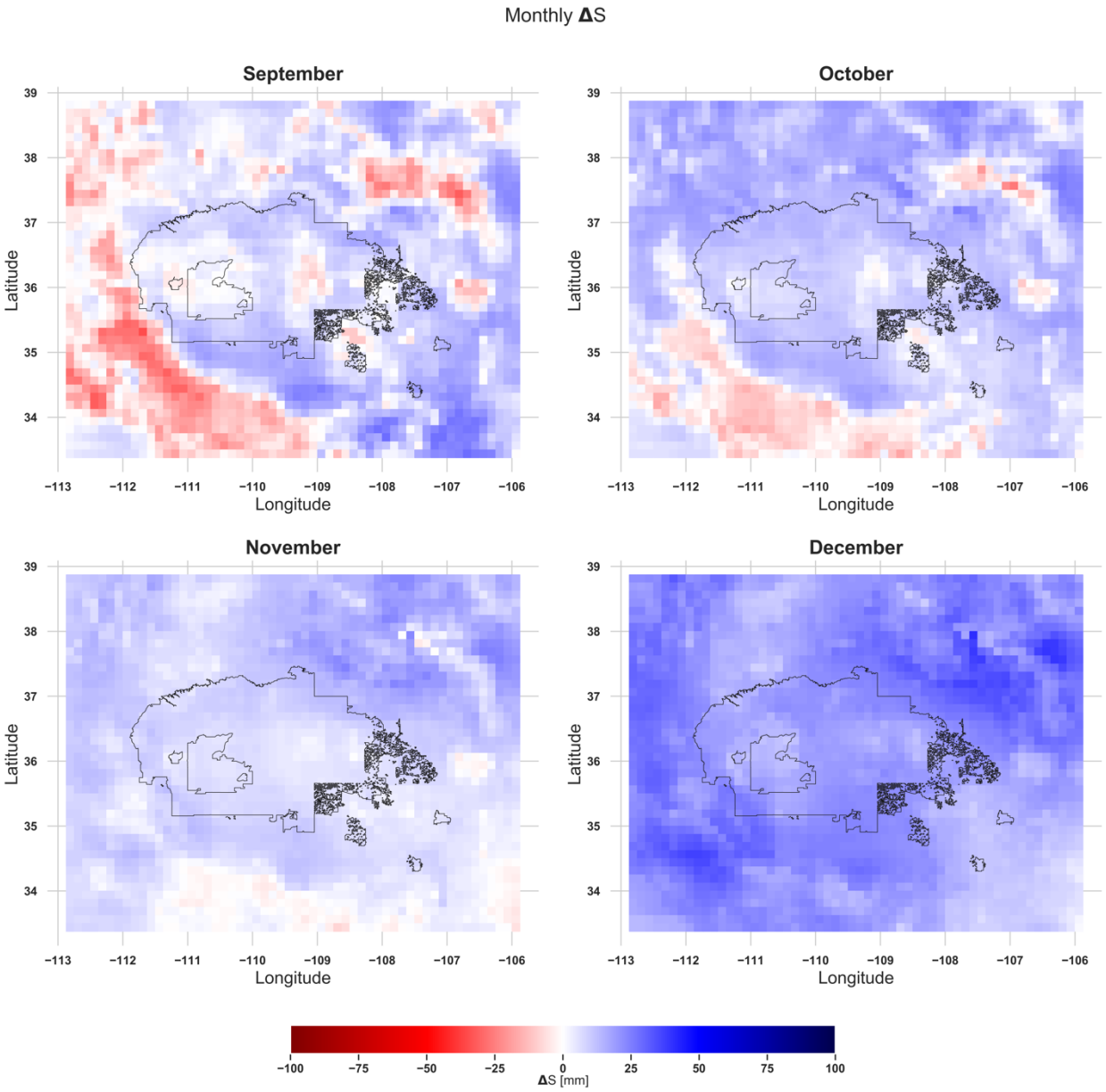

Figure 3.7. (continued).

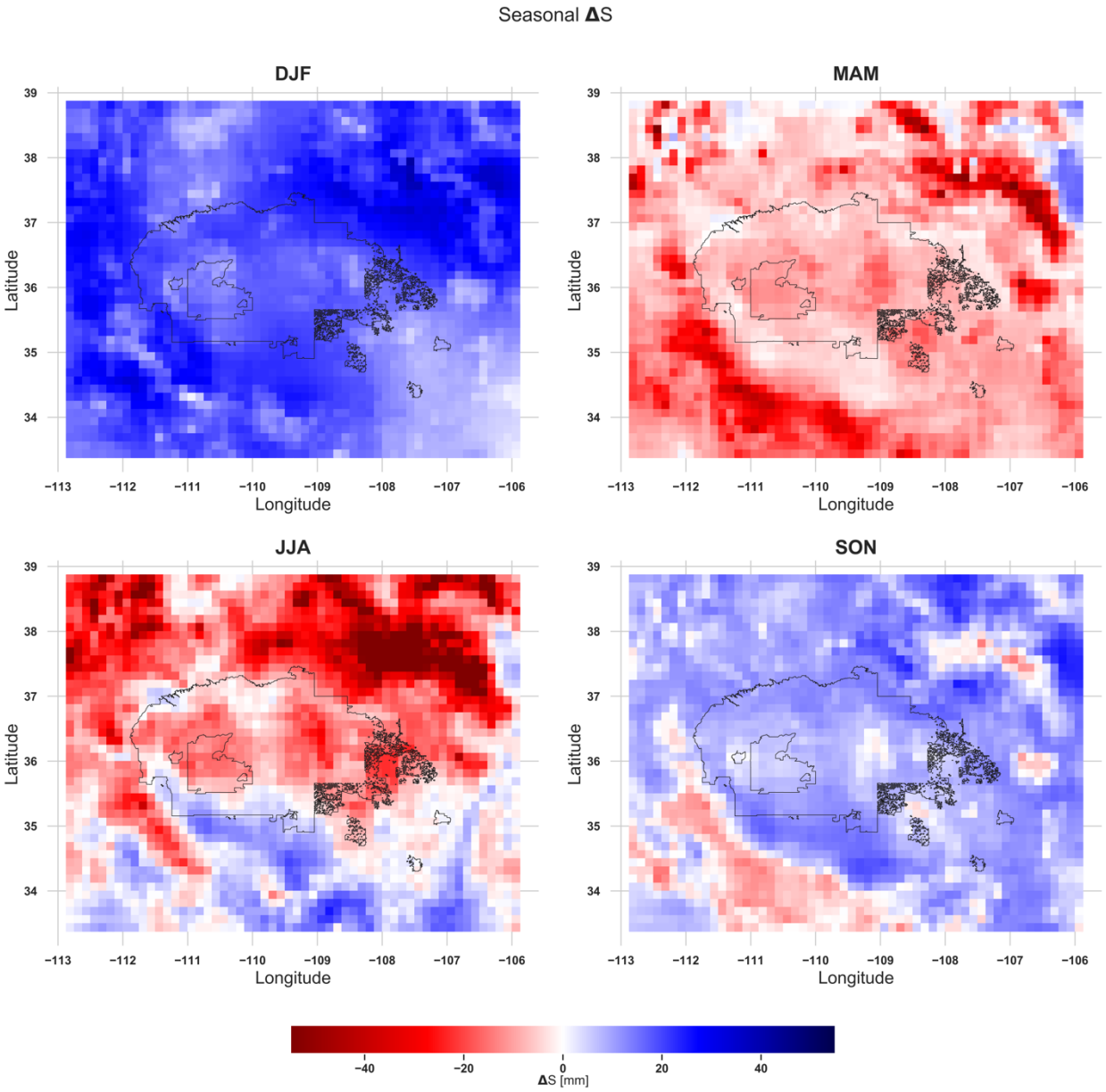

Figure 3.8. ΔS by season for the Navajo Nation and FCR on a 0.125º x 0.125º grid.

CHAPTER 4

UTILIZING SATELLITE OBSERVATIONS TO ESTABLISH A PRECIPITATION PER LIVESTOCK METRIC[3]

[3] Long, K. A. and Shepherd, J. S. (2020). Utilizing satellite observations to establish a precipitation per livestock metric. To be submitted to *Applied Geography.*

Abstract

The water security crisis on the Navajo Nation has deeply impacted *Diné* families. Furthermore, disappearing surface water reservoirs on the Navajo reservation have decreased the supply of water to farmers, ranchers, and *Diné* families that rely on livestock for income, food security, and cultural traditional practices. As a result, the Navajo energy-water-food nexus (EWFN) has become threatened and will continue to be in jeopardy in the future as a result of anthropogenic climate change. Satellite precipitation observations have provided scientists with a novel way to study the impacts of hydroclimate on the EWFN. Recently, impactful precipitation metrics have been developed using space-borne precipitation measurements to study the available precipitation for global human populations. In light of the Navajo water security crisis, a precipitation per livestock (PPL) metric is established as a "proof of concept" to contextualize water availability and water stress trends on the reservation as it relates to livestock populations. This research utilizes NASA's IMERG V06 Final Run and NLDAS-2 total evapotranspiration data to calculate an annual PPL metric and a seasonal precipitation-evapotranspiration-consumption metric. The annual PPL metric reveals that available precipitation for livestock is a function of the spatial trends in population and precipitation. The seasonal precipitation-evapotranspiration-consumption maps that serve as a proxy for water stress reveal that water surpluses and deficits are a function of temperature, where higher temperatures drive evapotranspiration and consumption rates that result in water deficits despite annual peak precipitation and/or lower livestock populations. The PPL metric serves as an instructive tool to evaluate water stress on the Navajo Nation and is a novel precipitation metric employing remotely-sensed precipitation data.

4.1 Introduction

The security, protection, and sustainability of the global energy-water-food nexus (EWFN) has become a critical area of research as populations continue to grow. While the largest rates of population growth are occurring in urban centers, demands for food, water, and energy are expected to increase worldwide. Projections from *The World Economic Forum Report* [2011] on global risk estimate that by 2040, demands for food, water, and energy will increase by 50%, 30%, and 40% respectively. The projected increases in food, water, and energetic demands will place additional strain on less-developed countries, making it difficult for these populations to adapt to these changes. Anthropogenic climate change is also expected to impact the EWFN. Climate change forced by greenhouse gas emissions is expected to increase food and water scarcity, which will ultimately drive prices for these commodities. As a result, developing countries and marginalized populations will experience the effects of future population growth, climatic changes, and shifts in demand disproportionately than their wealthier counterparts [*Bohle et al.*, 1994; *Groisman et al.*, 2001].

Hydroclimate is fundamental to EWFN function and vitality because precipitation inputs are inextricably linked to the function and interconnectedness of the synergistic relationships between each node in the EWFN. For example, inputs of energy and water are used in the production, processing, distribution, and consumption of food where energy production hinges on the availability of water and the supply and consumption of water require energy [*Shepherd et al.*, 2016]. From this example it is obvious that hydroclimate variability could potentially lead to significant impacts in the fluidity of the relationships between each branch of the EWFN and therefore should be taken into consideration when evaluating energy, water, and food security.

Remotely sensed data have been used to monitor the global EWFN from a hydroclimate perspective. NASA's space-borne precipitation observations have been utilized by several studies to identify the impacts of hydroclimate on urban centers, water availability, and gross/net primary production for agriculture [*Zhao and Running*, 2010; *Shepherd et al.*, 2013; *Stout et al.*, 2015; *Mitra and Shepherd*, 2016; *Shepherd et al.*, 2016; *Basheer et al.*, 2018]. In an effort to understand urban water stress, demands, and availability on a global scale, a novel precipitation metric has been developed [*Shepherd et al.*, 2016; *Haupt et al.*, 2019]. The authors established a Precipitation Per Person (PPP) metric that utilized NASA's Global Precipitation Measurement (GPM) remotely sensed precipitation observations in an effort to address global EWFN capabilities and vulnerabilities in the context of hydroclimate and urbanization.

While understanding the implications of hydroclimate on the EWFN in urban centers is significant, especially in light of future population projections, it is equally important to understand hydroclimate impacts on EWFN security in rural spaces and in developing and marginalized populations. The Navajo Nation, located on the semi-arid Colorado Plateau in the Four Corners Region of the southwestern United States, is currently facing a water security crisis. It is estimated that up to 40% of homes on the Navajo reservation lack potable water in their homes [*Navajo Nation Department of Water Resources*, 2000]. As a result of the current water scarcity on the Navajo reservation, socioeconomic issues, food insecurity, and energetic demands have increased. The median income for households in the Navajo Nation is $27,389, which is the lowest median income of any demographic in the country [*Arizona Rural Policy Institute*, 2010]. This means that many Navajo families will suffer from energy, water, and food security related issues disproportionately than other wealthier demographics.

Livestock populations are an essential component for the Navajo's economy and EWFN [*Henderson*, 1989; *Nania et al.*, 2014]. Cattle and sheep in particular contribute to enhanced food security on the Navajo Nation. Furthermore, cattle are often a significant source of income for some Navajo ranchers and farmers while horses and sheep are special markers for Navajo cultural identity and traditional practices [*McPherson*, 1998; *Benally*, 2011]. Navajo tradition teaches families to be morally obligated to care for their sheep herds and it is often said that "sheep are life" [*Witherspoon*, 1973]. Navajo also revere horses, which are considered highly valuable and sacred [*Roessel*, 1974]. However, overgrazing of the land in the early 20th century by large livestock populations inspired efforts spearheaded by Bureau of Indian Affairs (BIA) Commissioner John Collier to limit the head of livestock in the Livestock Reduction Act. The limitations on head counts of livestock still exist today to prevent overgrazing, where livestock head counts are enforced through permits. The livestock reduction efforts on the Navajo Nation have resulted in reduced sources of economic income and food security. Moreover, reduction efforts have also denied Navajo the ability to continue important cultural traditions and perpetuate significant cultural practices to future generations [*Henderson*, 1989; *McPherson*, 1998; *Benally*, 2011].

In order to maintain healthy livestock herds, animals require rangeland resources for grazing and also require access to reliable sources of water. The Navajo Nation Department of Agriculture estimated that the livestock on the reservation require between 1 to 2 million gallons of water a day [*Bureau of Reclamation*, 2018]. Currently, livestock populations rely on roughly 7,500 stock ponds supplied by surface water runoff and 1,200 windmill powered livestock wells that tap into shallow alluvial aquifers for sources of water [*Navajo Department of Water Resources*, 2011]. Unfortunately, many of these critical water resources for livestock are already

stressed and threatened. A withdrawal water supply stress index map from *Averyt et al.* [2013] shows that the watersheds encompassing the Navajo Nation exhibit indices >1.0, signaling that the demands for surface freshwater exceed the natural supply (Figure 4.1). These surface water resources that are already unable to provide sufficient supply become depleted during the summer when many of the surface stock ponds dry up as a result of increased evaporation rates from warm temperatures. These water sources are then unable to be replenished sufficiently in the fall, especially under drought conditions. The reduction of water in stock ponds in particular poses a unique threat to Navajo livestock food security as herds tend to congregate around water sources and forage for livestock sustenance can become rapidly depleted if water becomes scarce [*Nania et al.* 2014]. This emphasizes the vulnerability of Navajo food and water security that are highly susceptible to drought and changes hydroclimate.

In light of the large-scale water scarcity issue on the Navajo reservation, this research seeks to establish a novel precipitation per livestock (PPL) metric in order to assess the significance of hydroclimate on livestock populations. The PPL metric ultimately seeks to address the following questions:

1. What is the spatial distribution of available water from precipitation for livestock populations on the Navajo Nation?
2. How do seasonal changes in precipitation, evapotranspiration, and livestock water consumption dictate the spatial patterns of water deficits and surpluses on the Navajo Nation?

3. Can remotely sensed precipitation observations be useful in understanding the water demands for livestock populations, which are a critical component of the Navajo EWFN?

This research is motivated by current efforts to incorporate remotely sensed precipitation data in order to understand how hydroclimate can influence the interconnectedness of the EWFN where water availability is a key driver in the synergistic relationships between nodes. This metric is based off of the precipitation per person metric established by *Shepherd et al.* [2016] using NASA space-borne precipitation observations. This PPL metric is not meant to be a quantitative analysis of water availability, nor is it an exhaustive examination of a regional water budget. Instead, this innovative PPL metric is developed as a proof of concept and is intended to serve as an instructive tool to identify spatial trends in water demands on the reservation. Additionally, it aims to distinguish seasonal fluctuations in water surplus or deficits as a function of livestock populations while utilizing space-borne precipitation measurements to understand how precipitation influences the EWFN. In the following sections, geospatial analyses of annual PPL and seasonal water surpluses and deficits derived from precipitation-evapotranspiration-consumption of livestock are evaluated on a 0.1º x 0.1º grid.

4.2 Data and Methods

In the summer of 2019, NASA launched Integrated Multi-SatellitE Retrievals for GPM (IMERG) V06, which offers global precipitation estimates on a 0.1º x 0.1º grid. Data is made available for Early, Late, and Final runs which are available 4hrs, 14hrs, and 3.5 months after observation respectively [*Retrieved from*: https://giovanni.gsfc.nasa.gov/giovanni/; *Acker and Leptoukh*, 2007; *Huffman et al.*, 2019]. This research utilizes 16 years of precipitation data from

2001 to 2018 using NASA's IMERG V06 Final Run for annual and seasonal estimates. Precipitation data was collocated with the Food and Agriculture (FAO) 2010 Gridded Livestock of the World (GLW) datasets [*Gilbert et al.*, 2018] for cattle, horses, and sheep to produce PPL at a 0.1º x 0.1º resolution. These three species were chosen for the precipitation per livestock metric because due to the previously noted food security, cultural, and economic significances. The GLW dataset provides population data for individual species of livestock globally at 5-minute arc (~10km) resolution. The areal-weighted (AW) version of the GLW dataset was chosen as it derives population data from census polygons that are distributed homogenously [*Gilbert et al.*, 2018]. The GLW dataset is also available in a dasymetric (DA) version.

One important caveat to note in regard to the GLW dataset is that the sheep, horse, and cattle population data available for the Navajo Nation may be significantly under- or overrepresented. According to the United States Department of Agriculture's (USDA) National Agriculture Statistics Service (NASS) 2012 Census, the cattle population totals roughly 72,000 beef cattle, 51,000 horses, and 171,000 sheep on the Navajo Nation [*United States Department of Agriculture- National Agriculture Statistics Service*, 2012]. Numbers for the population totals in the GLW dataset for the Navajo Nation match up quite well for horses but exhibits an overrepresentation for cattle and a large underrepresentation for sheep. This large underrepresentation specifically of sheep may stem from many sources, including the issue of overstocking of sheep on the Navajo reservation. Overstocking has become a major issue on the Navajo reservation today. According to the Navajo Nation Livestock Inventory reported a total of 403,138 sheep while only 285,346 head were permitted [*United States Department of Agriculture*, 2007]. Overstocking of sheep is an ongoing problem that has been known to result in overgrazing of the landscape that ultimately contributes to desertification. While horse

populations matched up quite well between the USDA 2012 Agriculture Census and GLW dataset, it is estimated by the Bureau of Indian Affairs (BIA) that up to 60,000 feral horses roam the Navajo Nation [*Nania et al.*, 2014]. Further, the method of population estimates for livestock species in the AW version of the GLW dataset that spreads the average population over land that is appropriate for livestock may contribute to the population discrepancies. *Gilbert et al.* [2018] note that the AW version allows the population estimates to be independent of the influence of a variety of spatial variables but may produce more inexact populations.

Despite the discrepancies in accurate head counts of species population, it is important to be mindful of the fact that the primary goals of this PPL metric are to utilize the gridded geolocated livestock population dataset in combination with space-borne precipitation data as a proof of concept. The metric's primary purpose is to be used as an instructive tool to glean information about the spatial patterns of water availability for livestock to hypothesize the potential implications of hydroclimatic variability, especially in the context of anthropogenic climate change, rather than an accurate diagnostic and quantitative analysis of water security.

The annual precipitation used for this study was generated from average mm/day estimates from January 1, 2001- December 31, 2018 via the IMERG V06 Final Run product, which was then converted into tons/year. To produce the annual precipitation per livestock (PPL), the precipitation was divided by the combined population of cattle, horses, and sheep. Although this provides a novel metric of water availability for livestock based on precipitation, the actual natural supply of surface and groundwater reservoirs are balanced by precipitation, evapotranspiration, and runoff rates. A water budget is balanced between the inputs and outputs of water and can be described by the following equation:

$$\text{Precipitation} - \text{Runoff} - \text{Evapotranspiration} = \Delta\text{Storage} \quad (1)$$

Evapotranspiration rates can be exceedingly high in arid and semiarid regions, such as the environment the Navajo Nation is located in. Evaporation is the primary driver of hydrology in the region and is largely dependent upon moisture availability from precipitation [*Camacho Suarez et al.* 2015; Chapter 3]. To assess how water deficits and surpluses change throughout the year, precipitation-evapotranspiration-consumption maps are created on a seasonal basis. These maps are generated using the North American Land Data Assimilation System (NLDAS) VIC model evapotranspiration rate data from 2001-2018. NLDAS-2 data was retrieved from NASA'S Giovanni online data system which is developed and maintained by the NASA Goddard Earth Sciences (GES) Data and Information Services Center (DISC) [*Retrieved from*: https://giovanni.gsfc.nasa.gov/giovanni/; *Acker and Leptoukh*, 2007; *Mocko*, 2012; *Xia et al.*, 2012]. Species water consumption was based off of livestock water requirement data from *Meehan et al.* [2015]. In addition to the seasonal changes in precipitation and evapotranspiration that drive available water, seasonal changes in temperature can influence how much each species of livestock consumes water. Animal consumption of water is dependent on several parameters (i.e., species, weight, atmospheric temperature, etc.), which were taken into consideration when establishing species water consumption. In the seasonal analysis, larger amounts of water consumption were utilized in species calculations for seasons with higher average temperatures. A table of seasonal water consumption rates by species is found in Table 4.1.

4.3 Results

In the GLW dataset, the populations of cattle, horse, and sheep are roughly equal. It is important to reiterate that the species populations in the GLW dataset may present large under- or overrepresentations of the actual population on the Navajo Nation. The population maps for each species of animal as well as the total combined population of livestock for the Navajo Nation can be found in Figure 4.2. The cattle population is most dense in the southeastern portions of the reservation, and the population density decreases from east to west. The horse population is most dense in the central section of the reservation and the sheep population is more evenly distributed with higher population densities also in the center. In the combined total livestock population maps, the densest population of livestock animals is located in the middle of the reservation and the southeastern portions. The total livestock population distribution exhibits a decreasing trend moving westward. The least densely populated area for livestock species is found on the northern edge of the reservation (Figure 4.3).

The map of annual precipitation exhibits a broad area of relatively low precipitation in tons/year (Figure 4.4). This area extends from the northern edge of the reservation along the San Juan River and extends to the southerly edge of the reservation. There are also lower amounts of precipitation found in a latitudinal band across the central part of the Navajo reservation. Higher amounts of precipitation are found in the southwestern and southeastern corners as well as the most northern fringes of the reservation boundaries. Since these precipitation observations were derived from IMERG V06, it is important to note than in some regions of high complex terrain (i.e. Chuska Mountains), precipitation estimates may be significantly underestimated (Chapter 2).

To create the annual precipitation per livestock maps, the annual precipitation in ton/year was divided by the total livestock population. Figure 4.5 reveals that the largest amounts of PPL

are found along the northern fringes of the reservation as well as some plots southeast of the main portion of the reservation. Lower PPL is widespread throughout most of the reservation identified by the orange and red. Moderate precipitation amounts are available for the western portion of the reservation and along the eastern fringe. The low PPL correspond to the larger populations of livestock in these areas in combination with lower precipitation amounts. High PPL is also driven by population, where higher amounts are seen in less populated areas despite relatively lower annual precipitation.

While this paper seeks to identify trends in potential available water for Navajo livestock populations from precipitation through the annual PPL, a more advantageous method of determining water availability and revealing areas on the Navajo reservation where water stress may occur is to assess PPL on a seasonal basis and include considerations for evapotranspiration and consumption. As discussed in Chapter 3, evapotranspiration is a significant driver of water availability in the Four Corners Region and on the Navajo Nation and varies primarily as a function of seasonal temperatures and moisture from precipitation. The highest evapotranspiration rates occur in the summer as a result of warm temperatures and increased rainfall from the monsoon. High evapotranspiration rates drive deficits in the water balance throughout the reservation despite regional peak precipitation amounts from the North American Monsoon season (Chapter 2; Chapter 3).

Water consumption is also largely influenced by atmospheric temperatures. Average temperatures were derived from NLDAS temperature data. On average, temperatures in the summer are roughly 25ºC, -0.4ºC in the winter, and spring and fall averages are around 12.6ºC (Table 4.1). Temperatures throughout the reservation may vary significantly depending on elevation and large diurnal temperature swings may be present. For example, in the summer,

temperatures can reach well over 37ºC during daylight hours while dipping down to 10ºC overnight in clear conditions. High daytime temperatures characteristic of the summer months lead to increases of consumption of water during the day.

It is also important to consider consumption amounts of water by livestock species to understanding the distribution of water consumption in the livestock populations considered. Although the population for the three animal species in the GLW dataset is roughly equal, the consumption of water is not. Sheep consume less water (~1.4 gallons/day) while cattle and horses consume ~8.3 and ~9.5 gallons a day per individual animal. The annual water consumption by species assumes that on a yearly basis, individual cattle use roughly 3031.2 gallons/year (11.3 tons/year), horses use 3467.5 gallons/year (12.9 tons/year), and sheep use roughly 507.4 gallons/year (1.9 tons/year). From these numbers, it is clear that there will be insufficiencies in water availability from precipitation, resulting in increased regional water stress and demands. The seasonal precipitation-evapotranspiration-consumption maps aim to address the question of when and where these water deficits may arise.

Precipitation-evapotranspiration-consumption as a function of season reveals more about spatial water availability patterns throughout the year and can serve as a proxy for water stress (Figure 4.6). This analysis reveals that in DJF when the region experiences its secondary annual peak in precipitation as a result of the southward shift in the midlatitude storm track. Figure 4.7 shows the National Centers for Environmental Prediction (NCEP) North American Regional Reanalysis (NARR) composite mean 500mb geopotential heights for DJF and JJA between 2002 and 2018 [*Mesinger et al.*, 2006; available at https://psl.noaa.gov/]. In this reanalysis of composite 500mb geopotential heights, DJF shows the FCR upstream of a trough axis, resulting in increased precipitation to the region from the storm track. This is in contrast with the JJA

500mb geopotential height reanalysis where a strong ridge is present. In DJF when precipitation is enhanced and evapotranspiration and consumption rates are low due to lower temperatures, there is a widespread surplus of water (blue) for the entire reservation, signaling livestock water demands can be sufficiently met. During MAM where the precipitation is the lowest annually as the midlatitude storm track lifts out of the region and a dry regime from large scale ridging takes over, water stress is exacerbated by the warmer temperatures that drive evapotranspiration and consumption rates. As a result, much of the reservation has only slightly positive values (light green) for water availability, while areas in the central and southern portion of the reservation experience near zero water values (yellow). Some negative values crop up in the central portion of the reservation (orange) during MAM. By summer, daytime temperatures become exceedingly warm, driving evapotranspiration and livestock consumption rates up. While the North American Monsoon system brings the primary peak of annual precipitation to the region from July through September, straddling summer and fall seasons, the warm temperatures dictate water demands for livestock. In JJA, the largest surpluses of water are found along the boundaries of the reservation, where population of livestock is low. The largest deficits occur in the central and southern portions of the reservation, indicated by the bright orange and red. This coincides with large populations of livestock in these areas, where demand for water is high, especially during the summer. JJA exhibits the most widespread water stress for livestock populations. In SON, water availability begins to recover for much of the reservation except the central and southern portion, where again livestock populations are higher relative to other areas on the reservation. SON may also have increased water availability compared to MAM as a result of the monsoon bringing precipitation to the region through September and evapotranspiration and consumption rates declining as a result of declining temperatures. The decreased amounts of water that are

consistently found in the central southern portion of the reservation in MAM, JJA, and SON may also be influenced by locally higher evapotranspiration rates as seen in (Chapter 3) in combination with more densely populated livestock.

4.4 Discussion and Conclusion

This research establishes the first precipitation per livestock (PPL) metric based on remotely sensed precipitation observations. The PPL metric is created for the Navajo Nation utilizing NASA's Integrated Multi-SatellitE Retrievals for GPM (IMERG V06) Final Run, NLDAS evapotranspiration data, and consumption rates of three species based on livestock populations from the Global Livestock of the World (GLW) dataset. The PPL metric is based on Sh*epherd et al.*'s [2016] Precipitation Per Person (PPP) metric where the authors established precipitation metrics per capita to understand trends in water availability and stress globally in the context of urban areas. PPL is intended to provide similar insights on water availability and water stress, but for the Navajo's livestock population. This research is insightful because it not only considers the precipitation input, but also the seasonal consumption rates of the livestock demands that drive water demands. Cattle, horses, and sheep provide food security for some Navajo families and are economically and culturally valuable. Livestock are ultimately tied to the Navajo EWFN and are vulnerable to changes in hydroclimate, especially given the current issues with water scarcity on the Navajo reservation. This research applies space-borne precipitation observations to assess the spatial patterns of annual water availability and seasonal changes to water stress that contribute to the security and synergy of the EWFN on the Navajo reservation. The application of remotely sensed precipitation observations to assess EWFN in

other countries and on a global scale has been an ongoing effort, and this research attempts to apply these methods to address EWFN needs on the Navajo Nation.

In the annual PPL maps, available precipitation for livestock is a function of the spatial precipitation patterns and population distribution. The annual PPL maps are significant to understanding the natural hydroclimatic input of precipitation to meet basic livestock water demands. Seasonal precipitation-evapotranspiration-consumption maps on the Navajo Nation highlights the impact of seasonal temperatures that result in significant impacts to water stress due to increases in evapotranspiration rates and species consumption rates, where animals tend to consume more water in warmer temperatures. The significance of atmospheric temperature influence on water stress is supported by the fact that precipitation in the region is bimodal, where a significant portion of precipitation occurs in the summer and early fall from the North American Monsoon system and a secondary peak is found in winter. Seasonal precipitation-evapotranspiration-consumption maps reveal that despite a peak in annual precipitation during July, August, and September, significant deficits in available water, particularly in JJA in the central and southern portions of the Navajo reservation, are evident. The precipitation-evapotranspiration-consumption maps during JJA is in stark contrast with DJF when the secondary peak in precipitation occurs but there are widespread water surpluses on the reservation. The significant difference between the two seasons despite similar precipitation amounts is due to the increased evapotranspiration rates and consumption rates with increasing temperature. MAM and SON PPL are driven by a combination of both precipitation and temperature, which again is inextricably linked to evapotranspiration and consumption rates. MAM experiences broad deficits across the Navajo Nation as a result of sparse precipitation during spring and warming temperatures (12.1ºC). SON has a slightly higher temperature

(13.1ºC) but the monsoon seasons continues through September which lends to the higher water amounts during this season. Since fall and spring have similar temperatures, this suggests that differences in available water during these two seasons depends more on precipitation amounts. With that said, overall temperature seems to be a significant environmental driver in seasonal variation in water availability as it influences evapotranspiration and livestock consumption rates, with precipitation being a secondary factor.

While this novel precipitation metric can be instructive, there are sources of error that present potentially significant limitations to this study. The low spatial resolution of the GLW dataset compared to the high resolution of the precipitation and evapotranspiration datasets may produce inaccurate estimates of available water introduced by downscaling methods. Additionally, the GLW dataset produces population numbers that vary significantly with other documented species populations from the USDA and BIA, which may be a result of the methods in which livestock populations are derived in the areal-weighted (AW) version of the GLW dataset as well as overstocking issues [*United States Department of Agriculture*, 2007; *Nania et al.*, 2014; *Gilbert et al.*, 2018]. Furthermore, Chapter 2 of this dissertation establishes the limitations to the IMERG V06 Final Run product that may result in precipitation estimates being over- or underestimated depending on location and elevation. While there are some noteworthy limitations to the precipitation per livestock metric, this paper serves as a successful proof of concept. The PPL metric within this chapter is a prototype and future iterations will address the limitations that have been identified within this research.

The results of this paper will become increasingly more important in the context of anthropogenic climate change. Projections of human-induced climate change scenarios due to greenhouse gas forcing show potential alterations to the hydroclimate regime of the American

southwest. The region is expected to become drier from an increase in the frequency and duration of severe droughts, surface water resources are expected to decrease, and projected increased temperatures will contribute to increased evapotranspiration rates and will likely increase livestock water consumption rates [*Zekster et al.*, 2005; *Cayan et al.*, 2010; *MacDonald*, 2010; *Seager and* Vecchi, 2010; *Seager et al.*, 2013]. As a result of increased temperatures and increased droughts episodes, seasonal precipitation-evapotranspiration-consumption may become significantly altered and the increased water demands will contribute to widespread water deficits. In light of anthropogenic climate change, water availability for livestock is likely to change and will contribute to an increased risk of unmet livestock water demands.

Already, water security is a considerable threat to the Navajo, and that threat is expected to increase as a result of future climate change projections and hydroclimatic variability. The threat to water security will result in significant impacts to the livestock population and threaten Navajo EWFN security, leaving the Navajo Nation even more vulnerable to climate change. The decreased water availability for livestock will have substantial negative impacts to many Navajo families' source of income and food security, presenting many challenges to families in the face of climate change. Furthermore, water scarcity will contribute to a significant loss in Navajo cultural identity and way of life. Water scarcity for livestock populations, especially sheep, will risk the perpetuation of the Navajo cultural traditions to future generations, and may force more livestock reductions that have already harmed Navajo way of life.

Table 4.1. Species water consumption estimates by season. Some species consumption rates do not fluctuate as much as others. For example, horses require relatively the same amount of water a day until the temperatures get quite warm and consumption rates can increase dramatically, especially if the horse is active.

	DJF	**MAM**	**JJA**	**SON**
Temperature	-0.4ºC	12.1ºC	25ºC	13.1ºC
Daily Cattle Consumption	7.1 gal	8.3 gal	12.1 gal	8.3 gal
Daily Horse Consumption	9.5 gal	9.5 gal	17.2 gal	9.5 gal
Daily Sheep Consumption	1.02 gal	1.4 gal	1.8 gal	1.4 gal

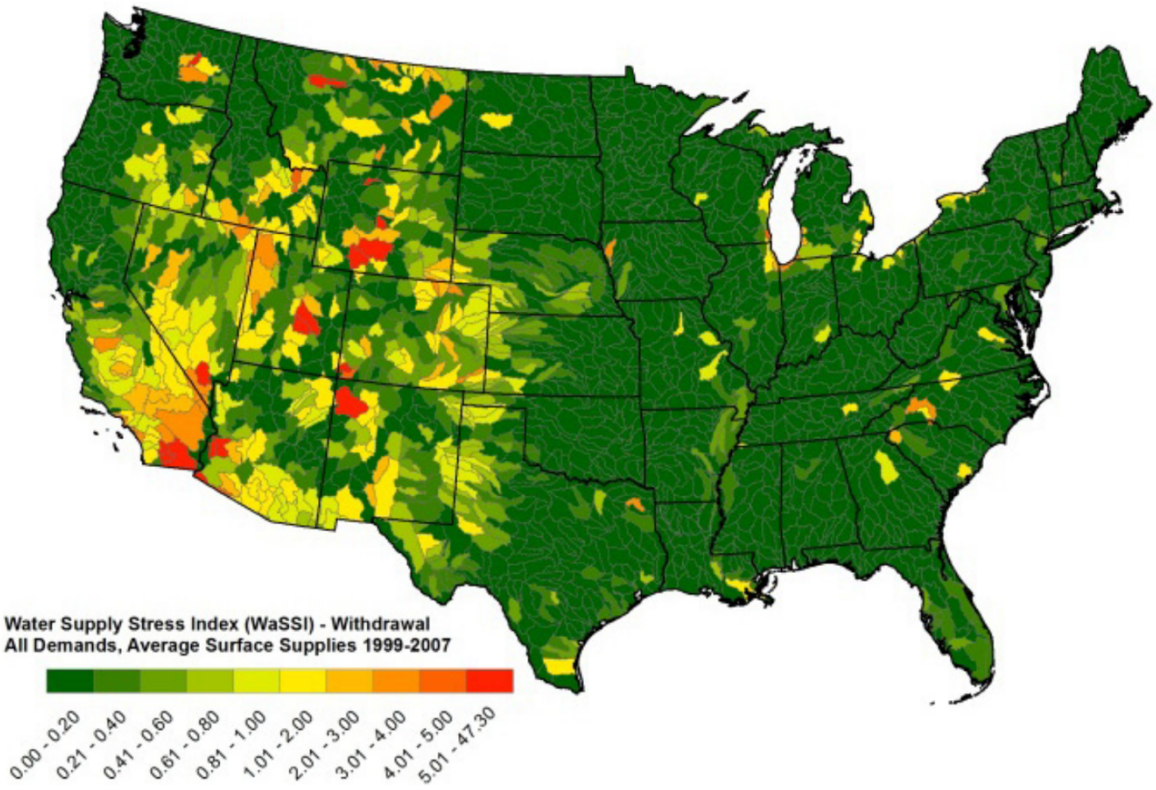

Figure 4.1. A map of withdrawal water supply stress index map that identifies watersheds where freshwater demands exceed supply. This image is reproduced from *Averyt et al.* [2013], with permission granted by the Institute of Physics copyright policy: https://iopscience.iop.org/page/copyright_notice.

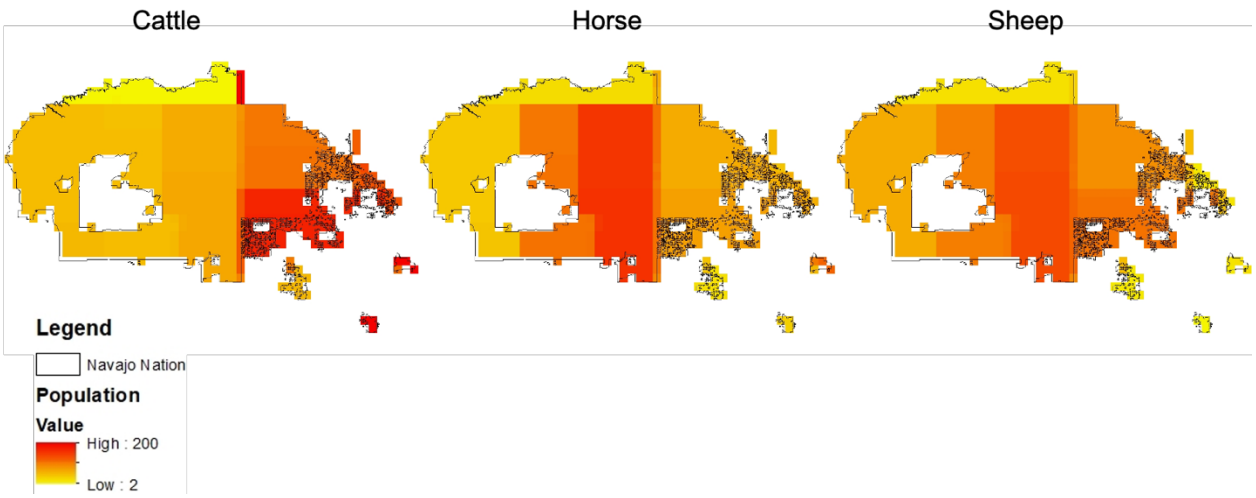

Figure 4.2. Maps of the cattle, horse, and sheep populations within the Navajo Nation on a 0.1º x 0.1º grid.

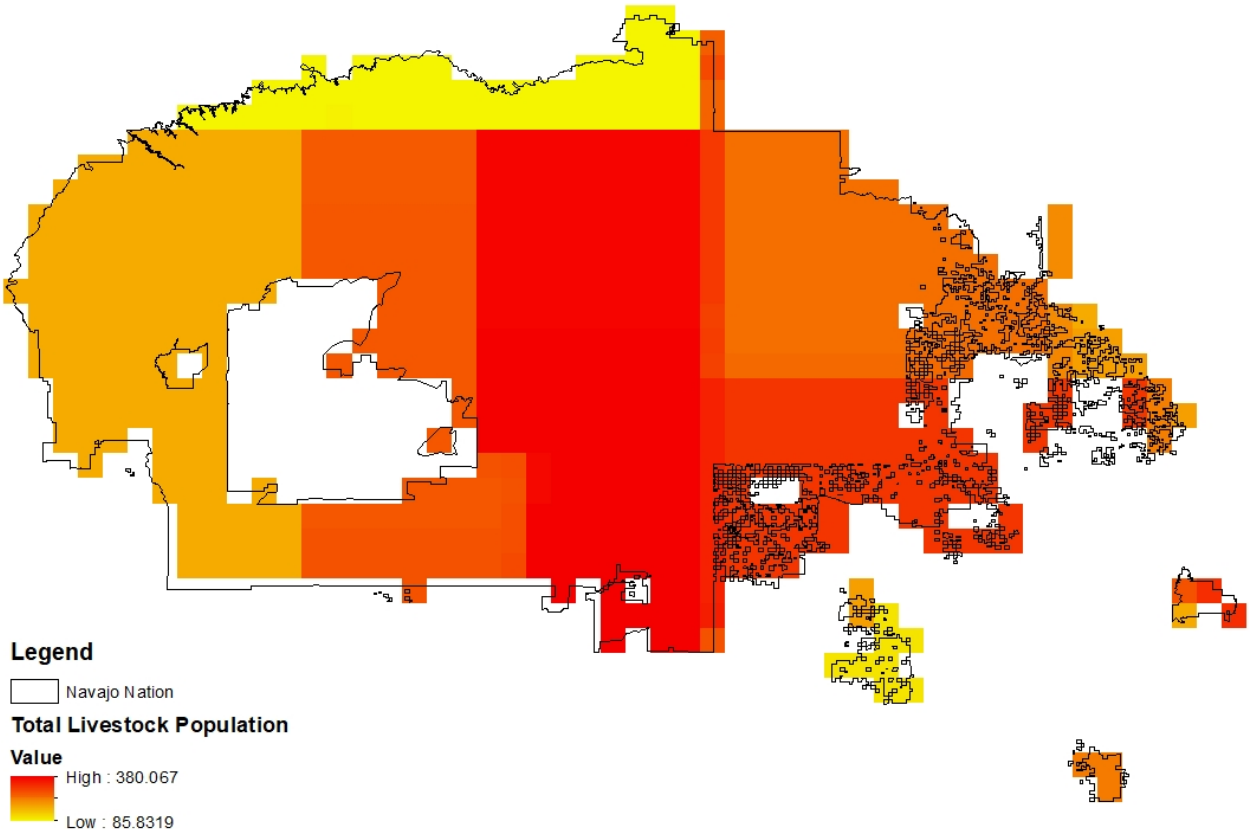

Figure 4.3. Map of the total (combined head counts of cattle, horse, and sheep) livestock population within the Navajo Nation on a 0.1º x 0.1º grid.

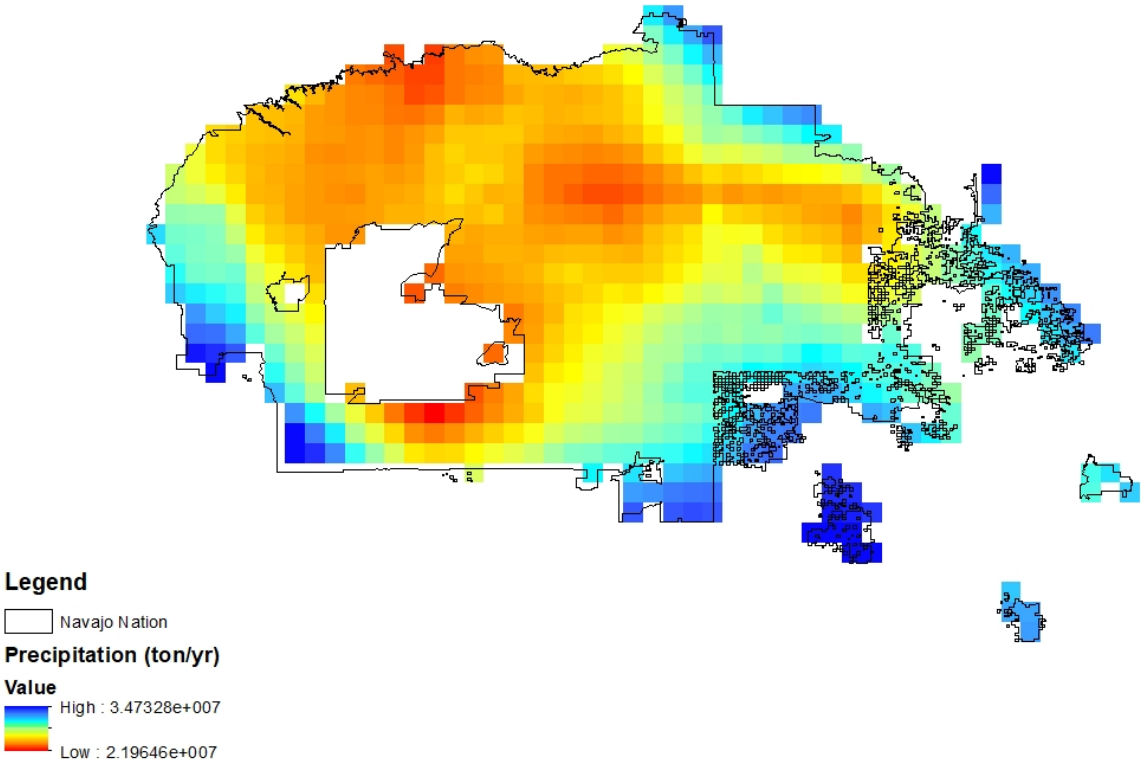

Figure 4.4. Average annual precipitation between 2002-2018 from IMERG V06 on a 0.1º x 0.1º grid in tons/year.

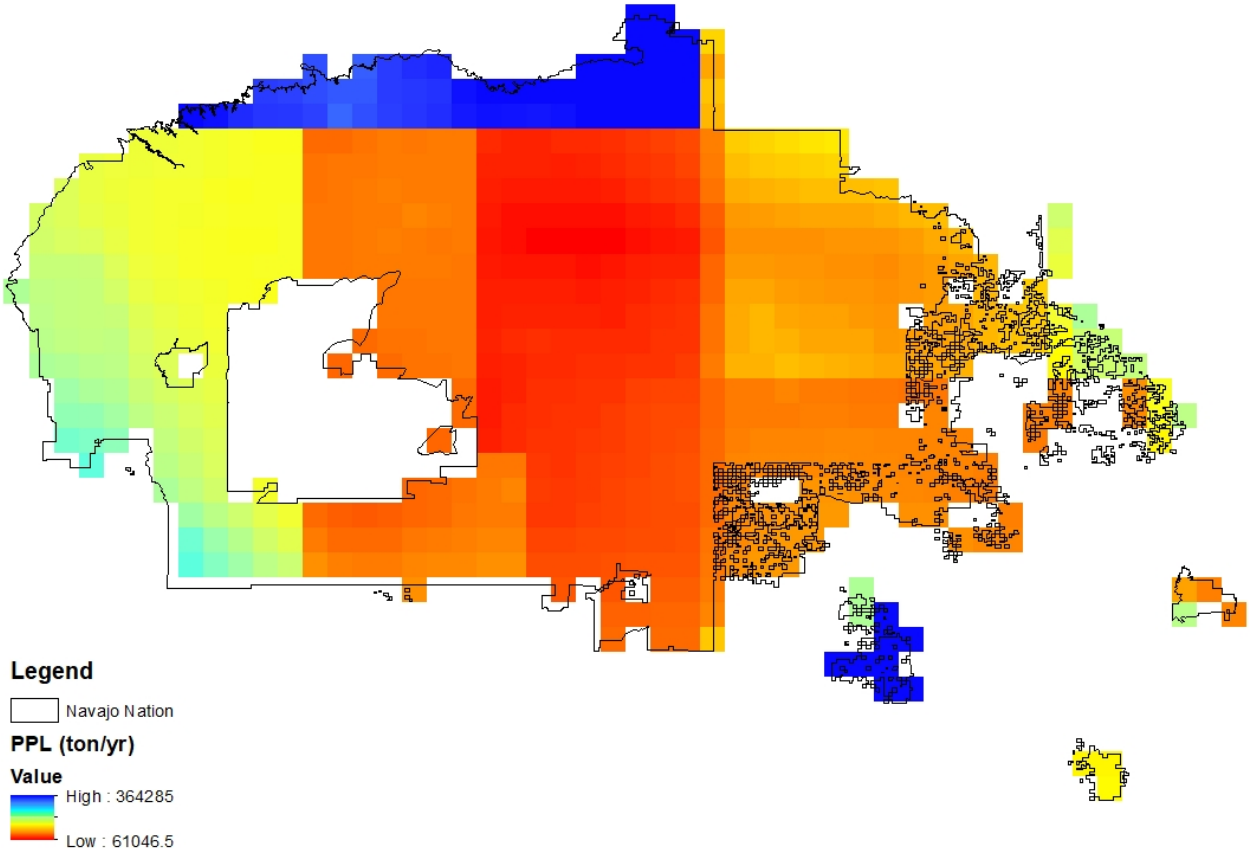

Figure 4.5. Annual precipitation per livestock (PPL) in tons/year on the Navajo Nation on a 0.1º x 0.1º grid. PPL is calculated as the annual average precipitation divided by the total (combined head counts of cattle, horse, and sheep) livestock population.

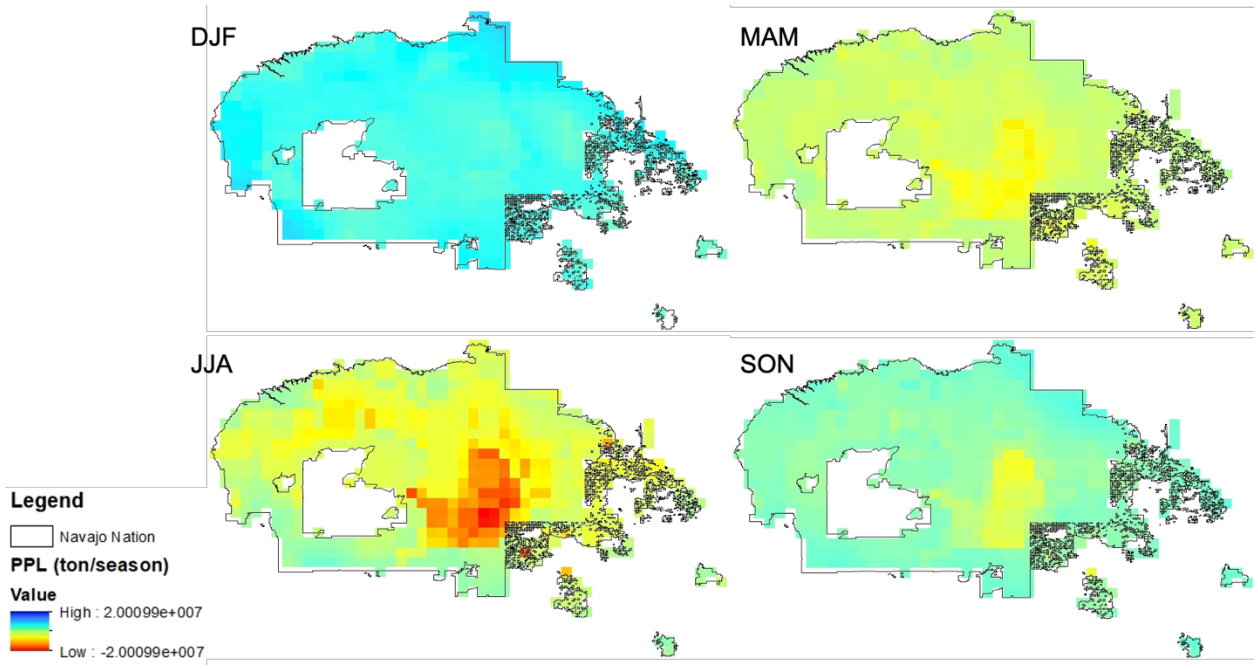

Figure 4.6. Seasonal precipitation-evapotranspiration-consumption maps in tons/season on the Navajo Nation on a 0.1º x 0.1º grid. Blue colors indicate surpluses, red colors indicate deficits, and yellow colors indicate a balance in water availability.

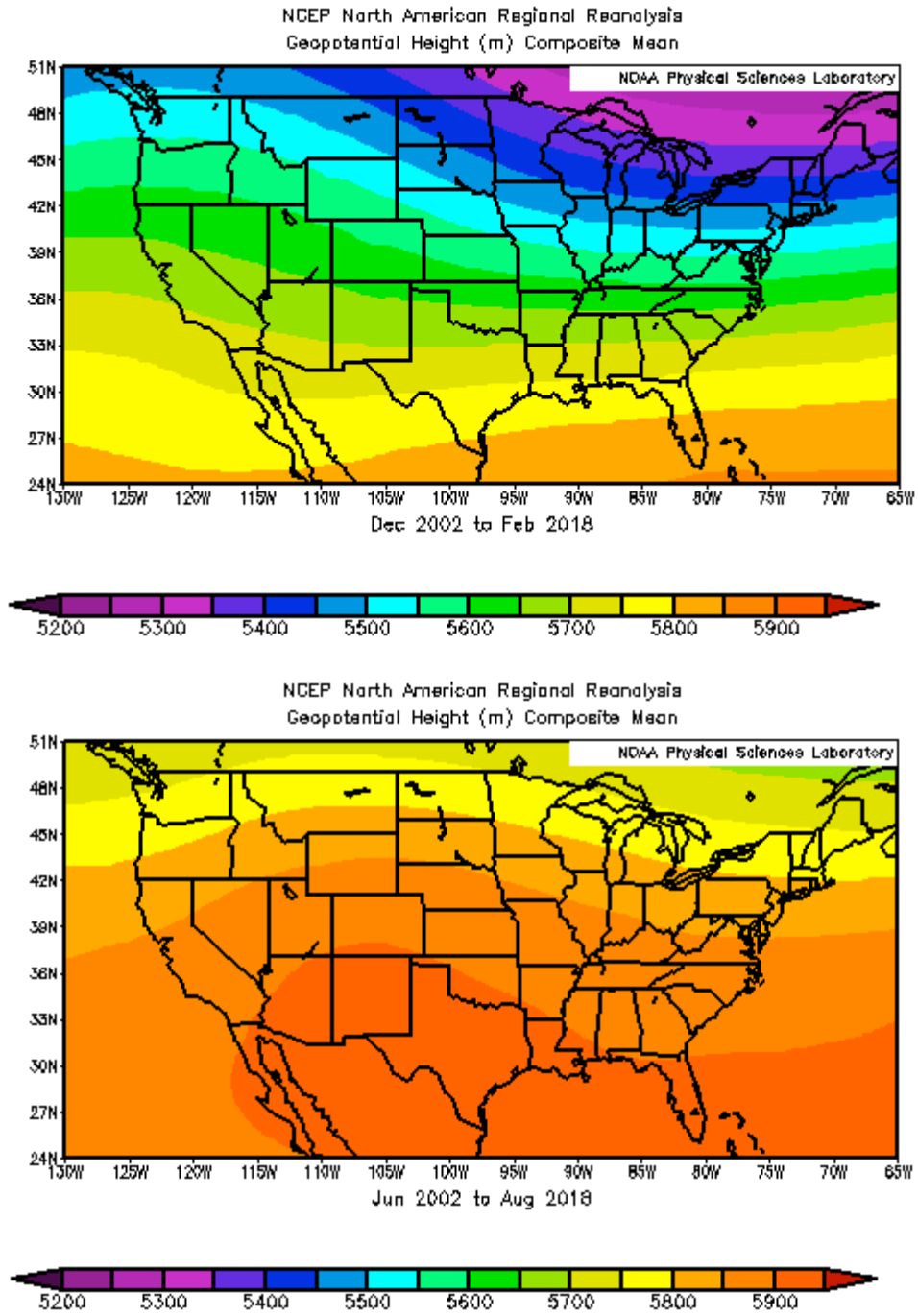

Figure 4.7. NCEP North American Regional Reanalysis (NARR) of composite mean 500mb geopotential heights for DJF and JJA between 2002 and 2018. DJF shows the FCR in a more active storm pattern than in JJA. NCEP Reanalysis data provided by the NOAA/OAR/ESRL PSL, Boulder, Colorado, USA, from their Web site at https://psl.noaa.gov/.

CHAPTER 5

CONCLUSION

This dissertation seeks to address the water security issues facing the Navajo Nation in the Four Corners Region (FCR) of the southwestern United States through remotely sensed precipitation measurements. The manuscripts within show that NASA IMERG V06 Final Run precipitation observations can be used as a tool to monitor precipitation and water resources, which are critical to the synergistic relationships between the energy-water-food nexus (EWFN) nodes. Through an exhaustive analysis of a satellite-derived precipitation measurement product performance, a geospatial water budget analysis, and an establishment of a novel precipitation per livestock (PPL) metric, the research in this dissertation provides a greater understanding of water availability, demands, and stress on the Navajo Nation and in the surrounding FCR. This dissertation's manuscripts will add to the growing scientific efforts to better understand and monitor hydroclimate as it relates to water resources for the Navajo Nation that equips the Navajo with a space-borne precipitation monitoring dataset, a detailed spatial analysis of the water budget, and proposes a new instructive precipitation metric to better meet the water demands of livestock populations. This research is executed in hopes of improving water security, that ultimately influences energy, food, and economic security for the Navajo as well as providing information on local hydroclimate that are likely to be impacted by future anthropogenically forced climate change scenarios.

The first manuscript in this dissertation (Chapter 2) provides an exhaustive analysis of NASA IMERG V06 Final Run. The satellite precipitation product is validated with Parameter-Elevation Regressions on Independent Slopes Model (PRISM) data to assess the performance of the product in the region. This manuscript demonstrates that the IMERG V06 Final Run product performs reasonably well in the summer when the region experiences warm temperatures and the North American Monsoon (NAM). Performance diminishes in the winter cool months, especially in elevations that are greater than 2500m. This is likely tied to the handling of precipitation phase by IMERG. The product is found to generally produce small to moderate overestimates in the study area, and can therefore be used as a monitoring tool for precipitation input as it relates to water resources and drought conditions. However, extreme underestimates were found in regions of high elevation (>2500m) where IMERG V06 Final Run cannot be utilized confidently for water monitoring purposes.

In the second manuscript (Chapter 3), a high-resolution geospatial analysis of the water budget is performed using IMERG V06 Final Run precipitation estimates and NLDAS-2 total evapotranspiration and runoff data. This research is novel as it utilizes remotely sensed precipitation data from NASA's newest version of IMERG and also provides a detailed analysis for the Navajo Nation and surrounding FCR. This research includes the greater FCR because the Navajo Nation does have rights to large surface water features such as the Colorado and San Juan Rivers whose streamflow is dependent upon snowmelt from high elevations mountain ranges (i.e. San Juan and Rocky Mountains). The geospatial water budget analysis revealed that the annual water storage, ΔS, is dominated by evapotranspiration processes that are driven by moisture availability (i.e. precipitation) as well as vegetation, which is elevation dependent. The winter was found to be the most critical season for ΔS since evapotranspiration rates are low. ΔS

becomes largely negative through the spring until the onset of the NAM. While NAM provides some replenishment of ΔS from precipitation, evapotranspiration rates are still high, which keeps ΔS low compared to winter despite the peak in precipitation. ΔS does not begin to recover until the fall when temperatures cool and evapotranspiration rates decrease. The seasonal analysis of total evapotranspiration, runoff, and ΔS reveal the spatial patterns and breakdown of the water budget. DJF and SON experience widespread surpluses of ΔS in the region while MAM and JJA experience large deficits. These results are vital to understanding the impacts of changes in hydroclimate for the Navajo Nation. Alterations to precipitation regimes from anthropogenic climate change as a result of increases in the frequency and magnitude of severe drought episodes and increases in temperature that will drive evapotranspiration rates will exacerbate the natural interannual variability of climate in the region. Having knowledge of the spatial patterns in ΔS will allow for the Navajo to better prepare for future hydroclimate change on a localized scale.

The final manuscript in this dissertation (Chapter 4) establishes a novel precipitation metric to evaluate the water availability for the Navajo livestock population. The precipitation per livestock (PPL) metric provides an instructive analysis of the annual water demands expected for Navajo livestock that provide economic income, enhance food security, and are central to traditional practices. The annual PPL reveals that available precipitation to support the water demands for livestock is a function of precipitation and population patterns. Areas of higher PPL generally have higher precipitation and lower livestock population. Low PPL is widespread throughout the central part of the reservation where livestock populations are high and precipitation is lower relative to other portions of the reservation. The precipitation-evapotranspiration-consumption maps reveal the surpluses and deficits of available water from

precipitation for livestock populations as a function of seasonal atmospheric temperature. Evapotranspiration and consumption rates are largely influenced by temperature where higher temperatures result in higher rates. The seasonal precipitation-evapotranspiration-consumption maps underscore the water stress incurred as a function of the warm daytime atmospheric temperatures that the FCR is characterized by in the summer that drive water demand for livestock populations. The PPL metric ultimately serves as an instructive tool to evaluate water stress on the Navajo Nation and is a novel precipitation metric employing remotely-sensed precipitation data to study the impacts of hydroclimate on a critical component of the energy-water-food nexus.

The research conducted in this dissertation largely focuses on the hydroclimate of the Navajo Nation and surrounding region. This research adds to the growing body of scientific literature that seeks to address hydroclimate monitoring on the Navajo reservation and in the greater FCR. The results of the manuscripts in this dissertation provide the Navajo with the knowledge of the behavior of a remotely sensed precipitation dataset that can be used to monitor precipitation, water resources, and drought conditions. It also provides the Navajo with a greater understanding of the localized impacts of the water budget so that it will be easier to identify areas of need, especially during periods of drought. The PPL metric identifies the basic water demands of livestock from precipitation while the seasonal precipitation-evapotranspiration-consumption maps provide a water stress guide to establish when and where water deficits and surpluses occur as a function of precipitation. These efforts aim to increase Navajo EWFN security by incorporating remotely sensed precipitation data to understand hydroclimate trends and patterns for the Navajo Nation. While this research aimed to establish baseline information of hydroclimate, the behavior of satellite-derived precipitation measurements in the region, and

the development of a prototype of a precipitation metric, it is important that the results from the manuscripts in this dissertation are eventually conveyed to Navajo stakeholders. The research in this dissertation was conducted with the goal of becoming more knowledgeable of the hydroclimate in the region and to uncover the strengths and limitations of novel remotely sensed tools and metrics that can be utilized effectively to monitor water resources in the region. Future collaboration with Navajo stakeholders, particularly the Navajo Nation Department of Water Resources, as well as Navajo farmers and ranchers, will ideally be sought to continue efforts in gaining a better understanding of water resource monitoring for the Diné.

REFERENCES

Acker, J. G., and Leptoukh, G. (2007). Online analysis enhances use of NASA earth science data. *Eos, Transactions American Geophysical Union*, *88*(2), 14-17, doi:https://doi.org/10.1029/2007EO020003.

Adams, D. K., and Comrie, A. C. (1997). The north American monsoon. *Bulletin of the American Meteorological Society*, *78*(10), 2197-2214, doi:https://doi.org/10.1175/1520-0477(1997)078<2197:TNAM>2.0.CO;2.

Adang, T. C., and Gall, R. L. (1989). Structure and dynamics of the Arizona monsoon boundary. *Monthly Weather Review*, *117*(7), 1423-1438, doi:https://doi.org/10.1175/1520-0493(1989)117<1423:SADOTA>2.0.CO;2.

Albrecht, T., Crootof, A., Scott, S. (2018). The Water-Energy-Food Nexus: A systematic review of methods for nexus assessment. *Environmental Research Letters*, *13*(4), 043002, doi:https://orcid.org/0000-0001-5114-8265.

Andrade Jr., E. R., and Sellers, W. D. (1988). El Niño and its effect on precipitation in Arizona and western New Mexico. *Journal of Climatology*, *8*(4), 403-410, doi:https://doi.org/10.1002/joc.3370080407.

Anjum, M. N., et al. (2019). Assessment of IMERG-V06 precipitation product over different hydro-climatic regimes in the Tianshan Mountains, North-Western China. *Remote Sensing*, *11*(19), 2314, doi: https://doi.org/10.3390/rs11192314.

Arizona Rural Policy Institute. (2010). Demographic analysis of the Navajo Nation using 2010 Census and 2010 American Community Survey estimates. Retrieved from http://gotr.azgo vernor.gov/sites/default/files/navajo_nation_0.pdf.

Averyt, K., Meldrum, J., Caldwell, P., Sun, G., McNulty, S., Huber-Lee, A., and Madden, N. (2013). Sectoral contributions to surface water stress in the coterminous United States. *Environmental Research Letters*, *8*(3), 035046, doi: 10.1088/1748-9326/8/3/035046.

Barlow, M., Nigam, S., and Berbery, E. H. (1998). Evolution of the North American monsoon system. *Journal of Climate*, *11*(9), 2238-2257, doi:https://doi.org/10.1175/1520-0442(1998)011<2238:EOTNAM>2.0.CO;2.

Barnett, T. P., Adam, J. C., and Lettenmaier, D. P. (2005). Potential impacts of a warming climate on water availability in snow-dominated regions. *Nature*, *438*(7066), 303-309, doi:https://doi.org/10.1038/nature04141.

Barnett, T. P. et al. (2008). Human induced changes in the hydrology of the western United States. *Science*, *316*(5866):1080–1083, doi:10.1126/science.1152538.

Basheer, M., Wheeler, K. G., Ribbe, L., Majdalawi, M., Abdo, G., and Zagona, E. A. (2018). Quantifying and evaluating the impacts of cooperation in transboundary river basins on the Water-Energy-Food nexus: The Blue Nile Basin. *Science of the Total Environment*, *630*, 1309-1323, doi:https://doi.org/10.1016/j.scitotenv.2018.02.249.

Behrangi, A., Bormann, K. J., and Painter, T. H. (2018). Using the Airborne Snow Observatory to assess remotely sensed snowfall products in the California Sierra Nevada. *Water Resources Research*, *54*(10), 7331-7346, doi:https://doi.org/10.1029/2018WR023108.

Benally, M. (2011). Bitter Water: Diné oral histories of the Navajo-Hopi land dispute. Tucson, AZ: University of Arizona Press.

Benson, L., Petersen, K., and Stein, J. (2007). Anasazi (pre-Columbian Native-American) migrations during the middle-12th and late-13th centuries–were they drought induced?. *Climatic Change*, *83*(1-2), 187-213, doi:https://doi.org/10.1007/s10584-006-9065-y.

Blöschl, G., Sivapalan, M., Wagener, T., Viglione, A., and Savenije, H.: Runoff prediction in ungauged basins, Cambridge University Press, 2013.

Blumenfeld, J. (2015, September 29). From TRMM to GPM: The Evolution of NASA Precipitation Data. Accessed on June 10, 2019. Retrieved from https://earthdata.nasa.gov/learn/articles/tools-and-technology-articles/trmm-to-gpm.

Blumenfeld, J. (2020). Using NASA Earth Science Data to Help Manage Water Resources in the Navajo Nation: A Data Chat with Vickie Ly. Accessed February 20, 2020. Retrieved from https://earthdata.nasa.gov/learn/data-chat/data-chat-vickie-ly.

Bohle, H. G., Downing, T. E., and Watts, M. J. (1994). Climate change and social vulnerability: toward a sociology and geography of food insecurity. *Global Environmental Change*, *4*(1), 37-48, doi:https://doi.org/10.1016/0959-3780(94)90020-5.

Boushaki, F. I., Hsu, K. L., Sorooshian, S., Park, G. H., Mahani, S., and Shi, W. (2009). Bias adjustment of satellite precipitation estimation using ground-based measurement: A case study evaluation over the southwestern United States. *Journal of Hydrometeorology*, *10*(5), 1231-1242, doi:https://doi.org/10.1175/2009JHM1099.1.

Brooks, R., and Corey, T. (1964). HYDRAU uc properties of porous media. *Hydrology Papers, Colorado State University*, *24*, 37.

Bureau of Reclamation. (2018). Colorado River Basin Ten Tribes Partnership Tribal Water Study Report. Accessed April 16, 2020. Retrieved from https://www.usbr.gov/lc/region/programs/crbstudy/tws/finalreport.html.

Camacho Suarez, V. V., Saraiva Okello, A. M. L., Wenninger, J. W., and Uhlenbrook, S. (2015). Understanding runoff processes in a semi-arid environment through isotope and

hydrochemical hydrograph separations. *Hydrology and Earth System Sciences*, *19*(10), 4183-4199, doi:10.5194/hess-19-4183-2015.

Carleton, A. M. (1986). Synoptic-dynamic character of 'bursts' and 'breaks' in the South-West US summer precipitation singularity. *Journal of Climatology*, *6*(6), 605-623, doi:https://doi.org/10.1002/joc.3370060604.

Carleton, A. M. (1987). Summer circulation climate of the American Southwest, 1945–1984. *Annals of the Association of American Geographers*, *77*(4), 619-634, doi:https://doi.org/10.1111/j.1467-8306.1987.tb00184.x

Carleton, A. M., Carpenter, D. A., and Weser, P. J. (1990). Mechanisms of interannual variability of the southwest United States summer rainfall maximum. *Journal of Climate*, *3*(9), 999-1015, doi:https://doi.org/10.1175/1520-0442(1990)003<0999:MOIVOT>2.0.CO;2.

Carrillo, C. M., Castro, C. L., Woodhouse, C. A., and Griffin, D. (2016). Low-frequency variability of precipitation in the North American monsoon region as diagnosed through earlywood and latewood tree-ring chronologies in the southwestern US. *International Journal of Climatology*, *36*(5), 2254-2272, doi:https://doi.org/10.1002/joc.4493.

Cayan, D. R., and Webb, R. H. (1992). El Niño/Southern Oscillation and streamflow in the western United States. Cambridge University Press, 29-86.

Cayan, D. R. (1996). Interannual climate variability and snowpack in the western United States. *Journal of Climate*, *9*(5), 928-948, doi:https://doi.org/10.1175/1520-0442(1996)009<0928:ICVASI>2.0.CO;2.

Cayan, D. R., Dettinger, M. D., Diaz, H. F., and Graham, N. E. (1998). Decadal variability of precipitation over western North America. *Journal of Climate*, *11*(12), 3148-3166, doi:https://doi.org/10.1175/1520-0442(1998)011<3148:DVOPOW>2.0.CO;2.

Cayan, D. R., Das, T., Pierce, D. W., Barnett, T. P., Tyree, M., and Gershunov, A. (2010). Future dryness in the southwest US and the hydrology of the early 21st century drought. *Proceedings of the National Academy of Sciences*, *107*(50), 21271-21276, doi:https://doi.org/10.1073/pnas.0912391107.

Cayan D.R. et al. (2013). Future Climate: Projected Average. In: Garfin G., Jardine A., Merideth R., Black M., LeRoy S. (eds) Assessment of Climate Change in the Southwest United States. NCA Regional Input Reports. Island Press, Washington, D.C.

Chen, F., and Li, X. (2016). Evaluation of IMERG and TRMM 3B43 monthly precipitation products over mainland China. *Remote Sensing*, *8*(6), 472, doi:https://doi.org/10.3390/rs8060472.

Cook, E. R., Woodhouse, C. A., Eakin, C. M., Meko, D. M., and Stahle, D. W. (2004). Long-term aridity changes in the western United States. *Science*, *306*(5698), 1015-1018, doi:10.1126/science.1102586.

Cozzetto, K., Chief, K., Dittmer, K., Brubaker, M., Gough, R., Souza, K., Ettawageshik, F., Wotkyns, S., Opitz-Stapleton, S., Duren, S., and Chavan, P. (2013). Climate change impacts on the water resources of American Indians and Alaska Natives in the U.S. *Climate Change*, *120*(3), 569–584, doi:doi:10.1007/s10584-013-0852-y.

Credo, J., Torkelson, J., Rock, T., and Ingram, J. C. (2019). Quantification of elemental contaminants in unregulated water across western Navajo Nation. *International Journal of Environmental Research and Public Health*, *16*(15), 2727, doi:10.3390/ijerph16152727.

Crimmins, M. (2006). Arizona and the North American Monsoon System. Tucson, AZ: The University of Arizona College of Agriculture and Life Sciences. Retrieved from https://extension.arizona.edu/sites/extension.arizona.edu/files/pubs/az1417.pdf.

Crimmins, M. A., Selover, N., Cozzetto, K., Chief, K., and Meadow, A. (2013). Technical Review of the Navajo Nation Drought Contingency Plan–Drought Monitoring. *Climate Assessment for the Southwest Tech. Rep*.

Daly, C., Neilson, R. P., and Phillips, D. L. (1994). A statistical-topographic model for mapping climatological precipitation over mountainous terrain. *Journal of Applied Meteorology*, *33*(2), 140-158, doi:https://doi.org/10.1175/1520-0450(1994)033<0140:ASTMFM>2.0.CO;2.

Daly, C., et al. (2008). Physiographically sensitive mapping of climatological temperature and precipitation across the conterminous United States. *International Journal of Climatology: a Journal of the Royal Meteorological Society*, *28*(15), 2031-2064, doi:https://doi.org/10.1002/joc.1688.

Dieter, C.A., Maupin, M.A., Caldwell, R.R., Harris, M.A., Ivahnenko, T.I., Lovelace, J.K., Barber, N.L., and Linsey, K.S. (2018). Estimated use of water in the United States in 2015: U.S. Geological Survey Circular 1441, 65 p., doi:https://doi.org/10.3133/cir1441. [Supersedes USGS Open-File Report 2017–1131.]

DeMenocal, P. B. (2001). Cultural responses to climate change during the late Holocene. *Science*, *292*(5517), 667-673, doi:10.1126/science.1059287.

Dornbusch and Associates, Prepared by Jim Merchant. (2006). Economic benefit/cost analysis - Navajo Gallup Water Supply Project.

Douglas, M. W. (1995). The summertime low-level jet over the Gulf of California. *Monthly Weather Review*, *123*(8), 2334-2347, doi:https://doi.org/10.1175/1520-0493(1995)123<2334:TSLLJO>2.0.CO;2.

Dunn, L. B., and Horel, J. D. (1994). Prediction of central Arizona convection. Part I: Evaluation of the NGM and Eta model precipitation forecasts. *Weather and Forecasting*, *9*(4), 495-507, doi:https://doi.org/10.1175/1520-0434(1994)009<0495:POCACP>2.0.CO;2.

El-Vilaly, M. A. S., Didan, K., Marsh, S. E., van Leeuwen, W. J., Crimmins, M. A., and Munoz, A. B. (2018). Vegetation productivity responses to drought on tribal lands in the four corners region of the Southwest USA. *Frontiers of Earth Science*, *12*(1), 37-51, doi:https://doi.org/10.1007/s11707-017-0646-z.

Erdei, E., Shuey, C., Pacheco, B., Cajero, M., Lewis, J., and Rubin, R. L. (2019). Elevated autoimmunity in residents living near abandoned uranium mine sites on the Navajo Nation. *Journal of Autoimmunity*, *99*, 15-23, doi:10.1016/j.jaut.2019.01.006.

Euler, R. C., Gumerman, G. J., Karlstrom, T. N., Dean, J. S., and Hevly, R. H. (1979). The Colorado plateaus: Cultural dynamics and paleoenvironment. *Science*, *205*(4411), 1089-1101, doi:0.1126/science.205.4411.1089.

Fairweather, M. L., Geils, B. W., and Manthei, M. (2008). Aspen decline on the Coconino national forest. In *In: McWilliams, Michael; Palacios, Patsy, comps. Proceedings of the 55th Annual Western International Forest Disease Work Conference; 2007 October 15-19; Sedona, AZ. Salem, OR: Oregon Department of Forestry. p. 53-62.* (pp. 53-62).

Ffolliott, P. F., and Stropki, C. (2008). Impacts of pinyon-juniper treatments on water yields: a historical perspective. *Ecology, Management, and Restoration of Piñon-Juniper and Ponderosa Pine Ecosystems*, 59.

Franchini, M., AND Pacciani, M. (1991). Comparative analysis of several conceptual rainfall-runoff models. *Journal of Hydrology*, *122*(1-4), 161-219, doi:https://doi.org/10.1016/0022-1694(91)90178-K.

Frankland, H.C., Turnbull, A.P., Wehmeyer, M.L., and Blackmountain, L. (2004). An exploration of the self-determination construct and disability as it relates to the Dine (Navajo) culture. *Education and Training in Developmental Disabilities*, 39(3), 191-205, URI: http://hdl.handle.net/1808/6218.

Garfin, G., Ellis, A., Selover, N., Anderson, D., Tecle, A., Heinrich, P., and Crimmins, M. (2007). Assessment of the Navajo Nation hydroclimate network. Arizona Water Institute Report AWI-07-21.

Gershunov A. et al. (2013). Future Climate: Projected Extremes. In: Garfin G., Jardine A., Merideth R., Black M., LeRoy S. (eds) Assessment of Climate Change in the Southwest United States. NCA Regional Input Reports. Island Press, Washington, D.C.

Gilbert, M., Nicolas, G., Cinardi, G., Van Boeckel, T. P., Vanwambeke, S. O., Wint, G. W., and Robinson, T. P. (2018). Global distribution data for cattle, buffaloes, horses, sheep, goats, pigs, chickens and ducks in 2010. *Scientific Data*, *5*(1), 1-11, doi:https://doi.org/10.1038/sdata.2018.227.

Groisman, P. Y., Koknaeva, V. V., Belokrylova, T. A., and Karl, T. R. (1991). Overcoming biases of precipitation measurement: A history of the USSR experience. *Bulletin of the American Meteorological Society*, *72*(11), 1725-1733, doi:https://doi.org/10.1175/1520-0477(1991)072<1725:OBOPMA>2.0.CO;2.

Groisman, P. Y., Knight, R. W., and Karl, T. R. (2001). Heavy precipitation and high streamflow in the contiguous United States: Trends in the twentieth century. *Bulletin of the American Meteorological Society*, *82*(2), 219-246, doi:https://doi.org/10.1175/1520-0477(2001)082<0219:HPAHSI>2.3.CO;2.

Guo, H., et al. (2016). Early assessment of integrated multi-satellite retrievals for global precipitation measurement over China. *Atmospheric Research*, *176*, 121-133, doi:https://doi.org/10.1016/j.atmosres.2016.02.020.

Gutzler, D. S., and Preston, J. W. (1997). Evidence for a relationship between spring snow cover in North America and summer rainfall in New Mexico. *Geophysical Research Letters*, *24*(17), 2207-2210, doi:https://doi.org/10.1029/97GL02099.

Gutzler, D. S., Kann, D. M., and Thornbrugh, C. (2002). Modulation of ENSO-based long-lead outlooks of southwestern US winter precipitation by the Pacific decadal oscillation. *Weather and Forecasting*, *17*(6), 1163-1172, doi:https://doi.org/10.1175/1520-0434(2002)017<1163:MOEBLL>2.0.CO;2.

Harrington Jr, J. A., Cerveny, R. S., and Balling Jr, R. C. (1992). Impact of the Southern Oscillation on the North American southwest monsoon. *Physical Geography*, *13*(4), 318-330, doi:https://doi.org/10.1080/02723646.1992.10642460.

Hashemi, H., Nordin, M., Lakshmi, V., Huffman, G. J., and Knight, R. (2017). Bias correction of long-term satellite monthly precipitation product (TRMM 3B43) over the conterminous United States. *Journal Of Hydrometeorology*, *18*(9), 2491-2509, doi:https://doi.org/10.1175/JHM-D-17-0025.1.

Haupt, S. E. et al. (2019). 100 years of progress in applied meteorology. Part III: Additional applications. *Meteorological Monographs*, *59*, 24-1, doi:https://doi.org/10.1175/AMSMONOGRAPHS-D-18-0012.1.

Henderson, E. (1989). Navajo livestock wealth and the effects of the stock reduction program of the 1930s. *Journal of Anthropological Research*, *45*(4), 379-403, doi:https://doi.org/10.1086/jar.45.4.3630516.

Hereford, R., and Webb, R. H. (1992). Historic variation of warm-season rainfall, southern Colorado Plateau, southwestern USA. *Climatic Change*, *22*(3), 239-256, doi:https://doi.org/10.1007/BF00143030.

Higgins, R. W., Yao, Y., and Wang, X. L. (1997). Influence of the North American monsoon system on the US summer precipitation regime. *Journal of Climate*, *10*(10), 2600-2622, doi:https://doi.org/10.1175/1520-0442(1997)010<2600:IOTNAM>2.0.CO;2.

Higgins, R. W., Mo, K. C., and Yao, Y. (1998). Interannual variability of the US summer precipitation regime with emphasis on the southwestern monsoon. *Journal of Climate*, *11*(10), 2582-2606.

Higgins, R. W., and Shi, W. (2000). Dominant factors responsible for interannual variability of the summer monsoon in the southwestern United States. *Journal of Climate*, *13*(4), 759-776, doi:https://doi.org/10.1175/1520-0442(2000)013<0759:DFRFIV>2.0.CO;2.

Higgins, R. W., Shi, W., and Hain, C. (2004). Relationships between Gulf of California moisture surges and precipitation in the southwestern United States. *Journal of Climate*, *17*(15), 2983-2997, doi:https://doi.org/10.1175/1520-0442(2004)017<2983:RBGOCM>2.0.CO;2.

Hoerling M.P. et al. (2013). Present Weather and Climate: Evolving Conditions. In: Garfin G., Jardine A., Merideth R., Black M., LeRoy S. (eds) Assessment of Climate Change in the Southwest United States. NCA Regional Input Reports. Island Press, Washington, D.C.

Hoover, J., Gonzales, M., Shuey, C., Barney, Y., Lewis, J. (2017). Elevated arsenic and uranium concentrations in unregulated water sources on the Navajo Nation, USA. *Exposure and Health,* 9, 113–124, doi:https://doi.org/10.1007/s12403-016-0226-6.

Hoover, J. H., Coker, E., Barney, Y., Shuey, C., and Lewis, J. (2018). Spatial clustering of metal and metalloid mixtures in unregulated water sources on the Navajo Nation–Arizona, New Mexico, and Utah, USA. *Science of The Total Environment*, *633*, 1667-1678, doi:https://doi.org/10.1016/j.scitotenv.2018.02.288.

Hrachowitz, M., Bohte, R., Mul, M. L., Bogaard, T. A., Savenije, H. H. G., and Uhlenbrook, S. (2011). On the value of combined event runoff and tracer analysis to improve understanding of catchment functioning in a data-scarce semi-arid area. *Hydrology & Earth System Sciences*, *15*(6), doi:10.5194/hess-15-2007-2011.

Huffman, G.J., E.F. Stocker, D.T. Bolvin, E.J. Nelkin, Jackson Tan. (2019). GPM IMERG Final Precipitation L3 1 month 0.1 degree x 0.1 degree V06, Greenbelt, MD, Goddard Earth Sciences Data and Information Services Center (GES DISC), Accessed: December 10, 2019, doi:10.5067/GPM/IMERG/3B-MONTH/06.

Huffman, G. J., Bolvin, D. T., Braithwaite, D., Hsu, K., Joyce, R., Kidd, C., Nelkin, E. J., Soroosh, S., Tan, J., and Pingping, X. (2019). NASA global precipitation measurement

(GPM) integrated multi-satellite retrievals for GPM (IMERG). *Algorithm Theoretical Basis Document (ATBD) Version*, *06*. Retrieved from https://docserver.gesdisc.eosdis.nasa.gov/public/project/GPM/IMERG_ATBD_V06.pdf.

Hunter, T., Tootle, G., and Piechota, T. (2006). Oceanic-atmospheric variability and western US snowfall. *Geophysical Research Letters*, *33*(13), doi:https://doi.org/10.1029/2006GL026600.

Ingram, J. C., Jones, L., Credo, J., and Rock, T. (2020). Uranium and arsenic unregulated water issues on Navajo lands. *Journal of Vacuum Science and Technology A: Vacuum, Surfaces, and Films*, *38*(3), 031003, doi:10.1116/1.5142283.

Ivanic, M., and Martin, W. (2008). Implications of higher global food prices for poverty in low-income countries. *Agricultural Economics*, *39*(s1), 405-416, doi:https://doi.org/10.1111/j.1574-0862.2008.00347.x.

Lee, G. W., and Zawadzki, I. (2005). Variability of drop size distributions: Time-scale dependence of the variability and its effects on rain estimation. *Journal of applied meteorology*, *44*(2), 241-255, doi:https://doi.org/10.1175/JAM2183.1.

Legates, D. R., and DeLiberty, T. L. (1993). Precipitation measurement biases in the United States 1. *Journal of the American Water Resources Association*, *29*(5), 855-861, doi:https://doi.org/10.1111/j.1752-1688.1993.tb03245.x.

Li, D., Wrzesien, M. L., Durand, M., Adam, J., and Lettenmaier, D. P. (2017). How much runoff originates as snow in the western United States, and how will that change in the future?. *Geophysical Research Letters*, *44*(12), 6163-6172, doi:https://doi.org/10.1002/2017GL073551.

Liang, X., D. P. Lettenmaier, E. F. Wood, and S. J. Burges (1994), A simple hydrologically based model of land surface water and energy fluxes for GCMs, J. Geophys. Res., 99, 14,415–14,428, doi:10.1029/94JD00483.

Liang, X., Wood, E. F., and Lettenmaier, D. P. (1996). Surface soil moisture parameterization of the VIC-2L model: Evaluation and modification. *Global and Planetary Change*, *13*(1-4), 195-206, doi:https://doi.org/10.1016/0921-8181(95)00046-1.

Lo, F., and Clark, M. P. (2002). Relationships between spring snow mass and summer precipitation in the southwestern United States associated with the North American monsoon system. *Journal of Climate*, *15*(11), 1378-1385, doi:https://doi.org/10.1175/1520-0442(2002)015<1378:RBSSMA>2.0.CO;2.

Lohmann, D. K. E. et al. (2004). Streamflow and water balance intercomparison of four land surface models in the North American Land Data Assimilation Systems project. *Journal of Geophysical Research*, *109*, D07S91.

MacDonald, G. M. (2010). Water, climate change, and sustainability in the southwest. *Proceedings of the National Academy of Sciences*, *107*(50), 21256-21262, doi:https://doi.org/10.1073/pnas.0909651107.

Maddox, R. A., McCollum, D. M., and Howard, K. W. (1995). Large-scale patterns associated with severe summertime thunderstorms over central Arizona. *Weather and Forecasting*, *10*(4), 763-778, doi:https://doi.org/10.1175/1520-0434(1995)010<0763:LSPAWS>2.0.CO;2.

Maghsood, F. F., Hashemi, H., Hosseini, S. H., and Berndtsson, R. (2020). Ground validation of GPM IMERG precipitation products over Iran. *Remote Sensing*, *12*(1), 48, doi: https://doi.org/10.3390/rs12010048.

Maurer, E. P., Stewart, I. T., Bonfils, C., Duffy, P. B., and Cayan, D. (2007). Detection, attribution, and sensitivity of trends toward earlier streamflow in the Sierra Nevada. *Journal of Geophysical Research: Atmospheres*, *112*(D11), doi:https://doi.org/10.1029/2006JD008088.

McPherson, R. S. (1998). Navajo livestock reduction in southeastern Utah, 1933-46: History repeats itself. *American Indian Quarterly*, *22*(1/2), 1-18.

Meehan, M. A., Stokka, G. L., and Mostrom, M. S. (2015). *Livestock Water Requirements*. NDSU Extension Service.

Mesinger, F. et al. (2006). North American regional reanalysis. *Bulletin of the American Meteorological Society*, *87*(3), 343-360, doi:https://doi.org/10.1175/BAMS-87-3-343.

Mitchell, D.L., Ivanova, D., Rabin, R., Brown, T.J., Redmond, K. (2002). Gulf of California sea surface temperatures and the North American Monsoon: mechanistic implications from observations. *Journal of Climate*, *15*(17), 2261–2281, doi:10.1175/1520-0442(2002)015<2261:GOCSST>2.0.CO;2.

Mitchell, K. E. et al. (2004). The multi-institution North American Land Data Assimilation System (NLDAS): Utilizing multiple GCIP products and partners in a continental distributed hydrological modeling system. *Journal of Geophysical Research: Atmospheres*, *109*(D7), doi:https://doi.org/10.1029/2003JD003823.

Mitra, C., and Shepherd, J. M. (2015). A global perspective. *The Routledge Handbook of Urbanization and Global Environmental Change*, 152.

Mock, C. J. (1996). Climatic controls and spatial variations of precipitation in the western United States. *Journal of Climate*, *9*(5), 1111-1125, doi:https://doi.org/10.1175/1520-0442(1996)009<1111:CCASVO>2.0.CO;2

Mocko, D. NASA/GSFC/HSL (2012), NLDAS Primary Forcing Data L4 Monthly 0.125 x 0.125 degree V002, Greenbelt, Maryland, USA, Goddard Earth Sciences Data and Information Services Center (GES DISC), doi:10.5067/Z62LT6J96R4F.

Morin, J., and Benyamini, Y. (1977). Rainfall infiltration into bare soils. *Water Resources Research*, *13*(5), 813-817, doi:https://doi.org/10.1029/WR013i005p00813.

Mote, P. W., Hamlet, A. F., Clark, M. P., and Lettenmaier, D. P. (2005). Declining mountain snowpack in western North America. *Bulletin of the American Meteorological Society*, *86*(1), 39-50, doi:*https://doi.org/10.1175/BAMS-86-1-39*.

Nania, J., Cozzetto, K., Gillett, K., Duren, N., Tapp, A.M., Eitner, M. and Baldwin, B. (2014). Considerations for climate change and variability adaptation on the Navajo Nation. University of Colorado, Boulder, Colorado. Retrieved from: https://scholar.law.colorado.edu/cgi/viewcontent.cgi?article=1002andcontext=books_reports_studies.

NASA Goddard Space Flight Center, Ocean Ecology Laboratory, Ocean Biology Processing Group. Moderate-resolution Imaging Spectroradiometer (MODIS) Aqua MODISA_L3m_SST v2014 Data; NASA OB.DAAC, Greenbelt, MD, USA. doi:10.5067/AQUA/MODIS/L3M/SST/2014.

NASA Goddard Space Flight Center, Ocean Ecology Laboratory, Ocean Biology Processing Group. Moderate-resolution Imaging Spectroradiometer (MODIS) Terra MOD13C2 v006 Data; NASA OB.DAAC, Greenbelt, MD, USA.

Navajo Department of Water Resources [NDWR]. (2000). Water resource development strategy for the Navajo Nation. Fort Defiance, AZ.

Navajo Department of Water Resources [NDWR]. (2003). Navajo Nation drought contingency plan. Fort Defiance, AZ.

Navajo Department of Water Resources [NDWR]. (2011). Draft water resource development strategy for the Navajo Nation. Fort Defiance, AZ.

Navajo Epidemiology Center. (2013). Navajo population profile 2010 U.S. Census. Retrieved from http:// www.nec.navajo-nsn.gov/Portals/0/Reports/ NN2010PopulationProfile.pdf.

Navajo Water Project. Accessed on May 10, 2020 from https://www.navajowaterproject.org/.

Navarro, A., García-Ortega, E., Merino, A., Sánchez, J. L., Kummerow, C., and Tapiador, F. J. (2019). Assessment of IMERG precipitation estimates over Europe. *Remote Sensing*, *11*(21), 2470, doi:https://doi.org/10.3390/rs11212470.

Neely, B. et al. (2001). Southern Rocky Mountains: An ecoregional assessment and conservation blueprint. *Prepared by the Nature Conservancy with support from the USDA Forest*

Service, Rocky Mountain Region, Colorado Division of Wildlife, and Bureau of Land Management.

Nesbitt, S. W., and Anders, A. M. (2009). Very high resolution precipitation climatologies from the Tropical Rainfall Measuring Mission precipitation radar. *Geophysical Research Letters*, *36*(15), doi:https://doi.org/10.1029/2009GL038026.

New, M., Todd, M., Hulme, M., and Jones, P. (2001). Precipitation measurements and trends in the twentieth century. *International Journal of Climatology: A Journal of the Royal Meteorological Society*, *21*(15), 1889-1922, doi: https://doi.org/10.1002/joc.680.

Parker, K. (2010). Population, immigration, and the drying of the Southwest. *Center for Immigration Studies*. Retrieved from https://cis.org/sites/cis.org/files/articles/2010/water.pdf.

Peterson, T. C., et al. (1998). Homogeneity adjustments of in situ atmospheric climate data: a review. *International Journal of Climatology: A Journal of the Royal Meteorological Society*, *18*(13), 1493-1517, doi:10.1002/(SICI)1097-0088(19981115)18:13<1493::AID-JOC329>3.0.CO;2-T.

Pilgrim, D. H., Chapman, T. G., and Doran, D. G. (1988). Problems of rainfall-runoff modelling in arid and semiarid regions. *Hydrological Sciences Journal*, *33*(4), 379-400, doi:https://doi.org/10.1080/02626668809491261.

Prat, O. P., and Barros, A. P. (2009). Exploring the transient behavior of Z–R relationships: Implications for radar rainfall estimation. *Journal of Applied Meteorology and Climatology*, *48*(10), 2127-2143, doi:https://doi.org/10.1175/2009JAMC2165.1.

PRISM Climate Group, Oregon State University, http://prism.oregonstate.edu, created 4 Feb 2004.

Redsteer, M. H., Bemis, K., Chief, K., Gautam, M., Middleton, B. R., Tsosie, R., and Ferguson, D. B. (2013). Unique challenges facing southwestern tribes. In *Assessment of Climate Change in the Southwest United States* (pp. 385-404). Island Press, Washington, DC.

Robinson, D. A., Lebron, I., Ryel, R. J., and Jones, S. B. (2010). Soil water repellency: A method of soil moisture sequestration in pinyon–juniper woodland. *Soil Science Society of America Journal*, *74*(2), 624-634, doi: 10.2136/sssaj2009.0208.

Roessel, R., and Johnson, B. H. (1974). *Navajo livestock reduction: A national disgrace*. Dine College Pr.

Ropelewski, C. F., and Halpert, M. S. (1986). North American precipitation and temperature patterns associated with the El Niño/Southern Oscillation (ENSO). *Monthly Weather Review*, *114*(12), 2352-2362, doi:https://doi.org/10.1175/1520-0493(1986)114<2352:NAPATP>2.0.CO;2.

Rose, C. W. (1968). Water transport in soil with a daily temperature wave. II. Analysis. *Australian Journal of Soil Research., 6*(1), 45-57.

Rowson, D. R., and Colucci, S. J. (1992). Synoptic climatology of thermal low-pressure systems over south-western north America. *International Journal of Climatology*, *12*(6), 529-545, doi:https://doi.org/10.1002/joc.3370120602

Rui, H., and Mocko, D. (2014). Readme Document for North America Land Data Assimilation System Phase 2 (NLDAS-2) Products; The National Aeronautics and Space Administration: Greenbelt, MD, USA.

Salzer, M. W. (2000). Temperature variability and the Northern Anasazi: Possible implications for regional abandonment. *Kiva*, *65*(4), 295-318, doi:10.1080/00231940.2000.11758414.

Salzer, M. W., and Kipfmueller, K. F. (2005). Reconstructed temperature and precipitation on a millennial timescale from tree-rings in the southern Colorado Plateau, USA. *Climatic Change*, *70*(3), 465-487, doi:https://doi.org/10.1007/s10584-005-5922-3.

Seager, R., and Vecchi, G. A. (2010). Greenhouse warming and the 21st century hydroclimate of southwestern North America. *Proceedings of the National Academy of Sciences*, *107*(50), 21277-21282, doi:https://doi.org/10.1073/pnas.0910856107.

Seager, R., Ting, M., Li, C., Naik, N., Cook, B., Nakamura, J., and Liu, H. (2013). Projections of declining surface-water availability for the southwestern United States. *Nature Climate Change*, *3*(5), 482-486, doi:https://doi.org/10.1038/nclimate1787.

Serreze, M. C., Clark, M. P., Armstrong, R. L., McGinnis, D. A., and Pulwarty, R. S. (1999). Characteristics of the western United States snowpack from snowpack telemetry (SNOTEL) data. *Water Resources Research*, *35*(7), 2145-2160, doi:https://doi.org/10.1029/1999WR900090.

Sevruk, B. (1982). Methods of correction for systematic error in point precipitation measurement for operational use. Operational Hydrology Rep. 21, World Meteorological Organization, Geneva.

Sharifi, E., Eitzinger, J., and Dorigo, W. (2019). Performance of the state-of-the-art gridded precipitation products over mountainous terrain: A regional study over Austria. *Remote Sensing*, *11*(17), 2018, doi:https://doi.org/10.3390/rs11172018.

Shepherd, J. M., Andersen, T., Strother, C., Horst, A., Bounoua, L., and Mitra, C. (2013). Urban climate archipelagos: A new framework for urban impacts on climate. *Earthzine*. Retrieved from http://www.earthzine.org/2013/11/29/urban-climate-archipelagos-a-new-framework-for-urban-impacts-on-climate/.

Shepherd, J.M., Burian, S., Liu, C., and Bernardes, S. (2016) Satellite precipitation metrics to study the energy-water-food nexus within the backdrop of an urbanized globe. *Earthzine*.

Retrieved from: https://earthzine.org/satellite-precipitation-metrics-to-study-the-energy-water-food-nexus-within-the-backdrop-of-an-urbanized-globe/.

Sheppard, P. R., Comrie, A. C., Packin, G. D., Angersbach, K., and Hughes, M. K. (2002). The climate of the US Southwest. *Climate Research*, *21*(3), 219-238, doi:10.3354/cr021219.

Shuttleworth, W. J. (1993). Evaporation In: Maidment, DR Handbook of hydrology.

Singer, S.L., and Woods, S. (2014) Navajo Nation energy and water consumption. United States. doi:10.2172/1389937.

Smith, W. P., and Gall, R. L. (1989). Tropical squall lines of the Arizona monsoon. *Monthly Weather Review*, *117*(7), 1553-1569, doi:https://doi.org/10.1175/1520-0493(1989)117<1553:TSLOTA>2.0.CO;2.

Stout, D. T., Walsh, T. C., and Burian, S. J. (2017). Ecosystem services from rainwater harvesting in India. *Urban Water Journal*, *14*(6), 561-573, doi:https://doi.org/10.1080/1573062X.2015.1049280.

Sungmin, O., Foelsche, U., Kirchengast, G., Fuchsberger, J., Tan, J., and Petersen, W. A. (2017). Evaluation of GPM IMERG Early, Late, and Final rainfall estimates using WegenerNet gauge data in southeastern Austria. *Hydrology & Earth System Sciences*, *21*(12), doi:https://doi.org/10.5194/hess-21-6559-2017.

Tang, M., and Reiter, E. R. (1984). Plateau monsoons of the Northern Hemisphere: A comparison between North America and Tibet. *Monthly Weather Review*, *112*(4), 617-637, doi:https://doi.org/10.1175/1520-0493(1984)112<0617:PMOTNH>2.0.CO;2.

Tsinnajinnie, L. M., Gutzler, D. S., and John, J. (2018). Navajo Nation snowpack variability from 1985-2014 and implications for water resources management. *Journal of Contemporary Water Research & Education*, *163*(1), 124-138, doi:https://doi.org/10.1111/j.1936-704X.2018.03274.x.

Tulley-Cordova, C. L., Strong, C., Brady, I. P., Bekis, J., and Bowen, G. J. (2018). Navajo Nation, USA, precipitation variability from 2002 to 2015. *Journal of Contemporary Water Research and Education*, *163*(1), 109-123, doi:https://doi.org/10.1111/j.1936-704X.2018.03273.x.

Ulbrich, C. W., and Lee, L. G. (1999). Rainfall measurement error by WSR-88D radars due to variations in Z–R law parameters and the radar constant. *Journal of Atmospheric and oceanic Technology*, *16*(8), 1017-1024, doi:https://doi.org/10.1175/1520-0426(1999)016<1017:RMEBWR>2.0.CO;2.

United States Department of Agriculture. (2007). Navajo Nation Profile: 2007 Census Of Agriculture. U.S. Department of Agriculture.

United States Department of Agriculture-national Agriculture Statistics Service (NASS). (2012). Navajo Nation Summary by Agency. Accessed April 16, 2020. Retrieved from https://www.nass.usda.gov/Statistics_by_State/Regional_Office/Mountain/includes/more_features/Navajo_Chapterhouse_Summary/Navajo-Nation-Summary-by-Agency.pdf.

United States Environmental Protection Agency [U.S. EPA]. (2001) Drinking water infrastructure needs survey: American Indian and Alaska native village water systems survey. USEPA, Washington.

United States Environmental Protection Agency [U.S. EPA] Region IX. (2008). Navajo Nation drinking water source sampling: February-March 2008. Retrieved from https://www.epa.gov/sites/production/files/2016-06/documents/2008-08-28-navajo-drinking-water-source-sampling.pdf.

United States Geological Survey (USGS). (2014). USGS Small-scale Dataset - 1:1,000,000-Scale Contours of the Conterminous United States 201404 Shapefile: U.S. Geological Survey.

University of Washington Computational Hydrology Group. (2016). VIC Model Overview. Retrieved January 15, 2020, from https://vic.readthedocs.io/en/master/Overview/ModelOverview/.

Watson, A. I., López, R. E., and Holle, R. L. (1994). Diurnal cloud-to-ground lightning patterns in Arizona during the southwest monsoon. *Monthly Weather Review*, *122*(8), 1716-1725, doi:https://doi.org/10.1175/1520-0493(1994)122<1716:DCTGLP>2.0.CO;2.

Welty, C. (2009). The urban water budget. In *The water environment of cities* (pp. 17-28). Springer, Boston, MA.

Wheater, H. S. (2002). Hydrological processes in arid and semiarid areas. *Hydrology of wadi systems, IHP-V, Technical documents in hydrology*, *55*, 5-22.

Witherspoon, G. (1973). Sheep in Navajo culture and social organization 1. *American Anthropologist*, *75*(5), 1441-1447, doi:https://doi.org/10.1525/aa.1973.75.5.02a00150.

Wood, E. F., Lettenmaier, D., Liang, X., Nijssen, B., and Wetzel, S. W. (1997). Hydrological modeling of continental-scale basins. *Annual Review of Earth and Planetary Sciences*, *25*(1), 279-300, doi:https://doi.org/10.1146/annurev.earth.25.1.279.

Woodhouse, C. A., and Meko, D. (1997). Number of winter precipitation days reconstructed from southwestern tree rings. *Journal of Climate*, *10*(10), 2663-2669, doi:https://doi.org/10.1175/1520-0442(1997)010<2663:NOWPDR>2.0.CO;2.

World Economic Forum. (2011). Global Risks 2011. 6th Edition. Retrieved from http://reports.weforum.org/global-risks-2011/.

Xia, Y. et al. (2012). Continental-scale water and energy flux analysis and validation for the North American Land Data Assimilation System project phase 2 (NLDAS-2): 1. Intercomparison and application of model products *Journal of Geophysical Research: Atmospheres*, *117*(D3), doi:10.1029/2011JD016048.

Xia, Y. et al. (2016). Basin-scale assessment of the land surface water budget in the National Centers for Environmental Prediction operational and research NLDAS-2 systems. *Journal of Geophysical Research: Atmospheres*, *121*(6), 2750-2779, doi:https://doi.org/10.1002/2015JD023733.

Zektser, S., Loáiciga, H. A., and Wolf, J. T. (2005). Environmental impacts of groundwater overdraft: selected case studies in the southwestern United States. *Environmental Geology*, *47*(3), 396-404, doi:https://doi.org/10.1007/s00254-004-1164-3.

Zhao, R. J., Zhang, Y. L., Fang, L. R., Liu, X. R., and Zhang, Q. S. (1980). The Xinanjiang model Hydrological Forecasting Proceedings Oxford Symposium, IASH.

Zhao, M., and Running, S. W. (2010). Drought-induced reduction in global terrestrial net primary production from 2000 through 2009. *Science*, *329*(5994), 940-943, doi:10.1126/science.1192666.